Thesis for the degree of Licentiate in Engineering

Automated Manufacture of Fertilizing Granules from Burnt Wood Ash

Thomas Svantesson

LUND
UNIVERSITY

Department of
Industrial Electrical Engineering and Automation
Lund University, SE-221 00 LUND, SWEDEN

Kalmar – Lund 2000

Department of
Industrial Electrical Engineering and Automation (IEA)
Lund Institute of Technology (LTH)
Lund University
P.O. Box 118
S-221 00 LUND
SWEDEN

http://www.iea.lth.se

ISBN 91-88934-16-0
CODEN:LUTEDX/(TEIE-1024)/1-133/(2000)

Printed in Sweden by Universitetstryckeriet, Lund University
Lund 2000

Hofstader's Law:

It always takes longer than you expect, even when you take into account Hofstader's Law

Abstract

This work considers control of an ash transformation process, which transforms wood ash produced at district heating plants into fertilizing granules. The manufactured granules are recycled back to the forest grounds, as a fertilizer, or as a tool to reduce the acidification in the forest soil at the spreading area. Other areas of application are, for example, structural fill and substitute for cement in ready-mix concrete.

The ash transformation process includes mixing, size reduction, granulation, drying, sorting and packing. Furthermore, the transformation process uses ETEC-dolomite that acts as a binding agent and therefore improves the strength of the produced granules. Due to the dolomite, the lime effect of the produced fertilizers is increased, whereas the leaching speed of the wood ash included heavy-metals is decreased. A robust machine is developed and controlled by an industrial control system in order to enable continuous and automatic manufacture. At present, the units for mixing and size reduction are fully implemented, built to comply with the industrial requirements for continuous operation. The remaining stages are controlled to a certain extent, but are still based on the earlier prototype.

Mixing ash/dolomite/water in order to obtain granular material is one method to stabilize wood ashes. The main problem is predicting the quantity of water to be added, since the necessary amount varies with the wood ash quality. The implemented controller is therefore able to determine this critical amount without any measure of the wood ash quality, as for example the ash carbon content. However, the produced granules do not benefit from high carbon content. Therefore, two potential on-line methods for carbons in ash monitoring are presented but not implemented due to financial reasons.

Acknowledgements

I am very grateful to all the people who have inspired and supported me during my work on this thesis.

First of all I would like to thank my supervisor, the always positive and enthusiastic Prof. Gustaf Olsson for accepting me as a Ph.D. student at his department. He controlled the evolution of the work and has always given a positive feedback. I also take this opportunity to thank Prof. Alexander Lauber for guidance and excellent support during all work at Kalmar University College.

I am indebted to the staff at Graninge - Kalmar Energi, especially Tommy Petersson, Daniel Jedfelt, Roger Andersson, Mats Petersson, Tomas Andersson, Per Snöberg and Bo Carlsson. They all have been a great support in this work. A special thanks to Bo Lindewald, who helped me to save the situation during the process breakdown, late evening, December 23, 1999.

I would like to thank Anders Hultgren for offering me the opportunity to become a Ph.D. student stationed at Kalmar University College. Furthermore, I would like to express my gratitude to everyone at IEA and the Department of Technology for the nice atmosphere and help with several of problems, especially Svante Andersson, Annika Augustsson, Anders Arpteg, Thomas Bergander, Olof Berglin, Martin Bojrup, Anita Borné, Magnus Eriksson, Per Fagrell, Jirina Fahlén, Jeanette Hedberg, Ulf Jeppsson, Bengt Johansson, Birgitta Johansson, Claes Johansson, Göran Johansson, Staffan Karlsson, Christine Knutsson, Wlodek Kulesza, Mattias Lindahl, Pär Lindahl, Gunnar Lindstedt, Erik Loxbo, Christer Lundberg, Peter Lundgren, Tommy Löfqvist, Jan Melin, Britt-Marie Nilsson, Leif Nilsson, Ronny Norlin, Åke Nyström, Stefan Petersson, Arvid Pohl, Christian Rosén, Carl-Johan Rydh, Olof Samuelsson, Harald Scherer, Camilla Sjögren, Håkan Skarrie, Lena Somogyi, Johan Tingström, Hans Veenhuizen and Jenny Wirandi.

I also thank myself, Morten Hemmingsson and Mats Larsson at IEA and Fredrik Gunnarsson, Division of Automatic Control, Linköping University for help with problems related to LaTeX.

The second, "green" group working in parallel on the environmental aspects of wood ash recycling has given me a lot of feedback and many great memories from project meetings. Thanks Tommy Claesson, for discovering the "new"

ash transformation process that utilize ETEC-dolomite and Sirkku Holmberg for helping me with all the chemical details and for support. I would also like to thank Britt-Marie Steenari, School of Chemical Engineering, Department of Environmental Inorganic Chemistry, Chalmers University of Technology for fruitful discussions related to the chemical properties of wood ashes, and Prof. Björn Zetraeus, The Bioenergy Centre at ITN, Växjö University for helping me to understand the art of combustion.

The material related to an impulse radar system for on-line measurement of carbon in wood ash would not have been presented in this thesis without Bernth Johansson and Johan Friborg, Malå GeoScience AB and Kjell Flodberg, Department of Earth Sciences, Geology, Earth Sciences Centre, Gothenburg. The formalities regarding the patent of the measuring system where neatly handled by Svetlana Jacobsdotter and Göran Borgö at the Business Relations Office. I also would like to thank Carl-Gunnar Nyquist at Atrium 21. To bad the patent was rejected.

Developing a machine for automatic wood ash transformation is a challenging task. In this work, I had many valuable discussions, and obtained a lot of help from Anders Axelsson, Chemical Engineering, Centre for Chemistry and Chemical Engineering, Lund University, Anders Ericson and the staff at Nobel Elektronik AB, Liebert Gustavsson, Dectron AB, Ulf Ivholt, ABB Automation products, Anders Johansson and Micael Grahn, IP Industri & Projektconsult AB, Lars-Johan Neander, NS Group, Lars Nestor, Sigma Benima AB, Gert Nordstöm, AB Nordströms konstruktionsbyrå and Sven Thege, the STG-group HB.

Furthermore, I also would like to thank Prof. Fredrik Gustafsson and Prof. Lennart Ljung, Division of Automatic Control, Linköping University, Prof. Rolf Johansson and Prof. Per Hagander, Department of Automatic Control, Lund Institute of Technology and Prof. Peter Wide at the Department of Technology, Örebro University, for the discussions related to the work presented in this thesis.

This project has been sponsored by the The Knowledge Foundation whose kind support is gratefully acknowledged.

Finally, I want to thank Josefine and the rest of my immediate family for the love and support they have given me during the completion of this work.

Kalmar, October 2000
Thomas Svantesson

Notations

Common abbreviations, and general notational conventions for mathematical symbols and operands follow. When local differences occur, they are clearly indicated in the text.

Symbols

A, B, C, D, F	Polynomials of order na, nb, nc, nd, nf.
$\mathbf{A}_t, \mathbf{B}_t, \mathbf{C}_t, \mathbf{D}_t$	The time varying matrices of a linear system.
α	Parameter used in the GMA-test.
$\in$	Belongs to.
$\mathbb{C}$	Field of complex numbers.
c	Concentration of a measured parameter.
$C_{uy}^2(\omega)$	Quadratic coherence spectrum.
$Ca(CO)_3$	Carbonate (calcite).
$Ca(OH)_2$	Slacked lime (portlandite).
CaO	Quicklime.
Cd	Cadmium.
CO_2	Carbon dioxide.
Cu	Copper.
d	Delay of the process.
$\overline{d}$	Granule mean diameter.
$\triangleq$	The left side is defined by the right side.
δ	Drying time for each granule.
e	White noise disturbance.
ε	Predictor residual.
ϵ_r	Relative permittivity (real dielectric constant).

$\eta(t)$	Viscosity.
$\mathbf{f}$	Vector of predicted free reponse.
Δf	Absolute bandwidth.
$F(\omega)$	The fourier transform of the continuous signal $f(t)$.
f_c	Carrier (center) frequency.
$F_s(\omega)$	The fourier transform of the sampled variable.
$\forall$	For all.
Φ_{uu}	Autospectra of the input u.
Φ_{yy}	Autospectra of the output y.
Φ_{vv}	Autospectra of the disturbance v.
Φ_{uy}	Cross spectrum between u and y.
$\boldsymbol{\varphi}$	Regression vector.
$\mathbf{G}$	GPC prediction matrix.
g	The impulse response of the process.
$G(q, \boldsymbol{\theta})$	The transfer function from u to y.
G_0	The true transfer function from u to y.
γ	Treshold used in the CUSUM-test.
h	Sampling time.
$H(q, \boldsymbol{\theta})$	The transfer function from e to y.
H_2O	Water.
H_{fb}	Feedback compensator.
H_{ff}	Feedforward compensator.
$\mathbf{I}$	Identity matrix of appropriate dimension.
I_i	Intensity of the incident light.
I_r	Intensity of the reflected light.
$\mathbf{K}$	Gain matrix in RLS.
k_1	Converts the input voltage into a pulse frequency.
k_2	The applied off-delay.
λ	Forgetting factor in RLS.
$L(q)$	Pre-filter (data-filter).
$\mathcal{M}$	Model set, model structure.
m_{uu}	Estimated mean.
μ^*	Estimated mean.
N_1	The minimum prediction horizon in the GPC.

N_2	The maximum prediction horizon in the GPC.
N_u	The control horizon in the GPC.
NO_X	Oxides of Nitrogen.
ν	Drift parameter in the CUSUM-test.
O_2	Oxygen.
$\mathbf{1}$	Column vector with all entries equal to one.
ω	Frequency in rad/s.
ω_{fl}, ω_{fh}	Lower/upper break frequencies for the data filter.
ω_{alias}	The fundamental alias frequency.
ω_N	The nyquist frequency.
ω_s	The sampling frequency.
$\mathbf{P}$	Parameter covariance matrix in RLS.
$P_e(t)$	Normalized effective power.
$P_e(k)$	Periodic observations of $P_e(t)$.
P_e^{crit}	Critical effective power (mixture viscosity).
Pb	Lead.
$Q(t)$	Water flow.
Q_{max}	The maximum water flow.
$\mathbb{R}$	Field of real numbers.
$r(k)$	Slope of the set-point trajectory in the GPC.
$\widehat{\mathbf{R}}_{uu}(n)$	The correlation matrix.
$r_{uu}(\tau)$	The autocorrelation of a stochastic process u.
ρ	The control penalty in the GPC.
$\mathcal{S}$	True system.
$s(k)$	Distance measure.
σ	Conductivity.
$\{\cdot\}$	Sequence of numbers.
t_k	Sampling times.
τ	Time-delay of a system.
$\boldsymbol{\theta}$	Vector of unknown parameters.
$\hat{\boldsymbol{\theta}}$	Estimated parameter vector.
u	The process input.
$\mathbf{\Delta u}$	Vector of future control increments.
u_c	Setpoint for controller.

u_f, y_f	Filtered process output and input values.
v	External variable that represents disturbances.
$\mathbf{w}$	Vector of future references.
$w(k)$	Reference trajectory for the GPC.
w_s^o	The mesh diameter for the oversized screen.
w_s^p	The mesh diameter for the product screen.
y	The process output.
$\hat{y}(k+i\|k)$	The expected value of $y(k+i)$ at time k.
y_F	Filtered measurement before A/D conversion.
Zn	Zinc.

Operators and Functions

$\arg\min_x f(x)$	The minimizing argument of $f(x)$.
$\|z\|$	Absolute value of $z \in \mathbb{C}$.
$\mathbf{A}^{-1}$	The inverse of the matrix $\mathbf{A}$.
$\mathbf{A}^T$	The transpose of the matrix $\mathbf{A}$.
$\mathbf{A}^H$	The hermitian transpose of the matrix $\mathbf{A}$.
$E\{X\}$	The expected value of a stochastic variable X.
$F_X(x)$	The probability distribution function.
$f_X(x)$	The probability density function.
mod	Modulus, i.e., the signed remainder after division.
$\|\mathbf{x}\|_p$	Norm of vector, $\|\mathbf{x}\|_p \triangleq (\sum_{i=1}^n \|x_i\|^p)^{1/p}$.
p	Differential operator, $p \triangleq d/dt$.
q, q^{-1}	Forward/backward shift operator, $qy(k) = y(k+1)$.
s	Laplace transform variable.
sign	Signum function.
sinc	Sinc function, $\text{sinc}(t) \triangleq \sin(\pi t)/\pi t$.
log	Natural logarithm.
$Var\{X\}$	The variance of a stochastic scalar X.

Acronyms

ACAA	American Coal Ash Association.
A-D	Analog-to-Digital.
ARX	AutoRegressive with eXternal input.
ARMAX	AutoRegressive MovingAverage with eXternal input.
CARIMA	Controlled AutoRegressive Integrating MovingAverage.
CIFA	Carbon In Fly Ash.
COMLI	COMmunication LInk.
CPU	Central Processing Unit.
CUSUM	CUmulative SUM.
D-A	Digital-to-Analog.
DDE	Dynamic Data Exchange.
FETC	The Federal Energy Technology Center.
GMA	Geometric Moving Average.
GPC	Generalized Predictive Control.
GPR	Ground Penetrating Radar.
HA	Hardware Alarms.
HMI	Human Machine Interface.
IEC	International Electrotechnical Commission.
IMP	Internal Model Principle.
LOI	Loss-On-Ignition.
MPC	Model Predictive Control.
NIR	Near InfraRed.
ODBC	Open Data Base Connectivity.
OE	Output Error.
PC	Personal Computer.
PE	Persistent Excitation.
PM	ProgramModules.
PID	Proportional Integral Derivative.
PLC	Programmable Logic Controller.
PRBS	Pseudo Random Binary Sequence.
RLS	Recursive Least Square.
SA	Software Alarms.
SCADA	Supervision, Control and Data Acqusition.

SFC	Sequential Function Chart.
SM	SubModules.
UWB	Ultra-Wide Band.
VM	VariableModules.
WAS	Wood Ash Stabilization.

Glossary

Agglomerate	Reshaping fine powder into larger particles.
ETEC-dolomite	Mineral used as a binding agent.

Contents

Chapter 1

Introduction

1.1 Background

Sweden supports the resolution concerning the environment and progress, which was taken at the U.N. convention, UNCED, Rio 1992. After this, it is now our obligation to aim for a lasting development. We should encourage an environmentally-sound use of renewable resources of energy, and furthermore the adaptation to the ecological cycle. The today active system for producing energy with biomass fuel is included in the resolution taken at the U.N., but still, the adaptation to the ecological cycle is not fully brought to an end.

Recycling of wood ashes from burnt wood (back to the forest grounds) is of great ecological importance. However, the ash cannot be recycled directly after combustion. There are several reasons for this, one being the volatility of wood ashes. This problem is of interest to companies that burn large amounts of wood in district heating plants and in other applications. Every year about 300 000 tons [43] of wood ash is produced in Sweden after combustion in heating plants and other applications that use biomass fuel. The ash, which contains fertilizing substances such as K, Mg, Ca, P and S [30], i.e., the substances that the trees initially are absorbing from the soil when growing, are today deposited as waste. This is not a good solution from an environmental point of view and contradicts the U.N. resolution. From January 1, 2000, there is a new deposit law for organic material in Sweden. The cost of 850 SEK/ton deposited wood ash also adds an economic incentive to recycle wood ash. Therefore, the aim is to implement a closed-loop system as symbolized by Figure 1.1, in which the wood ash is recycled back to the forest grounds.

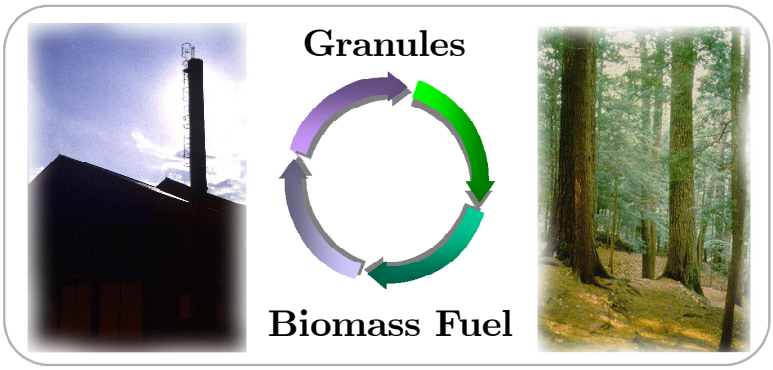

Figure 1.1: The closed-loop system.

The ash cannot be recycled directly after combustion without some pre-processing; its volatility would cause severe spreading problems. At the combustion an oxidation occurs. Therefore, primarily, all substances in the wood ash appear as oxides [60]. This implies that many components in the wood ash become *alkaline* and *reactive*. Hence, a direct spreading would cause heavy damage to the vegetation. Other drawbacks of the direct spreading are that the fertilizing substances are then emitted too fast or the ash could clog up the pores of the surrounding living plants. The idea is to transform the ashes into a product that easily could be recycled. The product should be manufactured locally at the heating plant and then distributed to the forests nearby.

As pointed out earlier, wood ashes are difficult to handle because of their volatility. It is therefore necessary to *stabilize* the wood ash before transportation and scattering. It is also necessary to stabilize the ash in order to control the leaching speed of the nutrients and the wood ash included heavy-metals, as for example cadmium (Cd), copper (Cu), lead (Pb) and zinc (Zn) [19]. In stabilized wood ash, heavy-metals are sparingly soluble. Thus, the heavy-metal emission from recycled (stabilized) wood ashes are comparable with the felling remains left at the felling area. It is also shown that berries and fungus do not obtain any higher concentrations of heavy-metals after spreading of stabilized wood ash [36]. It is recommended to recycle an amount of wood ash that will add a total heavy-metal concentration comparable to the take out at the felling. Then the forest soils are not supplied with more heavy-metals compared to the take out, thus resulting in a non-increasing concentration.

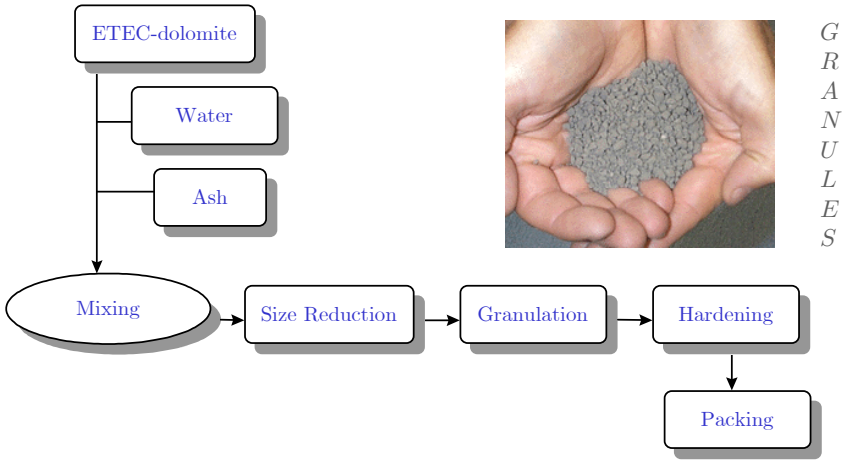

Figure 1.2: The general ash transformation process.

A researcher at Kalmar University College (Ph.D. Tommy Claesson) has devised a novel method to transform wood ashes into fertilizing *granules*, easy to handle and with adequate properties for recycling [30]. The solution is to mix the ash with water and a mineral (called ETEC-dolomite) that acts as a binding agent. The ETEC-dolomite, which is imported from Estonia, also reduces the acidification in the forest soil at the spreading area. Furthermore, the intensity of the heavy-metal emissions from the produced fertilizers are even more reduced due to the ETEC-dolomite.

The machine for automated manufacture is based on a pilot equipment that has been used to granulate the mixture of ash, dolomite and water. This prototype was developed by Graninge - Kalmar Energi in cooperation with Kalmar University College. The prototype consists of five different processing units, which are indicated by Figure 1.2. The ash, ETEC-dolomite and water are first mixed into a material that is used for granulation. When a suitable mixture is obtained, the batch is put into a feeder that gradually forces the material through a raster, which reduces the size of the passing mixture. The small particles created pass through a drum granulator where the actual granulation occurs. The granulated material is dried and hardened before it is packed.

Earlier, the prototype was controlled manually, and the granule properties then depended on the operator's knowledge and experience. The operator determined the mixture quality by taking a sample and analyzing the con-

sistency by squeezing it. This solution was expensive because of labor costs. Furthermore, the work was monotonous, making it even more difficult to maintain a good and uniform quality of the fertilizing granules. The purpose of this research is to go from *art to science*.

1.2 Objective

The objective is to develop the idea outlined above into a well-proven, professional method for recycling the ashes. The granule manufacture should be *automatic* and *batch-wise,* all the way from mixing the ingredients to packing the finished products. The ash transformation process should be capable of handling 2 tons of wood ash per day and be integrated with the heating plant computer system so that information easily can be exchanged between the local control system and the system used for supervision. Since there are several stages in this process, which all will run concurrently, it is necessary to use real-time control. Because of the industrial environment, an industrial control system is suitable as a base. The control system should not only be able to interact with the process. It should also be able to interact with the *operator*. It is very important to emphasize that the *man-machine interface* plays an essential role in these kind of applications. If the operator does not understand the information he/she is receiving, it is impossible to take the correct decision about the next step in the process. Therefore, it is important to also facilitate the exchange of information between the *user* and the equipment to be controlled. A well designed interface not only makes work conditions more pleasant, but also helps considerably to reduce errors and thus limit the extent of possible damage.

Since each stage in the ash transformation process earlier has been controlled manually, it is important to utilize the knowledge that the original process operator's possesses. This could help a great deal on the way from art to science in process experiments, controller design and software development.

1.3 Related Works

Research related to recycling of fly ash produced at coal-filed boilers are well known. The American Coal Ash Association (ACAA) reports that utilities and other coal-burning facilities generate nearly 50 million tons of fly ash annually [15]. Of this total, approximately 37 million tons are landfilled, while only 22%, or 13 million tons are reused. Applications in which fly ash is commonly used are substitute for portland cement in ready-mix concrete and structural fill. The greatest factor limiting the reuse of greater volumes of

fly ash is poor ash quality, primarily due to the presence of excessive *unburnt carbon*, which restricts usage of ash in ready-mix concrete, the largest market for fly ash in USA.

The research related to recycling of *wood ashes* back to the forest grounds are in its infancy. To summarize, there is a large amount of papers published that deal with the leaching properties of recycled wood ash. When considering techniques to manufacture products suitable for recycling, there is not that much published. The work in the area of wood ash recycling and related topics can be divided into several different categories, as for example:

Techniques for Wood Ash Agglomeration

In [38] several techniques used to agglomerate wood ashes are presented thoroughly. The advantages of using a *drum granulator* is presented in [30]. A number of experiments in Sweden to agglomerate wood ashes, on going or finished, are documented in [39]. Nordenberg presents a solution where a stirrer technique is adopted to transform the wood ash into granules. The solution requires four hours/day of labor work. The company RENOMA [43] granulates both lime, ashes and different sludges, either separately or combined. Their aim during 1999 was to handle one third of the total amount of wood ashes produced in Sweden.

Chemical Properties of Ashes

In [19], wood ashes from 10 heating plants and peat ashes from 3 plants were analysed to determine their contents of nutrients and heavy-metals and corresponding solubilities. In addition to pulverulent fly ashes, the investigation also included fly ashes hardened by adding water. Eriksson shows that the hardening gives decreases in pH and electrical conductivity suggesting that this process decreases the solubility of the fly ashes. Several aspects of ash chemistry are also discussed in the Ph.D. thesis by Steenari [48] .

Leaching Properties

The impact on the environment, leaching properties, how and where the stabilized wood ash should be recycled are presented in [18]. This reference also includes the opinion about wood ash recycling from the Swedish national environment protection board and the Swedish national board of forestry.

Measurement of Unburnt Carbon in Wood Ashes

Most of the methods today are developed for coal-fired boilers. Several off/on-line methods are available. The Loss-On-Ignition (LOI) test is the standard

off-line method for determination of carbon content in fly ash. However, in [7] it is shown that this conventional test method is not an accurate measure of unburnt carbon in fly ash. If there are significant quantities of slacked lime (portlandite) $Ca(OH)_2$ and carbonate (calcite) $CaCO_3$ in the fly ash, which, along with the particulate carbon lose weight under the high-temperature oxidation conditions of the LOI test, the weight loss from these minerals easily exceed that due to carbon resulting in gross errors in the LOI tests for fly ashes. The Federal Energy Technology Center (FETC), U.S. Department of Energy is every year organizing a conference on unburnt carbon in utility fly ash. Good publications from FETC on the topic of on-line Carbon In Fly Ash (CIFA) monitoring are [29], [57] and [53].

1.4 Problem Description

There are always some unburnt remains of carbon in the ash. This is so because the combustion is not always optimal due to varying quality of the biomass fuel, and due to different combustion loads. The amount of unburnt carbon influences the overall granule properties in a very definable way: if the amount of unburnt carbon is high, this will decelerate the self-hardening process for a granule with no binding agent [38], [60]. It should also be pointed out that the produced granules do not benefit from high carbon contents, since their fertilizing properties will then deteriorate. If there is a high carbon content present, the wood ash should be sorted out to be reburnt instead of being used for granule manufacture. If the wood ash is reburnt, the amount of unburnt carbon decreases and the ash can be used in the transformation process. Hence, there is a need for an accurate on-line measure of the wood ash carbon content.

It should be stressed that it is "fairly easy" to decrease the carbon content in the fly ash and thus improve the burner efficiency by increasing the oxygen ratio during combustion. On the other hand, the burner then produces high NO_X levels at elevated O_2. This is not permitted by the authorities and puts us into a dilemma. To optimize the combustion efficiency without elevated NO_X levels is an interesting control problem – however not within the scope of this thesis.

Mixing ash/dolomite/water in order to obtain granular material is one method to stabilize wood ashes. The main problem is predicting the quantity of water to be added, since the necessary amount varies with the wood ash quality. If the quantity of water exceeds the necessary amount one will obtain a mixture useless for granular material. Therefore, accurate water control is crucial. In [30], it is suggested that if a high content of unburnt carbon is present, the

mixture needs more water. This indicates that the process dynamics change due to the varying composition of the wood ash. If the dynamics are not time invariant, basic control theory may not be sufficient to cope with the problem. One suggested method to solve control problems with systems where the process dynamics change is to use *Adaptive Control*. The theory of Adaptive Control is well known and used in numerous of industrial applications today [63].

1.5 Outline and Contributions

This thesis addresses both the practitioner and the more theoretically inclined reader. Terms written in *italics* are generally index words found at the end of the thesis. Uncertain readers are advised to look up the meaning of common abbreviations, and general notational conventions for mathematical symbols and operands. The thesis is divided into six main sections, not counting the introduction in this chapter nor the concluding chapter.

Chapter 2 presents the suggested control structures and the selected control principles for each stage of the ash transformation process that are automated. Further, a short survey of the design procedure and implementation methods is given. The objective is to provide the reader without prior knowledge with an understanding of these methods.

On-line measurement of carbon in wood ash is the main issue in Chapter 3. Motivations for on-line monitoring are given and available methods are surveyed. The philosophy of a measuring device based on *impulse radar* is also described.

Chapter 4 presents the chemical properties and the empirical modeling of wood ash stabilization. As in Chapter 2, a survey of some topics in *system identification* is given for the reader unfamiliar with the topic. Further, the experimental setup and the results from the first and second stage experiments in the system identification procedure are presented. The chapter finishes with a summary and concluding remarks.

Control of the Wood Ash Stabilization (WAS) process using different control strategies to detect the critical amount of added water is discussed in Chapter 5. Three strategies are evaluated; a probing strategy, the Geometric Moving Average (GMA) test and the CUmulative SUM (CUSUM) test, all three adequate for successful implementation.

The process operations based on the pilot equipment developed by Graninge - Kalmar Energi in cooperation with Kalmar University College are presented in Chapter 6. The general philosophy applied during the development and implementation of the control program for the ash transformation process is discussed in Chapter 7. Finally, in Chapter 8 the main topics and contributions of the thesis are summarized and some topics for future research and development are outlined.

The main contributions of this work may be summarized as follows:

- A robust machine is developed and controlled by an industrial control system in order to enable automated manufacture of fertilizing granules from burnt wood ash.
- Different approaches for on-line Carbon In Fly Ash (CIFA) monitoring are surveyed and a measuring device based on *impulse radar* is presented.
- A new method is developed and implemented in order to predict the necessary amount of added water in the WAS process.

1.6 Academic Work

The main parts of the material presented in this thesis have been published earlier. Below are all the publications by the author listed.

Conference Papers

The ash transformation concept presented in this thesis was filed together in

- T. Svantesson, A. Lauber and G. Olsson. Automated Manufacture of Granules from Burnt Wood Ash. *V National Science-Technical Conference. Macro Levelling and Reclamation of Areas with use of By-Products Combustion*, Svinoujscie, Poland, October 14-17, 1998.

The empirical model of the WAS process presented in Chapter 4 was described in

- T. Svantesson, A. Lauber and G. Olsson: Viscosity Model Uncertainties in an Ash Stabilization Batch Mixing Process. *IEEE Instrumentation and Measurement Technology Conference,* Baltimore Maryland, USA, May 1-4, 2000.

Short versions of Chapter 5 appears in

- T. Svantesson and G. Olsson: Detection of Abrupt Parameter Changes in an Ash Stabilization Batch Mixing Process. *Swedish National Conference on Automatic Control, Reglermöte 2000*, Uppsala, Sweden, June 7-8, 2000.
- T. Svantesson and G. Olsson: Optimal Adaptive Control of an Ash Stabilization Batch Mixing Process using Change Detection. *IEEE International Conference on Control Applications*, Anchorage, Alaska, USA, September 25-27, 2000.

Other conference papers not included in the thesis.

- A. Hultgren, W. Kulesza, M. Lenells, T. Svantesson and A. Lauber: Virtual Real Time Measurement System with a Switched Kalman Filter. *IEEE Work Shop on Emergent Technologies & Virtual System for Instrumentation and Measurement.* Niagara Falls, Ontario, Canada, May, 1997.

Journals and Magazines

A popular science presentation of the project appears in

- T. Svantesson, S. Holmberg and T. Claesson: Granulerad aska ger näring till skogsbruket. (In Swedish) *Recycling Scandinavia* 1: 50-51, 1999.

Miscellaneous

- Patent-application of an impulse radar system for on-line CIFA monitoring.

Some of the material presented in Chapter 5 has been used in

- F. Gustafsson. *Adaptive filtering and change detection*, John Wiley & Sons, Ltd, 2000.

Chapter 2

Control Structures and Algorithms

2.1 Introduction

Several control structures and algorithms have to be applied to make the ash transformation process automatic. In all implementations, a computer is used to control the process. Practically all control systems that are implemented today are based on computers. Such systems can be viewed as approximations of *analog-control systems*, but this is a poor approach because the full potential of computer control is not used. At best the results are only as good as those obtained with analog control. It is much better to use *computer-control systems*, which base the control directly on discrete-time models, so that the full potential of computer control can be used. A more thorough discussion of this topic is to be found in [64].

2.2 Design: An Overview

Real control problems, like the ash transformation process, are often large and poorly defined, while control theory deals with well-defined problems. According to the dictionary, *structuring* can mean to construct a systematic framework for something. In this context, however, structuring is used to describe the gap between the real problems and the problems that control theory can handle.

The problem of structuring occurs in many disciplines. Formal approaches have also been developed. The terminology used here is borrowed from the

fields of computer science, where structuring of large programs has been subject of much work. There are two major approaches, top-down and bottom-up.

The *top-down* approach starts with the problem definition − the ash transformation process. The problem is then divided into successively smaller pieces, adding more and more details. The procedure stops when all pieces correspond to well-known problems. It is a characteristic of the top-down approach that many details are left out in the beginning. More and more details are added as the problem is subdivided.

The *bottom-up* approach starts with the small piece, which represents known solutions for subproblems. These are then combined into larger and larger pieces, until a solution to the large problem is obtained.

Top-Down Approach

The top-down approach involves the selection of control principles, choice of control variables and measured variables.

Control Principles

A control principle gives a broad indication of how a process should be controlled. The control principle thus tells how a process should respond to disturbances and command signals. The establishment of a control principle is the starting point for a top-down design. Several examples of control principles can be found in [64].

Choice of Control Variables

After the control principle has been chosen, the next logical step is to choose the control variables. The choice of control variables can often be limited for various practical reasons. Because the selection of control principle tells what physical variables should be controlled, it is natural to choose control variables that have a close relation to the variables given by the control principle. Because mathematical models are needed for the selection of control principles, these models also can be used for controllability studies when choosing control variables.

Choice of Measured Variables

When the control principle is chosen, the primary choice of measured variables is also given. If the variables used to express the control principle cannot

be measured, it is natural to choose measured variables that are closely related to these control variables. Typical examples found in chemical-process control, where temperatures - which are easy to measure - are used instead of compositions, which are difficult to measure.

Bottom-Up Approach

In a bottom-up approach to control system design, the choice of control variables and measurements comes first. Control-loops are then designed for the individual process operations of the system − the ash transformation process. At each iteration, different control designs are introduced in the local loops until a system, with the desired properties, is obtained. The controllers used to build up the system are the standard types based on the ideas of *feedback*, *feedforward, prediction* and *estimation, optimization* and *adaptation.*

2.3 Implementation Methods

Computer-Control

A computer controlled system can be described schematically as in Figure 2.1. The output from the process $y(t)$ is usually a continuous-time signal. The output is converted into digital form by the Analog-to-Digital (A-D) converter. The A-D converter can be included in the computer or regarded as a separate unit, according to one's preference. The conversion is made at the sampling times, t_k. The computer interprets the converted signal, $\{y(t_k)\}$ as a sequence of numbers, processes the measurements using an algorithm, and produces another sequence of "decision" or "control-variables", $\{u(t_k)\}$. This sequence is converted to an analog signal by a Digital-to-Analog (D-A) converter. The events are synchronized by the real-time clock in the computer. The digital computer operates sequentially in time and each operation takes a certain amount of time. The D-A converter must, however, produce a continuous-time signal. This is normally done by keeping the control signal constant between the conversions. In this case the systems runs open loop in the time interval between the sampling instants, because the control signal is constant irrespective of the values of the output. However, if the time interval between the sampling instants is short compared to the process dynamics, this will not deteriorate the performance of the control system.

The computer-controlled system contains both continuous-time signals and *sampled* or *discrete-time* signals. The mixture of different types of signals sometimes causes difficulties. In most cases it is, however, sufficient to de-

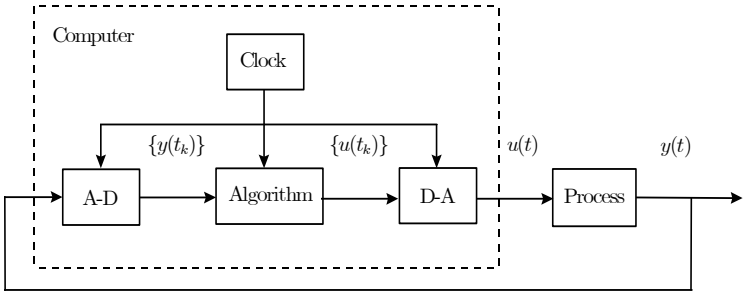

Figure 2.1: Schematic diagram of a computer controlled system.

scribe the behavior of the system at the sampling instants. The signal are then at interest only at discrete times. Such a system is called *discrete-time systems.* Discrete-time systems deal with sequences of numbers, so a natural way to represent these systems is to use *difference equations.*

Logic, Sequencing and Control

Industrial automation systems have traditionally had two components, controller and relay logic. Relays were used to sequence operations such as start-up and shutdown and they were also used to ensure safety of the operations by providing interlocks. Relays and controllers were handled by different categories of personnel at the plant. Instrument engineers were responsible of the controllers and the electricians were responsible for the relay systems. The so called Programmable Logic Controller (PLC) emerged in the beginning of the 1970s as replacements for relays. They could be programmed by electricians and in familiar notations, that is, as rungs of relay contact logic or as logic (AND/OR) statements. However, the PLC now include regularity control and data-handling capabilities as well, a development that has broadened the range of applications for it.

2.4 Control Methods

The *bottom-up* approach is used as design method for the ash transformation process. This section presents different control techniques and algorithms used for control of each stage (see Figure 1.2, Chapter 1) that is automated in the transformation process. As regarding the mixture quality control, we will emphasize the control algorithm based on Generalized Predictive Control (GPC).

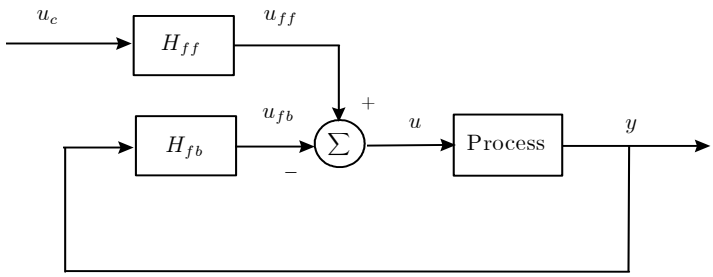

Figure 2.2: Block diagram of the two-degree-of-freedom controller used for control of the Wood Ash Stabilization (WAS) process.

The intended Carbon In Fly Ash (CIFA) analyzer provides the amount of unburnt carbon present in the wood ash. When this information is obtained, a controller should determine if the ash is to be used in the transformation process, or to be recycled for possible recombustion. This controller is programmed with AND/OR statements and affects the ash transformation process with discrete on/off control actions. See Figure 2.4 for a block diagram of a similar controller.

Mixture Quality Control

The schematic diagram of one of the proposed controllers for the mixture quality control problem is shown in Figure 2.2. This is a two-degree-of-freedom controller and its configuration has the advantage that the servo and regulation problems are separated. The feedback controller H_{fb} is designed to obtain a closed-loop system that is insensitive to process disturbances, measurement noise and model uncertainties. The feedforward compensator H_{ff} is then designed to obtain the desired servo properties. The single measurement y is the *normalized effective power* $P_e(t)$, which represents the rate of useful work being performed by the three-phase asynchronous machine used as stirrer drive. Hence, this measurement also represents the mixture viscosity. The setpoint u_c is therefore the desired effective power. The control input u is the variable flow of water $Q(t)$ added to the mixture of ash and dolomite. The controller is based on Generalized Predictive Control (GPC) [10], [6], [9], [63]. In [9] it is shown that a GPC is equivalent to a structure based on an optimal predictor plus a classical two-degree-of-freedom controller. In fact, for the unconstrained case, the closed loop system can be posed in the classical pole-placement controller [64]

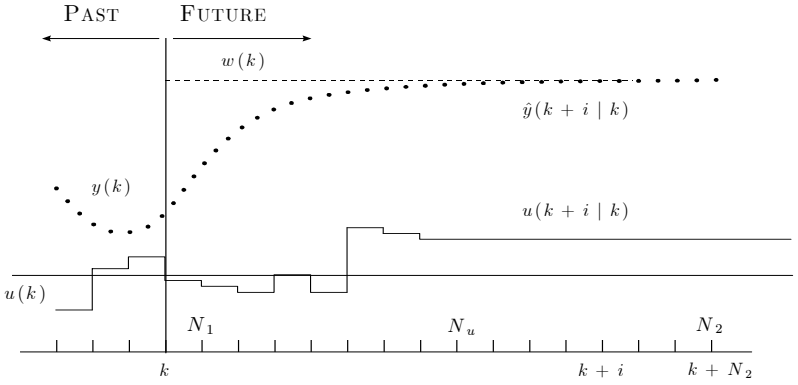

Figure 2.3: The strategy of MPC (Model Predictive Control).

$$R(q^{-1})\Delta u(k) = T(q^{-1})w(k) - S(q^{-1})y(k) \tag{2.1}$$

where R, S and T are polynomials in the *backward shift operator*. This control law can be considered as composed of a feedforward term (T/R) and feedback term (S/R), c.f. Figure 2.2. The control law (2.1) can also be interpreted as

$$\begin{aligned} \Delta u(k) \quad = \quad & -r_1\Delta u(k-1) - \cdots - r_{nr}\Delta u(k-nr) + t_0 w(k) + \\ & \cdots + t_{nt}w(k-nt) - s_0 y(k) - \cdots - s_{ns}y(k-ns) \end{aligned} \tag{2.2}$$

As seen in (2.2), the control signal $u(k) = u(k-1) + \Delta u(k)$ is based upon old control increments Δu, the used *reference trajectory* w and old measurements y. For example, in [64], it is shown that an incremental Proportional Integral Derivative (PID) controller is a special case of the general form (2.2).

The methodology of all the controllers belonging to the Model Predictive Control (MPC) family is characterized by the following strategy, represented in Figure 2.3.

1. The future outputs for a determined horizon N, called the *prediction horizon*, are predicted at each instant k using the process model. These predicted outputs $\hat{y}(k+i \mid k)$ for $i = N_1, \ldots, N_2$ depends on the known values up to instant k (past inputs and outputs) and on the future control signals $u(k+i \mid k)$, which are those to be sent to the system and to be calculated.

2. The set of future control signals is calculated by optimizing a determined criterion in order to keep the process as close as possible to the

reference trajectory $w(k)$ (which can be the setpoint itself or a close approximation of it). This criterion usually takes the form of a quadratic function of the errors between the predicted output signal and the predicted reference trajectory. The control effort is included in the objective function in most cases. An explicit solution can be obtained if the criterion is quadratic, the model is linear and there are no constraints. Otherwise, an iterative optimization method has to be used. Some assumptions about the structure of the future control law are also made in some cases, such as that it will be constant from a given instant.

3. The control signal $u(k \mid k)$ is sent to the process whilst the next control signals calculated are rejected, because at the next sampling instant, $y(k+1)$ is already known and step 1 is repeated with this new value and all the sequences are brought up to date. Thus $u(k+1 \mid k+1)$ is calculated (which in principle will be different to $u(k+1 \mid k)$ because of the new information available) using the *receding horizon control concept*.

Notice that the MPC strategy is very similar to the control strategy used in driving a car. The driver knows the desired reference trajectory for a finite *control horizon*, and by taking into account the car characteristics (mental model of the car) decides which control actions (accelerator, brakes and steering) to take in order to follow the desired trajectory. Only the first control actions are taken at each instant, and the procedure is again repeated for the next control decisions in a receding horizon fashion. Notice that when using classical control schemes, such as PID controllers, the control actions are essentially taken based on past errors. If the car driving analogy is extended, the PID way of driving a car would be equivalent to driving the car just using the mirror. This analogy is *not totally fair* with PID, because more information, (the reference trajectory) is used by MPC, and the PID controller includes a simple prediction provided by the derivative part. Notice that if a future point in the desired reference trajectory is used as setpoint for the PID, the differences between both control strategies would not seem so abysmal.

Earlier results [30] have shown that if there is a substantial amount of carbon present in the wood ash, the mixture needs more water to start the agglomeration process. This indicates that the process dynamics changes due to the varying quality of the wood ash. If the dynamics are not time invariant, traditional control theory may not be sufficient to cope with the problem. One suggested method to solve control problems with systems where the process dynamics change is to use *Adaptive Control.* The theory of Adaptive Control

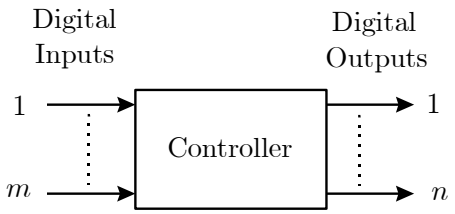

Figure 2.4: Block diagram of the size reduction controller.

is well known and used in numerous of industrial applications today [63].

The control objective is to regulate the normalized effective power $P_e(t)-$ an estimate of the mixture viscosity $-$ to the level P_e^{crit}, which represents a critical mixture viscosity. If more water is added to the ash stabilization process after P_e^{crit} has been reached, one will obtain a mixture useless for granular material [39], [49]. To cope with this problem, it is crucial to detect the level P_e^{crit}.

Size Reduction

This control problem essentially requires discrete control actions. The general schematic diagram of the controller for the size reduction is shown in Figure 2.4. However, the level in the feeder is continuously measured. This information is used to decide whether the feeder is full, partially filled or empty. The controller is programmed with AND/OR statements and affects the feeder with discrete on/off control actions. The output vector ($\mathbb{R}^{n\times 1}$) start/stops the feeder, controls the feeder direction etc.. Furthermore, the input vector ($\mathbb{R}^{m\times 1}$) monitors for example the overflow at the feeder inlet based on the information obtained from the continuous level measurement.

Granulation, Hardening, Sorting and Packing

The stages of granulation and hardening are only controlled to a certain extent. With control we here mean that the inputs to the actuators of the drum granulator and hardening furnace (see Chapter 6) have static values, which correspond to a desired system response (granule mean diameter and granule moisture content). Of course, this is not an adequate implementation if a uniform product quality is desired. For example, in the hardening process, the dynamics will change with the speed of the material through the dryer and the moisture content of the incoming material. On the other hand, this

implementation serves as a good initial solution. The sorting and packing is not yet automated and is thus handled manually.

2.5 Summary and Concluding Remarks

In this chapter, different control structures and control algorithms were outlined for the stages that are automated in the ash transformation process. In the remaining chapters, more detailed information are available. If the process dynamics of the WAS process are time-varying, it is favorable to adopt *adaptive* techniques. It is also crucial that the correct amount of water is added to the stabilization process in order to obtain a suitable mixture for granulation. The mixing procedure is performed batchwise which simplifies the control problem. Furthermore, the stages of granulation and hardening are only controlled to a certain extent − the inputs to the actuators of the drum granulator and hardening furnace have static values that correspond to a desired system response. It is also stated that the packing, today, is handled manually.

Chapter 3

Carbon Content Analysis - A Survey

3.1 Introduction

There are always some unburnt remains of carbon in the ash. This is so because the combustion is not always optimal. The lack of optimality is due to several reasons. Firstly, in the wintertime much energy must be produced to satisfy the needs of customers. As a result, there is an extraordinary high burner load during this period, which implies high carbon contents. At high burner loads, there are even situations when the wood ash is still glowing at the arrival of the recovery chute. However, this is very rare. Secondly, the quality of the biomass fuel may change several times a day. This will cause high carbon contents as long as the combustion parameters are not adapted to the new fuel.

The traditional methods to determine the carbon content of wood ashes have been mostly inaccurate and time consuming. This chapter presents a survey of the problems and available methods for off-line and on-line Carbon In Fly Ash (CIFA) monitoring. Good publications from The Federal Energy Technology Center on the topic of on-line CIFA monitoring are [29], [57] and [53]. For a survey of the economics motivations, see [42]. Another method presented in the academia for on-line monitoring are based on *photoacoustic detection*, which also has the potential for automatic, on-line monitoring [16]. A technique based on electrostatic separation for the removal of carbon in wood ash is presented in [1]. This method is interesting, but cannot be classified as an on-line measuring method for Carbon In Fly Ash.

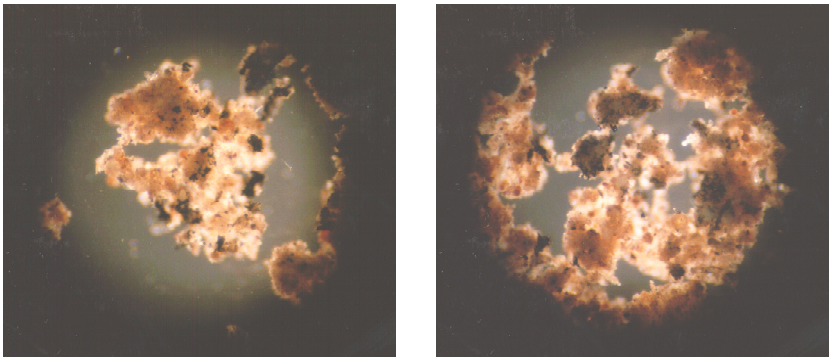

Figure 3.1: Two microscope photographs that show the carbon particles in a wood ash sample.

Problems in Determining the Carbon Content

In Figure 3.1 two microscope photographs show a close-up of a wood ash sample. As seen in the pictures dark areas are spotted in the wood ash. These dark areas are clusters of carbon particles. As a result of this observation it is natural to ask if there is a simple correlation between the wood ash carbon content and the color of the ash sample. If this is the case, the rash reader may claim that this problem is simple to solve, and states the following proposition: an ash sample that is properly burnt is *white*, otherwise the color of the sample should change according to the gray-scale and turn *darker* if the ash is not properly burnt. If this is so, the problem would be easy to solve with *Machine Vision*[1].

The more prudent reader (including the author of this thesis) would be a little more cautious. For example, consider the information given in Table 3.1. The table shows that the carbon content of the different samples analysed at Kalmar University College are of the same magnitude as the results obtained at Analys Centrum, which validate the results obtained at KUC. Both utilized the method of LOI − an off-line procedure where a sample is taken to be dried and reburnt; the weight loss of the sample, after it is reburnt (preceded by drying), is then proportional to the amount of unburnt carbon. When inspecting the samples it is concluded that they all have approximately the same color on the gray scale. In spite of this, as shown in the table, there is an *evident* difference between the carbon contents of the samples. The results in Table 3.1 should however be interpreted with caution. As mentioned earlier,

[1] Machine Vision is a form of artificial intelligence in which video images are converted into formats which are recognized by computers.

Carbon Content Analysis					
Nr	wl [%] KUC	wl [%] AC	**Nr**	wl [%] KUC	wl % AC
1	11.5	11.7	**6**	15.5	15.2
2	11.5	10.9	**7**	16	14.7
3	18	14.1	**8**	20.5	16.8
4	17	16.7	**9**	26	24.8
5	49	51.5	**10**	48	47.8

Table 3.1: The weight loss (wl) in percent of each ash sample provided from Graninge - Kalmar Energi. This series of ash samples was sent to Analys Center (AC) for validation, shown in the table for comparision.

if there are significant quantities of slacked lime (portlandite) $Ca(OH)_2$ and carbonate (calcite) $CaCO_3$ in the fly ash, this may cause problems since these substances, along with the particulate carbon lose weight under the high-temperature oxidation conditions of the LOI test. Then the weight loss from these minerals easily exceed that due to carbon, resulting in gross errors in the LOI tests for fly ashes [7]. Therefore, a second, more advanced analysis is carried through. Three different samples of wood ash with different qualities and colors are investigated. The more advanced analysis determines the amount of $CaCO_3$ and subtracts this from the weight lost under the high-temperature oxidation in order to obtain the *true* weight loss due to the carbon [19]. The results are shown in Table 3.2.

Carbon Content Analysis				
All measures are weight - %	**Sample 1**	**Sample 2**	**Sample 3**	Inst.
Total Carbon Content	59.6	35.4	8.5	**SP**
$CaCO_3$	0.63	0.86	2.0	**SP**
Unburnt Carbon	59.0	34.5	6.5	**SP**
Unburnt Carbon (wl)	61.4	35	3.5	**KUC**

Table 3.2: The more advanced method used at the Swedish National Testing and Research Institute (SP) in comparision with the results from the LOI test used at Kalmar University College (KUC).

The conclusion drawn from the results shown in Table 3.2 is that for the three ash samples used in the test, there is no difference between the two compared methods. However, this proves *nothing* for the samples presented in Table 3.1, and it cannot be excluded that the portlandite and calcite are the reason for these "strange" results. To continue the investigation, a photograph of the three samples is shown in Figure 3.2. Here a digital camera is used to

Figure 3.2: A photograph of the three samples presented in Table 3.2. The leftmost sample is **Sample 1**.

visualize the working conditions for any system based on machine vision. It is clear that there is a difference between the three samples. However, it is not easy to detect by visual means that the difference between the worst and best ash sample is as great as 53% of unburnt carbon. It should also be stressed that experimental results show that the color of the ash varies with different fuels (an unknown parameter) used at combustion. For example, the ash can sometimes be brown. Referring to Figure 3.1, a heuristic explanation to this observation may be that the color of the residue material (when the carbon particles are excluded) is varying as a result of the fuel composition. Hence, the presence of $Ca(OH)_2$ and $CaCO_3$ does not affect the color since they are not visible to the eye. These facts imply that a measuring method based on machine vision would be poor and that the theory of the rash reader will fail. Therefore, more precise methods are needed.

Motivation

Earlier work [38] shows that one could obtain problems to self-harden the wood ash if there is a substantial amount of unburnt carbon present. After the ash is stabilized with water, the presence of organic material (unburnt carbon) disturbs the hardening process. The method of self-hardening is not used in the ash transformation process presented in this thesis. Instead, a hardening furnace is used to obtain a hard surface of the produced granules. Further, the ETEC-dolomite act as a binding agent, which improves the strength of the produced granules.

In order to succeed with the ash transformation process, it is crucial that the correct amount of water is added to the mixture of ash/dolomite to obtain a material suitable for granulation [39], [49]. The problem is that this amount varies with the wood ash quality. If there is a correlation between the necessary amount of added water and the wood ash carbon content, one

solution would be to measure this parameter on-line and use this information to determine the optimum recipe of ash/dolomite/water. Furthermore, if the dynamics of the process are time-varying due to the varying wood ash qualities, the measurement of the wood ash carbon content could be used to gain-schedule the used controller. The problem with this approach is that an on-line measurement of the wood ash carbon content would be required.

A third motivation for on-line analysis is that if the wood ash contains a substantial amount of unburnt carbon ($> 50\%$), the fertilizing properties of the produced granules will deteriorate.

Today, at Graninge - Kalmar Energi, it is only possible to determine the CIFA (with any accuracy) by using the method of Loss-On-Ignition (LOI) [52]. This procedure takes about four hours and requires labor work. To avoid this procedure, an on-line measuring device would be convenient.

3.2 Different Approaches of On-line Analysis

Two types of on-line measurements exists for the assessment of unburnt carbon in wood ashes: *direct* and *indirect:*

- *Direct* methodologies use a laboratory-like procedure to weigh the collected ash and oxidize the sample. Determining the amount of unburnt carbon in the collected ash sample requires two quantities: the mass of the collected sample, and the amount of CO_2 released during oxidation. Direct carbon-in-ash measurements offer a high level of accuracy but has a quite long processing time, up to 15 minutes.

- *Indirect* methods include the attenuation of a light beam or microwaves, as well as measurements of ash capacitance. They can be capable of generating a high data rate, but with less accuracy than monitors employing a direct measurement method. This method is undoubtedly the most rapid on-line method.

Two *indirect* methods are considered for the task of CIFA analysis. The *Near InfraRed (NIR)* approach and the *impulse radar* approach. The latter is a new method for on-line monitoring of carbon in wood ash. During 1998, the author and *Malå GeoScience AB* applied for a patent of this novel measuring approach. Unfortunately, the patent was rejected. As a result, a prototype of the measuring device was not developed. Nevertheless, in section 3.2, the philosophy of the measuring device is presented.

Figure 3.3: An on-line NIR instrument for process control.

The NIR approach

On-line infrared measurement is usually performed with IR wavelengths between 1.0 and $2,5\mu m$. The measurement technique is based on the fact that various molecular groups can selectively absorb NIR light [4]. A typical on-line NIR sensor for process control is shown in Figure 3.3. The on-line sensor must be capable of detecting small changes in absorption and in this case of accurately relating these to the carbon content. Since NIR absorption is primarily concerned with absorptions by -OH, -CH, and -NH groups, most organic materials can be analyzed using absorption at different wavelengths. Absorption of NIR light in transmission and reflectance follows an exponential law (Beer-Lambert) and to a first approximation the following equation can be used for reflectance measurement:

$$\log \frac{I_i}{I_r} = Kc \tag{3.1}$$

where I_i is the intensity of the incident light, I_r the intensity of the reflected light, K is the absorption coefficient and c is the concentration of the measured parameter.

It is clear that by measuring the log ratio of incident and reflected intensities at the relevant absorption bands a signal proportional to concentration

would be obtained. In on-line analysis it is not possible to measure the incident light intensity and therefore at least one reference wavelength outside the region of absorption is used to approximate this. The reflected intensity at this wavelength is then *rationed* against that of the absorption, thus providing a measure of the amount of absorption irrespective of the level of illumination. A further important practical point in taking a ratio of the reference and measure signals is that factors other than concentration variations of the component under analysis affect both signals equally, and therefore cancel out in the calculation. Important examples of such factors in an industrial measurement are instrument-to-object distance, dust build-up on optical surfaces and atmospheric humidity variations, all of which cannot be controlled in most on-line applications. This simple two wavelength model helps to clearly describe the operation of an on-line instrument. In practice additional wavelengths are normally necessary but the principles of operation are similar. But one question remains: is it possible to separate the carbon from other substances in the wood ash when looking at the absorption?

The Impulse Radar approach

Conventional radar sends out short bursts of single-frequency (narrow band) electromagnetic energy in the microwave frequency range. Other radars step through multiple (wide-band) frequencies to obtain more information. An impulse, or a Ultra-Wide Band (UWB) radar sends *individual pulses* that contain energy over a very wide band of frequencies. The shorter the pulse, the wider the band, thereby generating even greater information. Because the pulse is so short, very little power is needed to generate the signal. An UWB radar is one having a very large bandwidth [55],

$$0 \leq \frac{\Delta f}{f_c} \leq 1 \tag{3.2}$$

where Δf is the *absolute bandwidth* and f_c is the *carrier (or center) frequency.* An UWB radar is characterized $0.25 < \Delta f / f_c \leq 1$.

The number of applications for Ground Penetrating Radar (GPR) is quite large [58]. It is mainly used for geological surveying, detecting of pipes and other buried objects [8]. The on-line CIFA analyzer utilizes the principle that the unburnt carbon found in fly ash affects the transmitted signal more than the ash itself. How an electromagnetic wave travels through a media is mainly determined by two properties; the *relative permittivity* ϵ_r (or dielectric constant) and the *conductivity* σ. The dielectrical properties determine the velocity of the electromagnetic wave through the media. The conductivity of the media determines how much of the input energy that is absorbed. Both these parameters are frequency dependent.

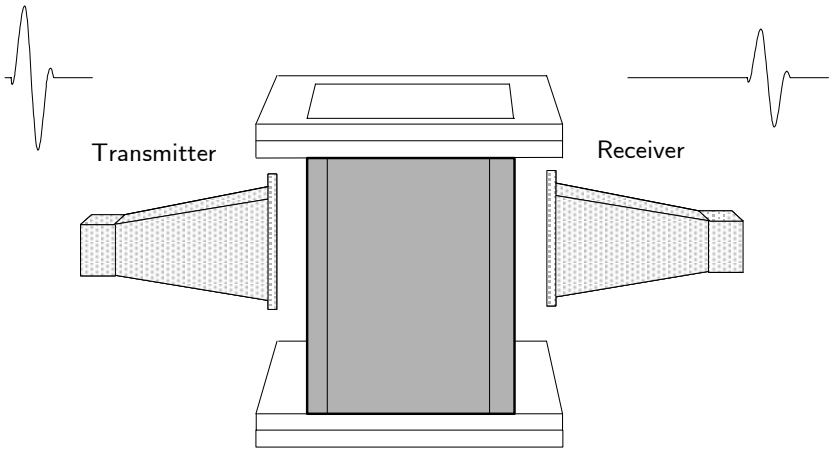

Figure 3.4: The impulse radar system for *indirect* on-line CIFA monitoring.

The objective is to utilize the impulse radar system to measure the *relative permittivity* ϵ_r (or dielectric constant) and the *conductivity* σ of an ash sample. The measuring device is depicted in Figure 3.4. The measuring system is installed on the recovery chute of the precipitator where the fly ash is removed. An impulse is sent from the transmitting horn-antenna through the ash sample and is received by another horn-antenna at the opposite side. The transmitted impulses have a very short duration of $1 - 10$ ns and a bandwidth of $100 - 800$ MHz.

Equipment for direct sampling at sampling frequencies necessary for this application is still expensive today, and most samplers rely on *repetitive sampling.* The impulse is transmitted several times and from each pulse one or several samples are taken. The trigger point for the sampler is delayed from pulse to pulse, such that after a number of pulses the whole waveform is sampled. The principle is shown in Figure 3.5, where 4 pulses are sampled with a sampling frequency of a fourth of the desired sampling frequency. The recorded measurement is then sent to a computer for further processing.

During one measuring cycle, the delay and attenuation of the received pulse are measured. The delay provides information about the *relative permittivity* ϵ_r of the ash sample, whereas the attenuation of the received pulse provides information about the *conductivity* σ. The ash sample collector is made of a non conducting material. In order to obtain a representative measurement it is important that the bulk density of the ash sample in the rectangular chute

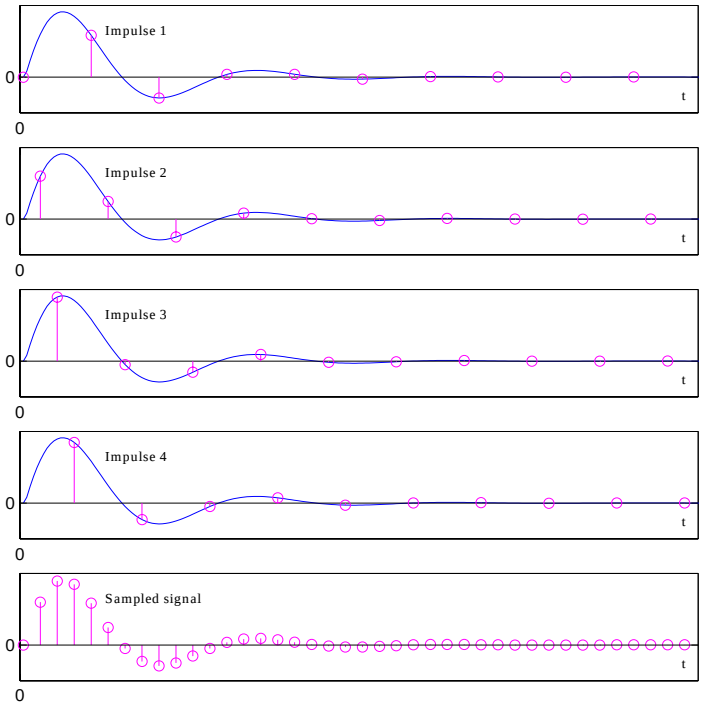

Figure 3.5: The principle of repetitive sampling.

is the same for each analysis. Finally, the parameters ϵ_r and σ are used to obtain the carbon content of the wood ash sample.

3.3 Summary and Concluding Remarks

There are always some unburnt remains of carbon in the ash. This is so because the combustion is not always optimal due to varying operating conditions. In this chapter two potential methods for on-line CIFA monitoring are presented. However, one disadvantage with the method of NIR spectroscopy is that only the top layer of the sample is analysed, i.e., this layer must be representative for the whole ash sample. A good reference on instru-

mentation and calibration for NIR spectroscopy is [41]. This reference also lists manufacturers of both laboratory and on-line equipment for NIR spectroscopy. Unfortunately, the absence of experimental results from a research colleague (not mentioned in the acknowledgments) make the evaluation of the method impossible.

It is concluded that the presence of $Ca(OH)_2$ and $CaCO_3$ does not affect the color of the wood ash, since these are not visible to the eye. On the other hand, this may result in gross errors in the LOI tests for fly ashes [7]. It is also concluded that experimental results show that the color of the wood ash varies with different fuels used at combustion. This implies that a measuring method based on machine vision would be poor.

The prices of the today available CIFA analyzers based on microwave methods, for example, the device presented in [17], are too expensive for the application of wood ash transformation. Also a direct methodology based on oxidation of the ash sample is expensive (≈ 1.5 MSEK). Therefore, at present, no on-line measuring device is installed. Instead, all wood ash is transformed into granules, i.e., no ash is sorted out to be reburnt. Furthermore, it is concluded that it is quite possible for the ash carbon content to attain a level of 60% of unburnt carbon, c.f. Table 3.2. Therefore, an attempt to optimize the burner efficiency has been launched and is ongoing. A solution to the problem of predicting the necessary amount of water in the ash stabilization procedure is presented in Chapter 5.

Chapter 4

Ash Stabilization - Empirical Modeling

4.1 Introduction

Mixing ash/dolomite/water in order to obtain granular material is one method to stabilize wood ashes. The main problem is predicting the quantity of water to be added, since the necessary amount varies with the wood ash quality [39], [49], [60]. In [49], it is reported that the critical water-to-ash ratio varies between ash types and must therefore be determined for each ash. However, one possible solution is to measure the mixture viscosity and study whether this parameter can be used to control the amount of added water. In this thesis, a novel method is presented where the viscosity is continuously estimated in the batch mixing process. The viscosity is estimated by measuring the normalized effective power $P_e(t)$, which represents the rate of useful work being performed by the three-phase asynchronous machine used as stirrer drive. In this chapter, an empirical model of the viscosity dynamics is developed.

First, an introduction to the general problems are given, followed by a presentation of the chemical properties of wood ash stabilization. Next, a survey of some topics in *system identification* is available for the reader unfamiliar with the topic. Further, the experimental setup and the results from the first and second stage experiments are presented, and the chapter ends with a summary and concluding remarks. The reader is encouraged to go back to Figure 1.2 in Chapter 1, if a reminder is necessary of the different stages in the ash transformation process.

For the mixing of the ash, ETEC-dolomite and water, a `Fejmert S-500` mixer

is utilized, see Appendix B. The dolomite and ash are mixed in the first step. The ratio between the two dry matters are always the same. The next step is to add water to start the *wood ash stabilization*. By measuring the normalized effective power $P_e(t)$, a good estimate of the mixture viscosity is obtained. This measurement provides information how to control the variable water flow. When the mixture quality is satisfactory, the material passes an outlet that is positioned at the bottom of the mixer. The batch ends up in a feeder that gradually forces the material through a raster that reduces the size of the passing mixture (see Figure 1.2). The feeder is rotating, and it is possible to obtain two directions of rotation. This is to prevent all superstructures that will occur due to the sticky mixture. A *high-pressure cleaning procedure* is provided to prevent any superstructure within the mixer. During this procedure a dust preventing system (see Appendix B) is controlled so that an underpressure is introduced into the mixer. This will seal the mixer so that no water is leaking out. After the cleaning procedure is finished, the mixer is ready to mix a new batch.

The Structure of the Problem

Earlier experiments have shown [30] that if a high content of unburnt carbon is present in the wood ash, the wood ash stabilization needs more water in order to be successful. This indicates that the process dynamics change due to the varying quality of the ash. The system is assumed to be described by the following general state space differential equation:

$$\begin{aligned} \frac{d\mathbf{x}_t}{dt} &= \mathbf{A}_t\mathbf{x}_t + \mathbf{B}_t\mathbf{u}_{t-\tau} \\ \mathbf{y}_t &= \mathbf{C}_t\mathbf{x}_t + \mathbf{D}_t\mathbf{u}_{t-\tau} \end{aligned} \tag{4.1}$$

where $\mathbf{A}_t, \mathbf{B}_t, \mathbf{C}_t$ and $\mathbf{D}_t$ denote the time varying matrices of the linear system, and τ denote the time-delay of the system. If the process dynamics are not time invariant, traditional control theory is not always sufficient to cope with the problem. One suggested method to solve control problems with systems where the process dynamics change is to use *Adaptive Control* [63]. An adaptive controller, being inherently nonlinear, is more complicated than a fixed gain controller. Before attempting to use adaptive control it is therefore important to investigate whether the control problem might be solved by traditional control methods. In the literature on adaptive control there are many cases in which these control methods can do as well as an adaptive controller. One way to proceed in deciding whether adaptive control should be used is given by the following discussion: if the process dynamics are *constant*, this leads to that a controller with *constant parameters* is selected. If the process dynamics are *varying*, then a controller with *varying parameters*

should be used. If the variations are *predictable,* a *gain-scheduling* should be used. And finally if the variations are *unpredictable,* this leads to the selection of an *adaptive controller.*

From here, two approaches are possible: control of the wood ash stabilization with the wood ash carbon content *known* or *unknown.*

1. If there is a correlation between different viscosity models and the wood ash carbon content, one solution would be to use the measurement from a CIFA monitor to gain-schedule the implemented controller. The problem with this solution is that an on-line measurement of the wood ash carbon content is required.
2. If the measurement of the carbon content is not available, indirect adaptive control could be used to on-line estimate the viscosity model dynamics and optimally control the ash stabilization process.

With support from the concluding remarks in Chapter 3, the latter of these two presented options is selected.

Chemical Properties of Wood Ash Stabilization

When stabilizing wood ashes that are well burnt (less than 10% of unburnt carbon) the following two reactions are dominating [38]. *Slacked lime* is produced by treating *quicklime* with water:

$$CaO + H_2O \longrightarrow Ca(OH)_2 + heat\ production \tag{4.2}$$

The reaction is fast and *exothermic.* When slacked lime is formed the stabilization starts through *carbonization* with help from the carbon dioxide available in the air:

$$Ca(OH)_2 + CO_2 \longrightarrow CaCO_3 + H_2O \tag{4.3}$$

This reaction is fast initially but is decreasing after $3 - 7$ days. The most important transformation is that of $Ca(OH)_2$ to $CaCO_3$, since it reduces the solubility of calcium and the alkalinity of the ash. Thus, a pH shock in the forest soil is avoided. These two reactions are dominating even if dolomite is mixed with wood ash. However, the presence of organic material (unburnt carbon) disturbs the hardening process.

4.2 System Identification

The notion of a mathematical model is fundamental to science and engineering. A model is a very useful and compact way to summarize the knowledge

about a process. The process models can sometimes be obtained from first principles of physics. It is more difficult to get the model of the disturbances, which is equally important. These models often have to be obtained from experiments. The types of models that are most often used are *state-space models* (internal models) and *input-output models* (external models). The models for the disturbances are for the internal models given as a dynamic system driven by white noise. For the external models the disturbances are often given in terms of *spectral densities* and *covariance functions*. Models for disturbances can, however, only rarely be determined from the first principles. Thus, experiments are often the only way to get models for the disturbances.

A process cannot be characterized by *one* mathematical model. A process should be represented by a *hierarchy* of models ranging from detailed and complex simulation models to very simple models, which are easy to manipulate analytically. The simple models are used for exploratory purposes and to obtain the gross features of the system behavior. The complicated models are used for a detailed check of the performance of the control system. The complicated models take a long time to develop. Between the two extremes, there may be many different types of models.

There are no general methods that always can be used to get a complete mathematical model. Each process or problem has its own characteristics. Some general guidelines can be given, but under no circumstances can they replace experience. Model building using physical laws requires knowledge and insight about the process.

In most cases it is not possible to make a complete model only from physical knowledge. Some parameters must be determined from experiments. This approach is called *system identification*, and the following discussion is inspired by [64], [31], [54] and [27].

The System Identification Procedure

The identification process amount to repeatedly selecting a model structure, computing the best model in the structure, and evaluating the properties of this model to see if they are satisfactory. The cycle run as follows [31]:

1. Design an experiment and collect input, output data from the process to be identified.

2. Examine the data. Some pre-treatment may have to be applied. Use the first half of data for identification, and the second half for validation.

3. Select a model structure.
4. Compute the best model in the model structure according to the input, output and the given criterion of fit.
5. Examine the properties of the model obtained.
6. If the model is good enough then stop, otherwise go back to the third step and try another model set. Other estimation methods can also be performed (fourth step), further pre-treatment can be applied to the data (first and second step).

System identification is thus the experimental approach to process-modeling as indicated by Figure 4.1.

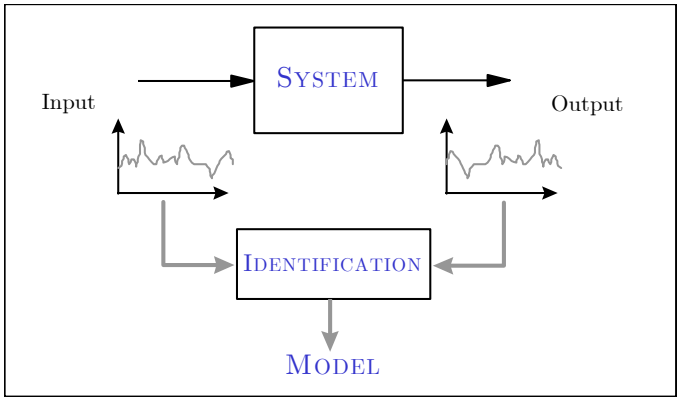

Figure 4.1: The approach of system identification for process-modeling.

The system identification procedure includes:

- *Experimental planning.*
- *Selection of model structure.*
- *Parameter estimation.*
- *Validation.*

When investigating a process where the *a priori* knowledge is poor, it is reasonable to start with transient or frequency-response analysis to get crude estimates of the dynamics and disturbances. The results can then be used to plan further experiments.

Experimental Planning

It is often difficult and costly to experiment with industrial processes. Therefore, it is desirable to have identification methods that do not require special input signals. Many "classic" methods depend strongly on having the input to be of a precise form, e.g., sinusoid or impulse. Other techniques can handle virtually any type of input signals at the expense of increased computations. One requirement of the input signal is that it should excite all process modes of interest sufficiently.

It is sometimes possible to base system identification on data obtained under closed-loop control of the process. This is very useful from the point of view of applications. For instance, adaptive controllers are based mostly on closed-loop identification. The main difficulty with data obtained from a process under feedback is that it may be impossible to determine the parameters in the desired model, i.e., the system is not identifiable, even if the parameters can be determined from a open-loop experiment. Identifiability can be recovered if the feedback is sufficiently complex. It helps to make the feedback nonlinear and time-varying, and to change the set points.

Model Structures

The *model structures* are derived from prior knowledge of the process and the disturbances. In some cases the only priori knowledge is that the process can be approximated by a linear system in a particular operating range. It is then natural to use general representations of linear systems. Such representation are called *black-box models*. An example of a generalized model structure is given in (4.4):

$$A(q)y(k) = \frac{B(q)}{F(q)}u(k) + \frac{C(q)}{D(q)}e(k) \tag{4.4}$$

where u is the input, y is the output, and e is a white noise disturbance and q is the *forward-shift operator.* The parameters, as well as the order of the models, are considered as unknown. Depending on which of the five polynomials A, B, C, D and F are used, different model-structures will arise. The AutoRegressive with eXternal input (ARX) model structure, which use the polynomials A and B in (4.4), is linear in the unknown parameters, but for example, in the AutoRegressive Moving Average with eXternal input (ARMAX) structure, which utilize the polynomials A, B and C in (4.4), the output can not be written as a linear regression.

Parameter Estimation Methods

Solving the parameter estimation problem requires:

- *Input-output data from the process.*
- *A class of models.*
- *A criterion.*

Parameter estimation can then be formulated as an optimization problem, where the best model is the one that best fits the data according to the given criterion. The results of the estimation problem depends, of course, on how the problem is formulated. For instance, the obtained model depends on the amplitude and frequency content of the input signal. There are many possibilities for combining experimental conditions, model classes and criteria. There are also many different ways to organize the computations. Consequently, there is a large number of different identification methods available. One broad distinction is between *on-line methods* and *off-line methods.* The on-line method gives estimations *recursively* when the measurements are obtained and is the only alternative if the identification is going to be used in an adaptive controller or if the process is time-varying. In many cases the off-line methods give estimates with higher precision and are more reliable, for instance in terms of convergence. This is due to the fact that an off-line formulation is a simpler problem to solve.

Criteria

When formulating an identification problem, a criterion is introduced to give a measure of how well a model fits the experimental data. The criteria can be postulated. By making statistical assumptions, it is also possible to derive criteria from probabilistic arguments. The criteria for discrete-time systems are often expressed as:

$$J(\boldsymbol{\theta}) = \sum_{k=1}^{N} g(\varepsilon(k)) \tag{4.5}$$

where $\boldsymbol{\theta}$ is a vector of unknown parameters, ε is the input error, the output error, or a *generalized error*. The prediction error is a typical example of a generalized error. The function g is frequently chosen to be quadratic, but it is possible for it to be of many other forms.

The first formulation, solution, and application of an identification problem where given by Gauss in his famous determination of the orbit of the asteroid Ceres [21]. Gauss formulated the identification problem as an *optimization*

problem and introduced the principle of least squares, a method based on the minimization of the sum of the squares of the error. Since then, the least-squares criterion has been used extensively. The *least-squares method* is simple and easy to understand. Under some circumstances it gives estimates with the wrong mean values (bias). However, this can be overcome by using various extensions. The least-square method is restricted to model structures where the output can be written as a *linear regression*. For a description of identification of other systems, good references are [31], [54] and [27].

When the disturbances of a process are described as a stochastic process, the identification problem can be formulated as a statistical parameter-estimation problem. It is then possible to use the *maximum-likelihood method*. This method has many attractive statistical properties. It can be interpreted as a least-square criterion if the quantity to be minimized is taken as the sum of squares of the prediction error. The maximum-likelihood method is a general technique that can be applied to a wide variety of model structures.

Model Validation

When a model has been obtained from experimental data, it is necessary to check the model in order to reveal its inadequacies. For *model validation*, it is useful to determine such factors as step responses, impulse responses, poles and zeros, model errors, and prediction errors. It is also a good approach to use another set of experimental data to validate the model. If the model does not pass the validation test, it must be revised i.e., we loop in the system identification procedure until a proper model is obtained. Since the purpose of the model validation is to scrutinize the model with respect to inadequacies, it is useful to look for quantities that are sensitive to model changes.

4.3 Experimental Setup

Measurement System

The mixture viscosity is estimated in the batch mixing process by measuring the normalized effective power $P_e(t)$, which represents the rate of useful work being performed by the three-phase asynchronous machine used as stirrer drive. The measurement system is depicted in Figure 4.2. One of three phases to the motor is connected to the primary side of a 100:5 current transformer. The secondary side of the transformer is connected to a power transducer (load measurement – EL-FI G3 power meter [35]) that electronically measures the input power to the asynchronous machine and compensates for

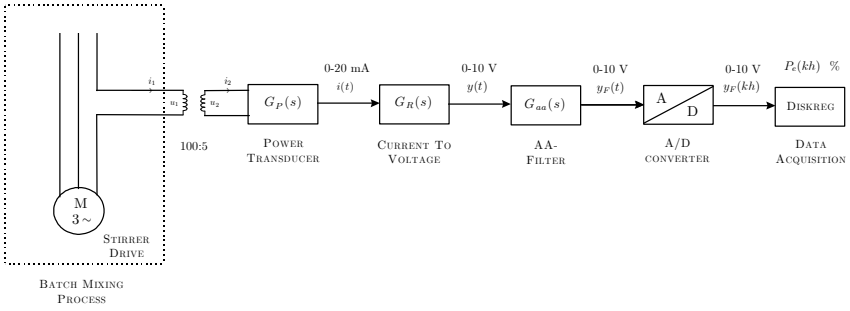

Figure 4.2: The setup used for measurement.

the internal losses in the induction motor. Thus, the transducer compensates for variations in the mains voltage and always estimates the actual power applied on the motor shaft. The electrical output from the transducer is a direct current $0 - 20\ mA$ and the dynamics $G_P(s)$ is given by the transfer function

$$G_P(s) = \frac{K}{1 + sT} \tag{4.6}$$

where K and T are user-adjustable parameters. The current from the power transducer is converted into a voltage of $0 - 10\ V$ with $G_R(s) = R = 500\ \Omega$. The anti-aliasing filter is a third order Butterworth-filter with a cut-off frequency of $3\ Hz$

$$G_{aa}(s) = \frac{1}{(\beta s + 1)\left(\beta^2 s^2 + \beta s + 1\right)} \tag{4.7}$$

where $\beta = (6\pi)^{-1}$. The sample time $h = 0.1\ s$ is used. The filtered signal $y_F(t)$ is A/D-converted and stored in `DISKREG`, a software package developed at the Department of Technology for real-time data acquisition and control. The power transducer is calibrated so that a voltage of $10\ V$ corresponds to full load, i.e. in `DISKREG` the range $0 - 10\ V$ is interpreted as $0 - 100\%$ of the maximum effective power $P_e(t)$.

Actuator

The water added during the ash stabilization procedure is the input to the WAS process. It is crucial that the water is distributed over a wide area, yielding a homogenous mixture [51]. To achieve this, spray nozzles and an

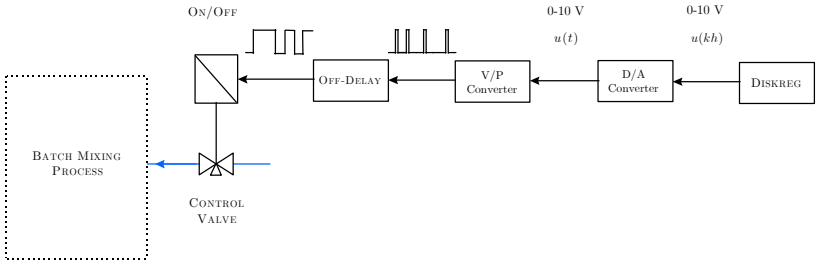

Figure 4.3: The setup used to generate the identification signal.

on/off control valve are adopted. The setup is depicted in Figure 4.3. As previous we use `DISKREG` but here as an input signal generator. The generated signal $u(kh)$ is D/A-converted and the Voltage/Pulse converter transforms the DC voltage into a proportional pulse frequency. Further, an off-delay is incorporated in such way that a continuously open valve is obtained if $u(t)$ reaches its maximum value. The time between the generated pulses increases with decreasing input voltage $u(t)$. The water flow $Q(t)$ to the WAS process is a linear function of the input voltage $u(t)$

$$Q(t) = f(u(t)) = u(t)k_1k_2Q_{\max} \tag{4.8}$$

where $u(t)$ is the input voltage (V), k_1 $(pulse/sV)$ is a constant that converts the input voltage into the corresponding pulse frequency and k_2 $(s/pulse)$ is the applied off-delay. The available flow $Q_{\max}$ $(liter/s)$ is approximately 0.3 $liter/s$. By using this approach, the flow of water is controlled with good precision and we comply with the constraints regarding a fine spray of water as input to the WAS process. A photograph of the experimental setup is shown in Figure 4.4.

4.4 First Stage Experiment

A standard procedure of identification is to start with some *first stage experiments*, which include simple experiments followed by continued experiments (*second stage experiments*). For a first stage experiment some simple input signal could be used. Dominating time constants in the output response and low-frequency noise can be evaluated from, for example, a step/pulse response. The first stage experiments are carried out with different amplitudes in order to determine the operating range of a *linear model*. The experimental

Figure 4.4: The experimental setup. The software `DISKREG` is used for data acquisition.

conditions for the first stage experiment are selected to be

$$\mathcal{H} : u \text{ is a } \textit{pulse sequence}\text{; each pulse has an amplitude of } \gamma \cdot 10\% \qquad (4.9)$$

where γ is an integer. The measurement of the normalized effective power $P_e(t)$ is only available as periodic observations of $P_e(t)$ sampled with a time interval h (the sampling period). Let the values of $P_e(t)$ be represented by a sequence

$$\{P_e(k)\}_{k=0}^{\infty}\,; \quad P_e(k) = P_e(kh) \quad \text{for } k = 0, 1, \ldots \qquad (4.10)$$

then the measurement of $P_e(k)$ can be expressed as

$$P_e(k) \;\triangleq\; y(k) = x(k) + v(k) = g(k) * u(k) + v(k) \qquad (4.11)$$

where $y(k)$ is an observation of a variable $x(k)$, the system input $u(k)$ convolved with the systems impulse response $g(k)$ corrupted by a variable $v(k)$, which is some external input that represents disturbances. The raw input-output data from the first stage experiment is shown in Figure 4.5. Here the sample time $h = 0.1\ s$ is used. In the figure it is seen that the process has "slow dynamics", which implies that the dynamics of the power transducer and anti-aliasing filter can be neglected. Due to the slow dynamics, the input and output are resampled to $h = 1\,s$ by decimation. The decimation is preceded by prefiltering. By observing the figure and disregarding the initial behavior (caused by gearbox oil heat-up in the stirrer drive, which implies

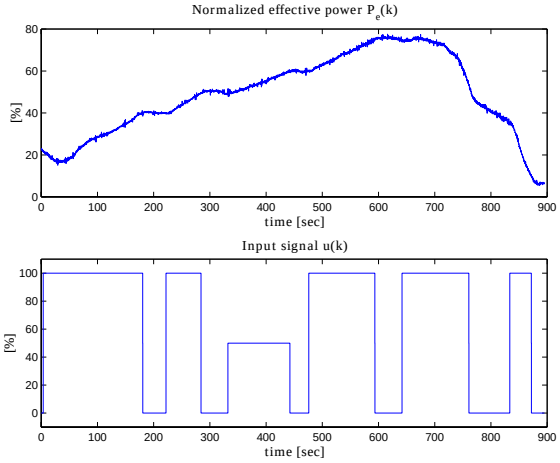

Figure 4.5: Raw input-output data from the first stage experiment.

decreased resistance), it may be inferred that the system has positive gain and no time-delay. This description of the system is valid up to $t \approx 700$ s. Then the mixture viscosity changes and the normalized effective power decreases rapidly giving a mixture useless for granulation.

Test of Linearity

The *coherence spectrum* is particularly interesting as a test of linearity in an input-output relationship. If we assume that (4.11) is valid, then the quadratic coherence spectrum between the two signals u and y is defined as the ratio

$$C_{uy}^2(\omega) = \frac{|\Phi_{uy}(i\omega)|^2}{\Phi_{uu}(i\omega)\Phi_{yy}(i\omega)} \tag{4.12}$$

where Φ_{uy} is the *cross-spectrum*, Φ_{uu} and Φ_{yy} are the *autospectra* of the input u and output y respectively. To see that the quadratic coherence always takes on a value in the interval $0 \leq C_{uy}^2(\omega) \leq 1$, we use that $\Phi_{uu} \in \mathbb{R}$ and rewrite equation (4.12) as

$$\begin{aligned} C_{uy}^2(\omega) &= \frac{\left|\Phi_{uy(i\omega)}\right|^2}{\Phi_{uu}(i\omega)\Phi_{yy}(i\omega)} = \frac{|G(i\omega)|^2 \Phi_{uu}^2(i\omega)}{\Phi_{uu}(i\omega)\Phi_{yy}(i\omega)} \\ &= \frac{|G(i\omega)|^2 \Phi_{uu}^2(i\omega)}{\Phi_{uu}(i\omega)\left(|G(i\omega)|^2 \Phi_{uu}(i\omega) + \Phi_{vv}(i\omega)\right)} \end{aligned} \tag{4.13}$$

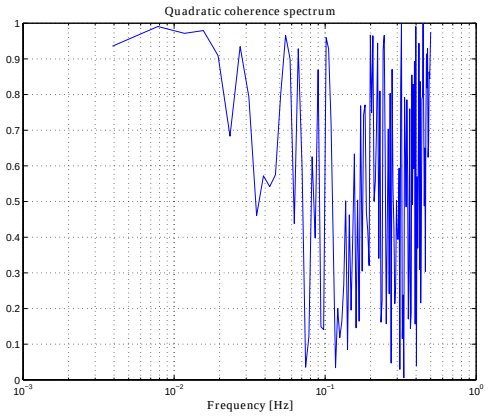

Figure 4.6: Empirical coherence spectrum $\hat{C}^2_{uy}(\omega)$.

which can be rewritten as

$$C^2_{uy}(\omega) = \frac{|G(i\omega)|^2}{|G(i\omega)|^2 + \frac{\Phi_{vv}(i\omega)}{\Phi_{uu}(i\omega)}} = \frac{1}{1 + \frac{\Phi_{vv}(i\omega)}{|G(i\omega)|^2 \Phi_{uu}(i\omega)}} \tag{4.14}$$

From (4.14) it is concluded that the quadratic coherence always takes on a value in the interval $0 \leq C^2_{uy}(\omega) \leq 1$, with a value close to one in the frequency range where the noise level is low ($\Phi_{vv} \ll \Phi_{uu}$) and if the system is linear [27]. The coherence function may thus be viewed as a type of correlation function in the frequency domain. Using the data set $Z^{100-700} = \{y(k), u(k)\}_{k=100}^{700}$, the coherence function estimate $\hat{C}^2_{uy}(\omega)$ is calculated and shown in Figure 4.6. The coherence spectrum with coherence close to 1 for frequencies up to $0.03\,Hz$ verifies that there is a satisfactory coherence between the two signals. This gives promise of successful identification with a linear model. Since a linear input-output relationship is observed in Figure 4.5, it may also be inferred that the noise level is larger, i.e., the magnitude of the input autospectrum Φ_{uu} is smaller for frequencies above $0.03\,Hz$. The results shown in Figure 4.6 should however be interpreted with caution since the viscosity dynamics seem to be time-varying.

The content of unburnt carbon present in the wood ash is the main parameter that determines the wood ash quality. For each experimental batch, the wood ash carbon content is determined by using the test of LOI [52]. Six repeated samples are taken from the batch used in the first stage experiments and

a confidence interval for the asymptotic distribution is calculated using the *Student's t-distribution*

$$\mu^* \pm t_{(n-1)_{\alpha/2}} \frac{\sigma^*}{\sqrt{n}} \tag{4.15}$$

where μ^* is the *estimated mean* of the n collected samples from the population, $n-1$ is the *degrees of freedom*, α is the *significance level* and σ^* is the *estimated standard deviation*. For the batch used in the first stage experiment, a 95%-confidence interval for the asymptotic distribution of the wood ash carbon content is 51.4 ± 0.8 % of unburnt carbon.

4.5 Estimating Process Dynamics

There may of course be several reasons why a model of a dynamical systems is sought. A common one is that the model is needed to design a regulator for the system. It is then important that available design variables are chosen so that the resulting model becomes as appropriate as possible for the control design. Originally, the idea was to fit the dynamics of the WAS process to a parametric model and to construct a model of the model errors that are present in the nominal model. This procedure is called *model error modelling* [32]. When the error models are linear, it is preferable to present the nominal model uncertainties in frequency domain. This approach is however not successful due to the fact that the process dynamics of the WAS are time-varying. Therefore, it is necessary to estimate a model on-line at the same time as the input-output data is received. The measurement of $P_e(k)$ can be expressed as

$$P_e(k) \triangleq y(k) = \boldsymbol{\varphi}^T(k,d)\boldsymbol{\theta}(k) + e(k) \tag{4.16}$$

where $\boldsymbol{\theta}(k)$ is a parameter vector containing the system parameters, d is the delay of the system, $\boldsymbol{\varphi}^T(k,d)$ is the regression vector and $e(k)$ is additive white noise. The estimated model parameters are expressed as a parameter vector $\hat{\boldsymbol{\theta}}$,

$$\hat{\boldsymbol{\theta}} = \left[\hat{a}_1, \ldots, \hat{a}_{na}, \hat{b}_1, \ldots, \hat{b}_{nb}\right] \tag{4.17}$$

where na and nb are the orders of the process denominator/numerator polynomials $A(q)$ and $B(q)$ respectively, c.f. equation (4.4). With a given time delay d, the regression vector $\boldsymbol{\varphi}$ can be written as

$$\boldsymbol{\varphi}(k,d) = [-y_f(k-1),\ \ldots, -y_f(k-n_a),\ u_f(k-1-d),\ \ldots, u_f(k-n_b-d)] \tag{4.18}$$

where y_f and u_f are the filtered process output and input values

$$y_f(k) = L(q)y(k) \qquad u_f(k) = L(q)u(k) \tag{4.19}$$

Here $L(q)$ is a suitable pre-filter (data-filter). See Section 4.8 (Appendix). The regressor $\boldsymbol{\varphi}$ is used to estimate the parameter vector $\hat{\boldsymbol{\theta}}$. The required least-square equations are [31]

$$\begin{aligned}
\hat{\boldsymbol{\theta}}(k) &= \hat{\boldsymbol{\theta}}(k-1) + \mathbf{K}(k)\left[y_f(k) - \boldsymbol{\varphi}^T(k,d)\hat{\boldsymbol{\theta}}(k-1)\right] \\
\mathbf{K}(k) &= \mathbf{P}(k)\boldsymbol{\varphi}(k,d) = \frac{\mathbf{P}(k-1)\boldsymbol{\varphi}(k,d)}{\lambda + \boldsymbol{\varphi}^T(k,d)\mathbf{P}(k-1)\boldsymbol{\varphi}(k,d)} \\
\mathbf{P}(k) &= \frac{1}{\lambda}\left[\mathbf{P}(k-1) - \frac{\mathbf{P}(k-1)\boldsymbol{\varphi}(k,d)\boldsymbol{\varphi}^T(k,d)\mathbf{P}(k-1)}{\lambda + \boldsymbol{\varphi}^T(k,d)\mathbf{P}(k-1)\boldsymbol{\varphi}(k,d)}\right]
\end{aligned} \tag{4.20}$$

where $\mathbf{P}$ is the parameter covariance matrix, $\mathbf{K}$ the gain matrix, and λ a forgetting factor. See Section 4.9 (Appendix) for a detailed derivation of how the forgetting factor λ influences the parameter estimate $\hat{\boldsymbol{\theta}}(k)$ given $\mathbf{P}(0)$ and $\hat{\boldsymbol{\theta}}(0)$. The Recursive Least Square (RLS) parameter estimator is implemented in `C-code` and incorporated in `SIMULINK S-functions` [50], [47]. The implemented algorithm uses the Bierman UD covariance factorization update, which is well suited for real-time implementation [5]. For more details on the algorithm, see Section 4.10 (Appendix). If the input sequence $u(k)$ of the first stage experiment is regarded to be sufficiently exciting, the RLS could be applied to this input-output data with different orders of an ARX model structure. To determine if the input is of sufficient complexity, the criterion of persistent excitation is used.

Definition 4.5.1 *Persistency of excitation* [27], [63].

A signal u fulfils the condition of Persistent Excitation (PE) of order n if the following limits exist

$$m_u = \lim_{N\to\infty} \frac{1}{N}\sum_{k=1}^{N} u(k) \tag{4.21}$$

$$r_{uu}(\tau) = \lim_{N\to\infty} \frac{1}{N}\sum_{k=1}^{N} u(k-\tau)u(k) \tag{4.22}$$

and if the correlation matrix

$$\widehat{\mathbf{R}}_{uu}(n) = \begin{bmatrix} \hat{r}_{uu}(0) & \hat{r}_{uu}(1) & \cdots & \hat{r}_{uu}(n-1) \\ \hat{r}_{uu}(-1) & \hat{r}_{uu}(0) & \cdots & \hat{r}_{uu}(n-2) \\ \vdots & \vdots & \ddots & \vdots \\ \hat{r}_{uu}(1-n) & \hat{r}_{uu}(2-n) & \cdots & \hat{r}_{uu}(0) \end{bmatrix} \tag{4.23}$$

is *positive definite* (See Appendix). □

Model set	na	nb	nk	$V_N(\hat{\boldsymbol{\theta}})$
$Ay = Bu + e$	1	1	1	0.3182
	2	1	1	0.1690
	2	2	1	0.1663
	3	1	1	0.1844
	3	2	1	0.2079
	3	3	1	0.2264

Table 4.1: Numerical values of the loss function $V_N(\hat{\boldsymbol{\theta}})$ for different ARX model orders when the RLS is applied to the data-set obtained from the first stage experiment. The strange result (increasing loss for increasing model order) may be caused by the abrupt change in the process dynamics since, in general, the convergence for the RLS is slower for a higher model order.

Persistent excitation of order n is sufficient to obtain consistent estimates of n parameters with the least-squares method. From the definition it is concluded that the input signal of the first stage experiment is PE of at least order 6.

The criteria for deciding the best model order was minimization of the mean square of the estimation error [34]

$$V_N(\hat{\boldsymbol{\theta}}) = \frac{1}{N}\sum_{k=1}^{N}\varepsilon^2(k) \tag{4.24}$$

where

$$\varepsilon(k) = L(q)y(k) - \boldsymbol{\varphi}^T(k,d)\hat{\boldsymbol{\theta}}(k-1) \tag{4.25}$$

The values of the loss function (4.24) for different model orders are shown in Table 4.1. Notice that $nk = d + 1$. Here, a low-pass data-filter

$$L(q) = \frac{1-f}{q-f} \tag{4.26}$$

with $f = 0.9$ is used. In the table it is observed that the loss function is minimized for a second order ARX model. However it may be useful to select a structure with $na = 2$, $nb = 1$ and $nk = 1$. When inspecting the input-output data shown in Figure 4.5 it may be inferred that the gain of the process dynamics switches sign when the mixture viscosity begins to decrease. If this structure is selected, the model may better capture this property. The reason is that if $nb = 2$, two parameters of small magnitude are identified in the numerator polynomial, whereas if nb is chosen to be one, this yields only one parameter to estimate in the B polynomial. As a result, an abrupt change of the system gain will be easier to track.

4.6 Second Stage Experiment

The second stage of experiments is characterized by a systematic design and execution of suitable experiments. These experiments were carried through at randomly selected occasions during a period of two months, in order to identify models for different wood ash qualities. A Pseudo Random Binary Sequence (PRBS) was used as an input signal during the identification experiments. This signal is implemented for example as

$$u(k) = 0.5(u_1 + u_2) + 0.5(u_1 - u_2)sign(w(k)) \tag{4.27}$$

where $w(k) \in [-1, 1]$ is a sequence of uniformly distributed random numbers, for example computer generated. The actual shape of the input signal should be adapted to the application. The viscosity dynamics are typically slow which implies that (4.27) must be modified so that the normalized effective power $P_e(t)$ is able to change adequately during two amplitude switches of the input sequence $u(k)$. This is achieved by only allowing the input sequence to change amplitude each N^{th} sample interval (called the *basic period*). With $u_1 = a$ and $u_2 = -a$ the correlation function for the PRBS sequence with basic period N can be shown to be [54]

$$r_{uu}(\tau) = \begin{cases} a^2 \frac{N-|\tau|}{N} & , \tau = 0, \pm 1, \ldots \pm N \\ 0 & , \ |\tau| > N \end{cases} \tag{4.28}$$

with the spectral density function

$$\Phi_{uu}(\omega) = \frac{a^2}{2\pi} \frac{1}{N} \frac{1 - \cos N\omega}{1 - \cos \omega} \tag{4.29}$$

As seen in (4.29) an input signal with most of its energy located in the low frequency range is obtained if N is large. This will excite the modes of the system that corresponds to slow dynamics. In the second stage experiments, N is selected to be 600.

An example of process input-output data and the convergence of the estimated parameters are shown in Figure 4.7. The figure clearly shows that the process dynamics are time-varying. For the experiment presented in Figure 4.7, a 95%-confidence interval for the asymptotic distribution of the batch wood ash carbon content is 40.9 ± 0.3 % of unburnt carbon. The second stage experiments yield the following physical interpretation of the viscosity dynamics, which also supports the results obtained in Table 4.1: since the mixture is accumulating water, an integrator is to be found in the process dynamics. Further, a time-constant is present, which depends on how the water is "diffused" into the mixture; in the beginning of the WAS procedure

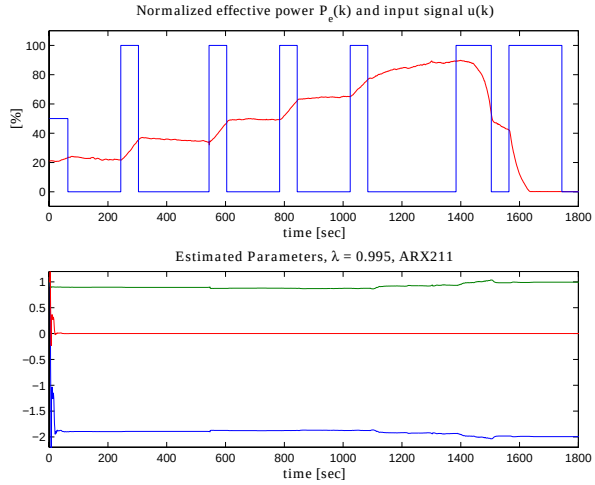

Figure 4.7: A selected second stage experiment. Here a PRBS sequence is used as an input sequence. In the lower plot, the convergence of three parameters in a second order ARX model identified with RLS is shown.

the dry mixture absorbs water fast, whereas at the end the mixture becomes more and more saturated and is not able to absorb water as fast as in the beginning. This implies a *grey box model* shown in Figure 4.8. From a system perspective, the gradual saturation of the mixture is explained as a time-varying time-constant, i.e., the time constant corresponds to a mode that decreases in speed. This implies that the system will, eventually, become a double integrator. This heuristic discussion is supported by Figure 4.9.

For each experiment, it is observed that the estimated process gain $\hat{b}_1$ switches sign (c.f. Figure 4.9) when the mixture viscosity begins to decrease. This property may be used to disable any control action during the WAS procedure. Further, there are strong indications that it is not only the accumulated quantity of water that is related to the instant when the process gain changes. In addition, this instant is also affected by the applied flow of water $Q(t)$ and the wood ash quality. For example, the accumulated amount of water at the viscosity change is 133 *liters* for the experiment shown in Figure 4.5, whereas the amount is only 85 *liters* for the experiment shown in Figure 4.7. When comparing the carbon content of the batches, which are 51.4 ± 0.8 % and 40.9 ± 0.3 % of unburnt carbon, this supports the theory that more water is required in the ash stabilization process if the carbon content is high [30].

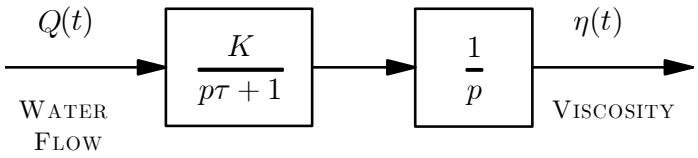

Figure 4.8: Gray box model for the dynamics of the WAS process. Here, p is the differential operator d/dt.

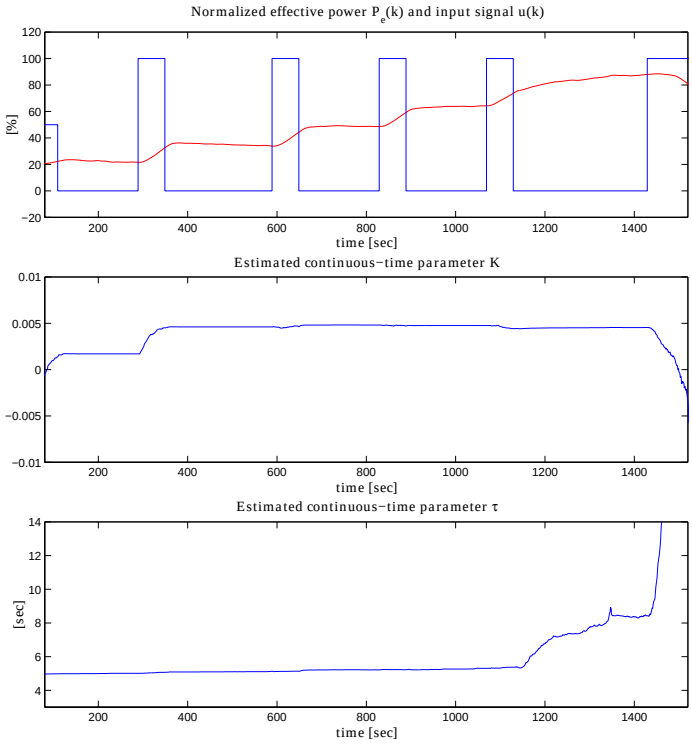

Figure 4.9: The estimated continuous-time parameters K and τ of the gray box model presented in Figure 4.8. It is observed that the time-constant τ is approximately 5 seconds at the beginning of the WAS process.

4.7 Summary and Concluding Remarks

In this chapter, the viscosity of the ash/dolomite/water mixture is estimated by measuring the normalized effective power $P_e(t)$, which represents the rate of useful work being performed by the three-phase asynchronous machine used as stirrer drive. It is shown that this measurement is well suited for control of the amount of added water to the WAS process. A second order ARX model structure has been selected. Recursive Least Square (RLS) is applied to estimate the time-varying dynamics. By using this approach, it is possible to track variations in the process dynamics due to varying wood ash quality.

It should be noticed that the selected ARX model could be exchanged for an identified Output Error (OE) model. The OE model structure is motivated by the interpretation that the random disturbances visible in $P_e(k)$ are caused by the stirrer, which is a part of the sensor (motor + stirrer). The sensor monitors the mixture viscosity, i.e., the random fluctuations are interpreted as measurement noise. However, the models identified with RLS maps the true measurement of $P_e(k)$ with good agreement in *deterministic simulations* [27]. This implies that the relation between the process input and output is well defined, i.e., the prediction of the normalized effective power $P_e(k)$ is not built upon old values of $P_e(k)$ only. This make the model most adequate for control of the WAS process.

Further, there are strong indications that it is not only the accumulated quantity of water that is related to the instant when the process gain changes. In addition, this instant is also affected by the applied flow of water $Q(t)$ and the quality of the wood ash. Therefore, to determine an critical water-to-ash ratio based only on CIFA measurements may give poor results. A solution for fast detection of the abrupt change in the process dynamics is presented in Chapter 5.

4.8 Appendix 4A - Choice of Data-filter

The system description is given in the form (c.f. equation (4.4))

$$y(k) = G(q^{-1}, \boldsymbol{\theta})u(k) + H(q^{-1}, \boldsymbol{\theta})e(k) \tag{4.30}$$

as the basic description of a linear system subject to additive random disturbances. Here

$$G(q^{-1}, \boldsymbol{\theta}) = \frac{B(q^{-1})}{F(q^{-1})} = \frac{b_1 q^{-1-d} + b_2 q^{-2-d} + \cdots + b_{nb} q^{-nb-d}}{1 + f_1 q^{-1} + \cdots + f_{nf} q^{-nf}} \tag{4.31}$$

and

$$H(q^{-1}, \boldsymbol{\theta}) = \frac{C(q^{-1})}{D(q^{-1})} = \frac{1 + c_1 q^{-1} + \cdots + c_{nc} q^{-nc}}{1 + d_1 q^{-1} + \cdots + d_{nd} q^{-nd}} \tag{4.32}$$

and $\{e(k)\}$ is a sequence of independent random variables with zero mean value and variance σ_e^2. For the case of an ARX model $G = B/A$ and $H = 1/A$. In this section we will explain and affect the distribution of the bias

$$G(e^{i\omega}, \boldsymbol{\theta}^*) - G_0(e^{i\omega}) \tag{4.33}$$

where $G_0(e^{i\omega})$ is the true transfer function and $G(e^{i\omega}, \boldsymbol{\theta}^*)$ is the limiting estimate of G. The case of most practical interest is probably to study the fit between $G(e^{i\omega}, \boldsymbol{\theta}^*)$ and $G_0(e^{i\omega})$. It is natural to consider the bias distribution of G to be the most important issue, since closed-loop stability of a regulator design will depend on the accuracy of G. The limiting parameter estimate is given by [31]

$$\boldsymbol{\theta}^* = \lim_{N\to\infty} \hat{\boldsymbol{\theta}}_N = \arg\min_{\boldsymbol{\theta}} \int_{-\pi}^{\pi} \left|G_0(e^{i\omega}) - G(e^{i\omega}, \boldsymbol{\theta})\right|^2 \underbrace{\frac{\Phi_u(\omega)}{\left|H(e^{i\omega}, \boldsymbol{\theta})\right|^2}}_{Q(\omega,\boldsymbol{\theta})} d\omega \tag{4.34}$$

This means that $Q(\omega, \boldsymbol{\theta})$ will be taken as the weighting function that determines the *bias distribution.* This bias distribution can in turn be affected by properly selecting the

Input spectrum $\Phi_u(\omega)$.	Noise model set.
Prefilter $L(q)$.	Prediction horizon k.

Notice that it is only the ratio $\Phi_u/|H|^2$ that determines the bias distribution; the values of the individual functions Φ_u, H and L are immaterial. If, for instance the input and outputs are filtered with the pre-filter

$$y_f(k) = L(q)y(k) \qquad u_f(k) = L(q)u(k) \tag{4.35}$$

this will affect the weighting function and the actual weighting function $Q(\omega, \boldsymbol{\theta})$ obtained is

$$\left|L(e^{i\omega})\right|^2 \cdot Q(\omega, \boldsymbol{\theta}) \tag{4.36}$$

To identify a system with non-zero mean one can, for example, remove the average value of the signals before they are used in the estimator to obtain a correct model. In recursive methods it is difficult to remove average values. An approach that works for signals with non-zero mean and drifting signals is to differentiate the signals, i.e. to multiply the regressor with $q - 1$. As differentiated signals are quite noisy, it is a good idea to low-pass filter the differentiated signals. Low-pass filtering also removes the undesired high frequency dynamics. A suitable data-filter is then [63]

$$L(q) = \frac{(q-1)(1-f)}{q-f} \tag{4.37}$$

With this filter a disturbance will be removed from the data, except for components in the frequency interval $(\omega_{fl}, \omega_{fh})$ where ω_{fl} is the lower break frequency and ω_{fh} is the upper break frequency for the data-filter, see Figure 4.10. The estimator will thus not be confused by low frequency drift. Hence,

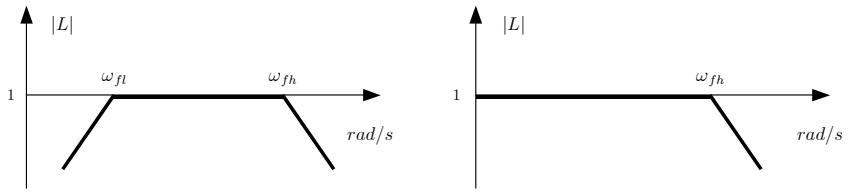

Figure 4.10: The amplitude curve of the bandpass filter (left) and the low pass filter (right).

if ω_{fh} is too high, the estimator may attempt to fit the model at too high frequencies.

Since it is assumed that no low frequency drift is present in the WAS process, a simple low-pass filter

$$L(q) = \frac{1-f}{q-f} \tag{4.38}$$

is implemented as data-filter. See Figure 4.10. Using a low pass filter as data-filter gives a good low frequency fit.

4.9 Appendix 4B - Interpretation of the RLS Algorithm

Consider the system

$$\mathcal{S}: \quad y_k = \boldsymbol{\varphi}_k^T \boldsymbol{\theta} + e_k \tag{4.39}$$

and the model

$$\mathcal{M}: \quad y_k = \boldsymbol{\varphi}_k^T \boldsymbol{\theta}$$

In the batch least-square [31] problem we consider the matrix

$$\mathbf{P}_k = \left[\sum_{i=1}^{k} \boldsymbol{\varphi}_i \boldsymbol{\varphi}_i^T \right]^{-1} \tag{4.40}$$

It satisfies the recursive equation

$$\mathbf{P}_k^{-1} = \mathbf{P}_{k-1}^{-1} + \boldsymbol{\varphi}_k \boldsymbol{\varphi}_k^T \tag{4.41}$$

By including the forgetting factor λ the corresponding RLS covariance matrix is obtained

$$\mathbf{P}_k^{-1} = \lambda \mathbf{P}_{k-1}^{-1} + \boldsymbol{\varphi}_k \boldsymbol{\varphi}_k^T \tag{4.42}$$

with the initial value $\mathbf{P}_0$. The solution is

$$\mathbf{P}_k^{-1} = \lambda^k \mathbf{P}_0^{-1} + \sum_{i=1}^{k} \lambda^{k-i} \boldsymbol{\varphi}_i \boldsymbol{\varphi}_i^T \tag{4.43}$$

The difference equation for $\mathbf{P}_k^{-1} \hat{\boldsymbol{\theta}}_k$ is given by

$$\mathbf{P}_k^{-1} \hat{\boldsymbol{\theta}}_k = \lambda \mathbf{P}_{k-1}^{-1} \hat{\boldsymbol{\theta}}_{k-1} + \boldsymbol{\varphi}_k y_k$$

with the initial values $\mathbf{P}_0$ and $\boldsymbol{\theta}_0$. The solution is

$$\mathbf{P}_k^{-1} \hat{\boldsymbol{\theta}}_k = \lambda^k \mathbf{P}_0^{-1} \hat{\boldsymbol{\theta}}_0 + \sum_{i=1}^{k} \lambda^{k-i} \boldsymbol{\varphi}_i y_i \tag{4.44}$$

Combining equations (4.43) and (4.44) gives

$$\hat{\boldsymbol{\theta}}_k = \left[\lambda^k \mathbf{P}_0^{-1} + \sum_{i=1}^{k} \lambda^{k-i} \boldsymbol{\varphi}_i \boldsymbol{\varphi}_i^T \right]^{-1} \left[\lambda^k \mathbf{P}_0^{-1} \hat{\boldsymbol{\theta}}_0 + \sum_{i=1}^{k} \lambda^{k-i} \boldsymbol{\varphi}_i y_i \right] \tag{4.45}$$

Hence,

- If $\lambda < 1$, the influences of the initial conditions tend to zero as $k \to \infty$.
- If $\lambda = 1$ and $\mathbf{P}_0 = \alpha \mathbf{I}$, then the influences of initial conditions tend to zero as $\alpha \to \infty$.

4.10 Appendix 4C - Bierman UDU^T Covariance Update

The three equations given in (4.20) denote one way to mechanize the recursive update of the estimates and the covariance matrix. Although widely accepted both in theory and practice, a straightforward implementation of the RLS algorithm is notorious for its poor numerical property in real application, which can easily destroy the performance of the RLS algorithm [5], [13]. This can be made clear by taking a look at the covariance updating formula

$$\mathbf{P}(k-1) - \frac{\mathbf{P}(k-1)\boldsymbol{\varphi}(k,d)\boldsymbol{\varphi}^T(k,d)\mathbf{P}(k-1)}{\lambda + \boldsymbol{\varphi}^T(k,d)\mathbf{P}(k-1)\boldsymbol{\varphi}(k,d)} \tag{4.46}$$

As time goes on, the covariance matrix converges to a matrix of very small magnitude, which implies that the covariance updating equation (4.46) may involve the subtraction of two almost equal matrices with very small magnitudes. This can easily result in poor numerical performance when implemented on digital computers with finite word length and round-of errors [13].

Many modified forms of the RLS algorithm exist to improve the numerical performance [34], [45], among which Bierman's UD factorization method [5], [56] is one of the most successful approaches. Mathematically, Bierman's method is equivalent to the RLS method. However, through a different formulation, namely, the UD factorization, Bierman's algorithm is numerically much more stable than the RLS algorithm [5], [56], [33]. In Bierman's method, instead of directly updating the covariance matrix $\mathbf{P}(k)$ using equation (4.46), a $\mathbf{UDU}^T$ factored form of the $\mathbf{P}(k)$ matrix,

$$\mathbf{P}(k) = \mathbf{U}(k)\mathbf{D}(k)\mathbf{U}(k)^T \tag{4.47}$$

is used. That is, at every time interval, $\mathbf{U}(k)$ and $\mathbf{D}(k)$, instead of $\mathbf{P}(k)$, are updated, where $\mathbf{D}(k)$ is diagonal and $\mathbf{U}(k)$ is an unit upper-triangular matrix. The UD factorization preserves the positive-definiteness (see Appendix A, Section A.1) of the $\mathbf{P}(k)$ matrix and updates the square root of the covariance matrix, thus the numerical condition can be considerably improved. Experiments show that for digital computer implementations, to obtain the same numerical accuracy, the UD algorithm can use about half the word length required by the conventional RLS algorithm [24], [56].

A stepwise implementation of Bierman's UD factorization algorithm is summarized in Algorithm 4.1. For detailed derivation and discussions, see [5], [56] and [34].

`Algorithm 4.1`: Bierman $\mathbf{UDU}^T$ Estimate-Covariance Update:

$\mathbf{v} = \mathbf{D}(k-1)\mathbf{f}, \quad \mathbf{f} = \mathbf{U}^T(k-1)\boldsymbol{\varphi}(k,d), \quad \alpha_0 = \lambda$

`for` $j = 1$ `to` n `do` $\quad \%\ n = na + nb$

$\alpha_j = \alpha_{j-1} + \mathbf{v}_j \mathbf{f}_j$

$\mathbf{D}_{jj}(k) = \alpha_{j-1}\mathbf{D}_{jj}(k-1)/\alpha_j\lambda$

$\mathbf{p}_j = -\mathbf{f}_j/\alpha_{j-1}, \quad \bar{\mathbf{K}}_j(k) = \mathbf{v}_j$

`for` $i = 1$ `to` $j-1$ `do`

$\mathbf{U}_{ij}(k) = \mathbf{U}_{ij}(k-1) + \mathbf{p}_j\bar{\mathbf{K}}_i(k)$

$\bar{\mathbf{K}}_i(k) = \bar{\mathbf{K}}_i(k) + \bar{\mathbf{K}}_j(k)\mathbf{U}_{ij}(k-1)$

`end`

`end`

The update gain $\mathbf{K}(k)$ is now given by:

$\mathbf{K}(k) = \bar{\mathbf{K}}(k)/\alpha_n$

Clearly, the UD factorization algorithm is a variant of the RLS algorithm in that the UD factorization technique is used to replace the covariance update (4.46) for more stable numerical performance. The UD factorization algorithm was motivated to be, and actually has also been widely regarded as, only a numerical enhancement to the RLS method.

Chapter 5

Control of the Ash Stabilization Process

5.1 Introduction

During the simulations in this chapter, an optimal adaptive controller is used to regulate the chemical process of the WAS. The model parameters of the time-varying process dynamics are estimated using the RLS parameter estimator, see Section 4.5. At each batch produced, an auto-tuning sequence with the controller disabled is carried through in order to obtain a good estimate of the process dynamics. After the auto-tuning sequence is completed, a Generalized Predictive Controller (GPC) is enabled to control the WAS process. The control objective is to regulate the normalized effective power $P_e(t)$ to the level P_e^{crit}, which is the point when the mixture totally saturates. It should be stressed that the level P_e^{crit} must be detected as fast as possible, since at the level P_e^{crit} only a small additional amount of water gives a mixture useless for granulation. For example, given a saturated batch of 250-300 kg, an additional amount of 2-4 liters of water results in a wet mixture. To cope with this problem, change detection is applied to reach the desired level P_e^{crit} without any pre-determined set-point.

Three methods are evaluated: a probing strategy, the GMA-test and the CUSUM-test, all three adequate for successful implementation. The used control strategies are presented and off-line simulations with a model of the physical process will evaluate the control performance. The GMA-test and the CUSUM-test are also evaluated by testing the detectors on two different data sets, before the best strategy is selected for real-time control of the WAS process.

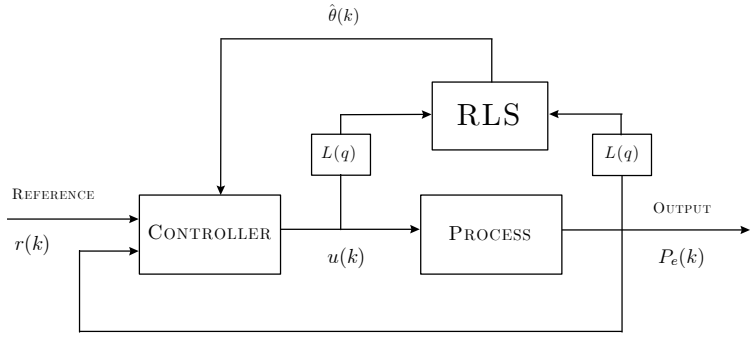

Figure 5.1: The structure of the closed loop system.

The GPC method was proposed by Clarke *et. al* [10] and has become a popular control method both in industry and academia. It has been successfully implemented in many industrial applications, showing good performance and a certain degree of robustness. It can handle many different control problems for a wide range of plants with a reasonable number of design variables, which have to be specified by the user depending upon the prior knowledge of the plant and control objectives. Advantages with the GPC controller, which make it suitable for control of the WAS process are:

- One design variable that is very useful comes with the penalty on the control signal − we can guarantee small control actions near the level P_e^{crit}.
- It is useful when future reference values are known. The objective is to control the process input $u(k)$ − the variable flow of water − in such way that the normalized effective power $P_e(t)$ initially follows a reference trajectory before the level P_e^{crit} is reached. This trajectory is constructed so that an appropriate flow of water is inserted to the WAS process.
- Constraints on the control signal are easily included in the controller − it is not possible to extract any added water.

5.2 Control using the GPC

The schematic of the closed loop system is shown in Figure 5.1. The model parameters of the time-varying WAS process dynamics are estimated using the RLS parameter estimator. The process inputs and outputs are filtered

with the data filter $L(q)$ to avoid difficulties with the parameter estimation. The estimated parameters are further used by a GPC that controls the relative effective power $P_e(k)$ given a ramp set-point trajectory with slope $r(k)$. The implemented control strategy disables the controller when the relative effective power $P_e(k)$ reaches the level P_e^{crit}.

Formulation of the GPC

The methodology of Generalized Predictive Control (GPC) is illustrated by using the loss function

$$J(N_1, N_2, N_u) = E\left\{\sum_{i=N_1}^{N_2}\left(\hat{y}(k+i \mid k) - w(k+i)\right)^2 + \sum_{i=1}^{N_u}\rho\left(\Delta u(k+i-1)\right)^2\right\} \tag{5.1}$$

subject to the equality constraints

$$\Delta u(k+i) = 0 \text{ for } i = N_u, \ldots, N_2 \tag{5.2}$$

Here $\hat{y}(k+i \mid k)$ is an optimum $i-$step prediction of the system output on data up to time k, N_1 is the minimum prediction horizon, N_2 is the maximum prediction horizon, N_u is the control horizon, ρ is a control penalty and $\Delta = 1 - q^{-1}$ is the difference operator. The future reference trajectory $w(k+i)$, can be calculated for example as

$$w(k+i) = w(k+i-1) + r(k+i) \tag{5.3}$$

where r is the slope set-point for the reference trajectory. Further a Controlled Auto-Regressive Integrating Moving-Average (CARIMA) model is used as a process model

$$A(q^{-1})y(k) = q^{-d}B(q^{-1})u(k-1) + C(q^{-1})\frac{e(k)}{\Delta} \tag{5.4}$$

where $u(k)$ and $y(k)$ are the control and output sequences respectively of the plant, and $e(k)$ is a zero mean white noise. A, B and C are the process polynomials in the backward shift operator

$$\begin{aligned} A(q^{-1}) &= 1 + a_1 q^{-1} + \cdots + a_{na} q^{-na} \\ B(q^{-1}) &= b_1 + b_2 q^{-1} + \cdots + b_{nb} q^{-nb+1} \\ C(q^{-1}) &= 1 + c_1 q^{-1} + \cdots + c_{nc} q^{-nc} \end{aligned} \tag{5.5}$$

and d is the time-delay of the system. The role of the Δ operator is to ensure integral action in the controller in order to cancel the effect of step output disturbances or model errors. Thus the nature of the plant description

(5.4) is to model the output as being corrupted by the effect of an additive random walk process. While this may not be a realistic model, its effect upon the controllers derived from it will be to force the ability to reject step output disturbances. This is entirely a reflection of the known nature of load perturbations arising. Thus, the GPC incorporates this noise model directly into its formulation in order to tailor its response for particular circumstances. This is a manifestation of the Internal Model Principle (IMP), see [6].

The key idea is to split the data into future and past components. We require the solution of two Diophantine equations [10], [6], [63]. Dropping the explicit arguments in q^{-1}, the first is

$$C = E_i A\Delta + q^{-i}F_i \tag{5.6}$$

Here

$$E_i = e_0^{(i)} + e_1^{(i)}q^{-1} + \cdots + e_{i-1}^{(i)}q^{-(i-1)} \tag{5.7}$$

and

$$F_i = f_0^{(i)} + f_1^{(i)}q^{-1} + \cdots + f_{nf}^{(i)}q^{-nf} \tag{5.8}$$

where $nf = \max(na, nc - i)$ [20]. The second Diophantine equation to solve is

$$E_i B = G_i C + q^{-i}H_i \tag{5.9}$$

Here

$$G_i = g_0^{(i)} + g_1^{(i)}q^{-1} + \cdots + g_{i-1}^{(i)}q^{-(i-1)} \tag{5.10}$$

and

$$H_i = h_0^{(i)} + h_1^{(i)}q^{-1} + \cdots + h_{nh}^{(i)}q^{-nh} \tag{5.11}$$

where $nh = \max(nc, nb + d - 1) - 1$ [20]. We find that

$$\begin{aligned}
y(k+i) &= \frac{B}{A}u(k+i-d-1) + \frac{C}{A\Delta}e(k+i) \\
&= \frac{B}{A}u(k+i-d-1) + \frac{F_i}{A\Delta}e(k) + E_i e(k+i) \\
&= \frac{B}{A}u(k+i-d-1) + \frac{F_i}{C}\left[y(k) - \frac{B}{A}u(k-d-1)\right] + E_i e(k+i) \\
&= \frac{B}{A}\left[1 - q^{-i}\frac{F_i}{C}\right]u(k+i-d-1) + \frac{F_i}{C}y(k) + E_i e(k+i) \\
&= \frac{E_i B}{C}\Delta u(k+i-d-1) + \frac{F_i}{C}y(k) + E_i e(k+i) \\
&= G_i\Delta u(k+i-d-1) + \frac{H_i}{C}\Delta u(k-d-1) + \frac{F_i}{C}y(k) + E_i e(k+i)
\end{aligned}$$

Hence, the optimal predictor for $y(k+i)$ at time k is obtained by replacing $e(k+i)$ by its expected value (zero):

$$\hat{y}(k+i \mid k) = G_i \Delta u(k+i-d-1) + \frac{H_i}{C}\Delta u(k-d-1) + \frac{F_i}{C}y(k) \quad (5.12)$$

In Chapter 4 it is shown that an ARX model structure of second order is sufficient to describe the process dynamics of the WAS adequately. This implies that the C polynomial can be chosen to be 1. When considering the set of i step ahead optimal predictors, we can write

$$\mathbf{y} = \mathbf{G}\boldsymbol{\Delta}\mathbf{u} + \mathbf{H}(q^{-1})\Delta u(k-d-1) + \mathbf{F}(q^{-1})y(k) \quad (5.13)$$

where

$$\begin{aligned}
\mathbf{y} &= \begin{bmatrix} \hat{y}(k+N_1 \mid k) \\ \hat{y}(k+N_1+1 \mid k) \\ \vdots \\ \hat{y}(k+N_2 \mid k) \end{bmatrix} \quad \boldsymbol{\Delta}\mathbf{u} = \begin{bmatrix} \Delta u(k) \\ \Delta u(k+1) \\ \vdots \\ \Delta u(k+N_u-1) \end{bmatrix} \\
\mathbf{G} &= \begin{bmatrix} g_{N_1-1} & 0 & \cdots & 0 \\ g_{N_1} & g_{N_1-1} & \cdots & 0 \\ \vdots & & \ddots & \vdots \\ \vdots & & & g_{N_1-1} \\ \vdots & & & \vdots \\ g_{N_2-1} & g_{N_2-2} & \cdots & g_{N_2-N_u} \end{bmatrix} \quad (5.14) \\
\mathbf{H}(q^{-1}) &= \begin{bmatrix} H_{N_1}(q^{-1}) \\ H_{N_1+1}(q^{-1}) \\ \vdots \\ H_{N_2}(q^{-1}) \end{bmatrix} \quad \mathbf{F}(q^{-1}) = \begin{bmatrix} F_{N_1}(q^{-1}) \\ F_{N_1+1}(q^{-1}) \\ \vdots \\ F_{N_2}(q^{-1}) \end{bmatrix}
\end{aligned}$$

Here $N_1 = d+1$ and $N_2 = d+N$, where N is the prediction horizon in the loss function (5.1). Notice that the last two terms in equation (5.13) only depend on the *past*. Now define

$$\mathbf{f} \triangleq \mathbf{H}(q^{-1})\Delta u(k-d-1) + \mathbf{F}(q^{-1})y(k) \quad (5.15)$$

The prediction can be written as

$$\mathbf{y} = \mathbf{G}\boldsymbol{\Delta}\mathbf{u} + \mathbf{f} \quad (5.16)$$

where $\mathbf{f}$ contains *known* components, $\boldsymbol{\Delta}\mathbf{u}$ contains *future* control increments and $\mathbf{G}$ is the lower triangular matrix containing the *step response coefficients*.

The dimension of $\mathbf{G}$ is $(N_2 - N_1 + 1) \times N_u$, since we have taken into account the constraints (5.2). The effect of altering N_1 is to delete rows from the top of $\mathbf{G}$ [6]. Expression (5.1) can be written as

$$J(N_1, N_2, N_u) = \|\mathbf{G}\boldsymbol{\Delta}\mathbf{u} + \mathbf{f} - \mathbf{w}\|_2^2 + \rho \|\boldsymbol{\Delta}\mathbf{u}\|_2^2 \tag{5.17}$$

where

$$\mathbf{w} = \begin{bmatrix} w(k+N_1) & w(k+N_1+1) & \cdots & w(k+N_2) \end{bmatrix}^T \tag{5.18}$$

Minimizing (5.17) with respect to $\boldsymbol{\Delta}\mathbf{u}$, assuming there are no constraints on the control signals, gives

$$\boldsymbol{\Delta}\mathbf{u} = \left(\mathbf{G}^T\mathbf{G} + \rho\mathbf{I}\right)^{-1} \mathbf{G}^T (\mathbf{w} - \mathbf{f}) \tag{5.19}$$

Notice that the control signal that is actually sent to the process is the first element of vector $\boldsymbol{\Delta}\mathbf{u}$, which is given by

$$\Delta u(k) = \mathbf{K} (\mathbf{w} - \mathbf{f}) \tag{5.20}$$

that is the first row of matrix $\left(\mathbf{G}^T\mathbf{G} + \rho\mathbf{I}\right)^{-1} \mathbf{G}^T$. This is the receding control concept.

If the delay d is known, the minimum prediction horizon is $N_1 = d + 1$. This is so because if the delay is known, there is no point in setting N_1 to be less than d since there would then be superfluous calculations in that the corresponding outputs cannot be affected by the first action $\Delta u(k)$. The usual choice of the maximum prediction horizon is $N_2 = d + \text{integer}\left(\frac{T_r}{h}\right)$, where T_r is the systems approximate rise time. The control horizon N_u is often selected to be considerably smaller compared to N_2 since this parameter essentially determines the size of the optimization problem.

Constrained GPC

In the previous section the control problem has been formulated considering all signals to possess an unlimited range. This is not very realistic because in practice all signals are subject to constraints. In our case the actuator has a limited range of action; a fully closed and a fully open position of the valve used for water control.

When the only constraints present are the maximum and minimum value of the control signal $u(k+i)$, the constraint can be written as

$$\mathbf{1}\,(u_{\min} - u(k-1)) \leq \mathbf{T}\mathbf{u} \leq \mathbf{1}\,(u_{\max} - u(k-1)) \tag{5.21}$$

where the matrix $\mathbf{T}$ is a lower triangular matrix whose entries are ones and $\mathbf{1}$ is a vector composed of ones. The optimal prediction of the process output can be written as

$$\mathbf{y} = \mathbf{G}\boldsymbol{\Delta}\mathbf{u} + \mathbf{f}_0 \tag{5.22}$$

we note that

$$\begin{aligned}
\boldsymbol{\Delta}\mathbf{u} &= \begin{bmatrix} \Delta u(k) \\ \Delta u(k+1) \\ \vdots \\ \Delta u(k+N_u-1) \end{bmatrix} = \begin{bmatrix} u(k)-u(k-1) \\ u(k+1)-u(k) \\ \vdots \\ u(k+N_u-1)-u(k+N_u-2) \end{bmatrix} \\
&= \begin{bmatrix} 1 & & & \\ -1 & 1 & & \\ & \ddots & \ddots & \\ & & -1 & 1 \end{bmatrix} \begin{bmatrix} u(k) \\ u(k+1) \\ \vdots \\ u(k+N_u-1) \end{bmatrix} - \begin{bmatrix} u(k-1) \\ 0 \\ \vdots \\ 0 \end{bmatrix} \\
&\triangleq \mathbf{D}\mathbf{u} - \mathbf{f}_1
\end{aligned} \tag{5.23}$$

If (5.23) is inserted in equation (5.22) we obtain

$$\mathbf{y} = \mathbf{G}\left(\mathbf{D}\mathbf{u} - \mathbf{f}_1\right) + \mathbf{f}_0 \;\triangleq\; \bar{\mathbf{G}}\mathbf{u} + \mathbf{f}_2 \tag{5.24}$$

where $\bar{\mathbf{G}}$ is a lower triangular matrix with all its diagonal elements equal to g_0 and its secondary elements are given by $g_i - g_{i-1}$. The objective function (5.17) can now with (5.23) be written as [9]

$$J(\mathbf{u}) = \frac{1}{2}\mathbf{u}^T\mathbf{A}\mathbf{u} + \mathbf{b}\mathbf{u} + c \tag{5.25}$$

where

$$\begin{aligned}
\mathbf{A} &= 2\left(\bar{\mathbf{G}}^T\mathbf{G} + \mathbf{D}^T\mathbf{D}\right) \\
\mathbf{b}^T &= 2\left(\left(\mathbf{f}_2 - \mathbf{w}\right)^T\bar{\mathbf{G}} - \mathbf{f}_1^T\mathbf{D}\right) \\
c &= \|\mathbf{f}_2 - \mathbf{w}\|_2^2 + \|\mathbf{f}_1\|_2^2
\end{aligned}$$

The problem has now been reduced to optimize a quadratic form (See Appendix A.1) with a constraint matrix

$$\min \frac{1}{2}\mathbf{u}^T\mathbf{A}\mathbf{u} + \mathbf{b}\mathbf{u} + c \tag{5.26}$$

$$\text{subject to} \begin{bmatrix} \mathbf{I}_{N\times N} \\ -\mathbf{I}_{N\times N} \end{bmatrix}\mathbf{u} \leq \begin{bmatrix} \mathbf{1}u_{\max} \\ -\mathbf{1}u_{\min} \end{bmatrix}$$

that is solved on-line at each sample interval using quadratic programming.

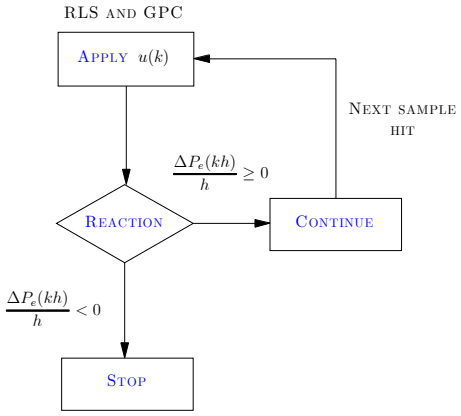

Figure 5.2: The probing strategy, where $\Delta = 1 - q^{-1}$ is the difference operator.

5.3 Detection of Critical Viscosity

The objective of this section is to develop methods to detect the critical mixture viscosity of the ash/dolomite/water.

Probing Strategy

The control objective is to regulate the normalized effective power $P_e(t)$ to the level P_e^{crit}, which represents the desired mixture viscosity. When P_e^{crit} is reached and nevertheless more water is added to the WAS process, this gives a mixture useless for granular material. To cope with this problem, a *probing strategy* is developed to reach the desired level P_e^{crit} without any fully pre-determined set-point trajectory. The strategy is shown in Figure 5.2 and is inspired by the work presented in [62]. The probing strategy works as follows: a ramp reference trajectory is generated and the GPC calculates the control signal increment $\Delta u(k)$ at each sample so that (5.25) is minimized. If the difference approximation of the derivative $\dot{P}_e(t)$ is negative, the controller is disabled and the probing strategy stops. If not, the probing strategy continues. Hence, the probing strategy also gives the ability to track changes in P_e^{crit} due to varying wood ash qualities. It should also be noticed that the strategy could include a linearly increasing control penalty ρ, yielding small control actions near the point P_e^{crit}.

Change Detection

Algorithmically, all proposed change detectors can be put into one of the following three categories:

- Methods using one filter, where a *whiteness test* is applied to the residuals.
- Methods using *two filters*, one slow and one fast, in parallel.
- Methods using *multiple filters* in parallel, each one matched to certain assumption on the abrupt changes.

The measurement of the normalized effective power $P_e(t)$ is only available as periodic observations of $P_e(t)$ sampled with an time interval h . Let the values of $P_e(t)$ be represented by a sequence

$$\{P_e(k)\}_{k=0}^{\infty}; \quad P_e(k) = P_e(kh) \quad \text{for } k = 0, 1, \ldots \tag{5.27}$$

then the measurement of $P_e(k)$ can be expressed as

$$P_e(k) \quad \triangleq \quad y(k) = \boldsymbol{\varphi}^T(k, d)\boldsymbol{\theta}(k) + e(k) \tag{5.28}$$

where $\boldsymbol{\theta}(k)$ is a parameter vector containing the system parameters, d is the delay of the system, $\boldsymbol{\varphi}^T(k, d)$ is the regression vector and $e(k)$ is an additive white noise. An adaptive parameter estimator is good at following slow variations in the system parameters. If the system is changed abruptly instead, for example if the gain of the system switches sign, it takes quite a long time before the filter adapts to the new system parameters. To improve the performance of the filter a change detector [22] can be added. The structure of the implemented change detector is shown in Figure 5.3:

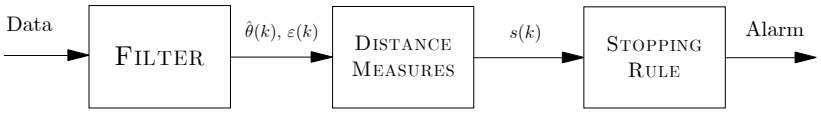

Figure 5.3: The principle of the one-filter approach for change detection.

In the one-filter approach, one adaptive filter is used to determine if there is a change in the system. If the estimated model is correct, the residuals $\varepsilon(k)$ from the filter should be white and gaussian. The change detector consists of three stages; filter, distance measures and stopping rules:

Filter

The implemented RLS parameter estimator discussed in Chapter 4 is here used as a filter. The RLS gives as an output the parameter estimate $\hat{\boldsymbol{\theta}}(k)$ and the residual $\varepsilon(k)$ at time k.

Distance Measures

After a change, either the mean or variance or both will change. This is indicated by the residuals $\varepsilon(k)$ from the filter, which become "large" in some sense. The main problem in statistical change detection is to decide what is meant by "large". Therefore a function $s(k)$, called *distance measure* of the residual, $\varepsilon(k)$, at time k is calculated to obtain a measurement of the distance to zero of the residual. Here, the implemented distance measure is the same as the residual [22], i.e., $s(k) = \varepsilon(k)$, which is useful for detecting a change in the mean.

Stopping Rules

If the residuals are white the expected value $E\{s(k)\}$, of $s(k)$ should be zero. A *hypothesis test* can be used to decide whether the model is correct or not

$$\begin{aligned} \mathcal{H}_0 &: \quad E\{s(k)\} = 0 \\ \mathcal{H}_1 &: \quad E\{s(k)\} \neq 0 \end{aligned} \tag{5.29}$$

This is essentially achieved by low-pass filtering $s(k)$ and comparing this value to a threshold γ. One such method is the GMA [44] test. A one-sided GMA-test[1] is

$$g(k) = \alpha g(k-1) - (1-\alpha)s(k), \qquad \text{alarm if } g(k) > \gamma \tag{5.30}$$

Here the parameter α is used to tune the low pass effect. Another method is the CUSUM-test [59], [3]. The one-sided CUSUM-test only detects if $g(k)$ is significantly larger than zero.

$$g(k) = \max\left(g(k-1) - s(k) - \nu, 0\right), \qquad \text{alarm if } g(k) > \gamma \tag{5.31}$$

Here the drift parameter ν and the threshold γ are design parameters used to tune the sensitivity of the change detector.

[1] To aid a visual comparison between the GMA and CUSUM-tests, we here use $\alpha g(k-1) - (1-\alpha)s(k)$ instead of the text-book version $\alpha g(k-1) + (1-\alpha)s(k)$ as a first order exponential filter.

5.4 Simulation Study

In order to evaluate the control performance, a model of the WAS dynamics has been built in `SIMULINK`. The experimental output and the predicted `SIMULINK` model output are shown in Figure 5.4. As seen in the figure the

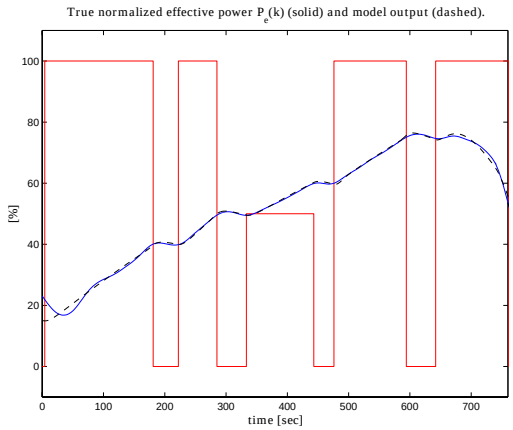

Figure 5.4: The input signal, $P_e(k)$ and the predicted `SIMULINK` model output. $P_e(k)$ is filtered with a low pass filter before plotted in the figure.

mixture becomes saturated at $t = 680$ sec. Hence, this is the point P_e^{crit}. The dynamics of the WAS are well described by a second order system with two real poles and a variable gain, see Section 4.6.

Two Simulation Examples

The RLS parameter estimator and the GPC algorithm with amplitude constraints on the control signal is implemented in `C-code` and incorporated in `SIMULINK S-functions` [47]. For the GPC, when $N_u = 1$, the step response matrix $\mathbf{G}$ becomes a vector and no matrix inversion is required for computing Δu. This choice is selected for simplicity and is valid for stable systems [10]. This choice of N_u also simplifies the optimization problem for the constrained GPC [11]. The implemented control strategies are evaluated by simulations, controlling the `SIMULINK` model of the time-varying WAS dynamics.

Two strategies are evaluated for comparison in the simulation study, the GMA-test and the probing strategy. The simulation results for both strategies are shown in Figures 5.5 and 5.6 respectively. In the simulations, a

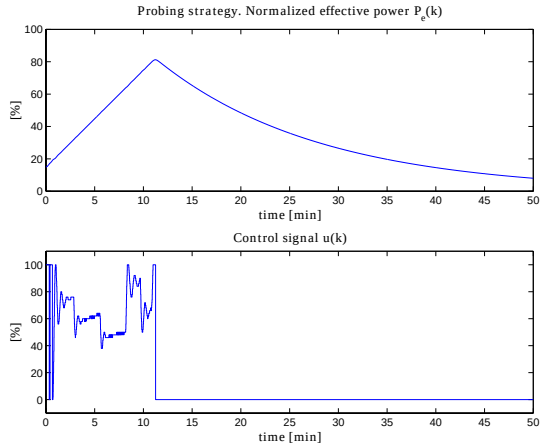

Figure 5.5: Simulation with the probing strategy, where $\lambda = 0.995$, $T_r = 10$, $\rho = 0.001$, $u_{\min} = 0$, $u_{\max} = 100$ and with a slope of the reference trajectory equal to 0.1. The RLS is turned off at $t = 20$ min to avoid estimator wind-up [63].

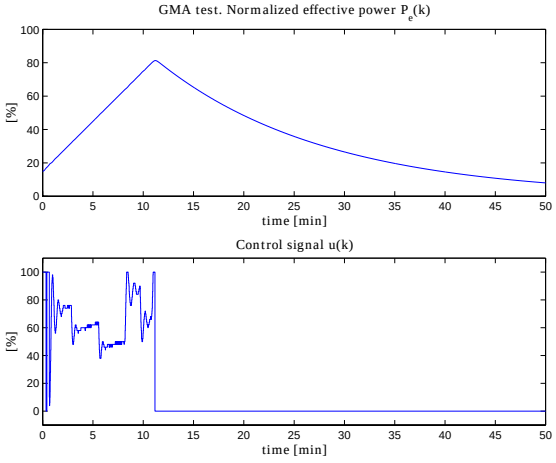

Figure 5.6: Simulation with the GMA-test as control strategy, where $\lambda = 0.995$, $T_r = 10$, $\rho = 0.001$, $u_{\min} = 0$, $u_{\max} = 100$. Here, the treshold $\gamma_{GMA} = 5 \cdot 10^{-3}$ has been used.

control signal quantization of 2% is included. Initially, an auto-tuning sequence with the controller disabled is carried through in order to obtain a good estimate of the process dynamics. After the auto-tuning sequence is completed, the GPC is enabled to control the WAS process. In Figure 5.5 it is seen that the probing strategy is successful in detecting the mixture saturation and stop the controller at $t = 11$ minutes. From $t = 11$ to $t = 50$ minutes the relative effective power $P_e(t)$ is still decreasing even if the control signal is zero. This phenomenon is also observed in real experiments. The explanation for this is that the diffusion process is still active giving a decreasing viscosity since the stirrer drive is running. To overcome this problem, the stirrer drive must be disabled when the normalized effective power has reached the point P_e^{crit}. Before the stirrer drive is disabled, a small amount of wood ash is added to the batch yielding a less sticky mixture. Hence, this can also be used as an additional control variable.

In Figure 5.6 we see that the GMA based control strategy also is successful in detecting the mixture saturation. The parameter α used to tune the low pass effect is here selected to be 0.9. Hence, the maximum value of the control signal $u(k)$ is 100%, which limits the bandwidth of the closed loop system. If the control signal would however be non-constrained, the mixture absorption properties would still limit the magnitude of the maximum control signal.

Conclusions

In this section it has been shown that an optimal adaptive controller combined with a control strategy will overcome the difficulties in controlling the chemical process of wood ash stabilization. Two control strategies were evaluated: Adaptive control combined with a probing strategy and adaptive control with the GMA-test. The results of the simulations listed with comments on good (+) or poor (−) properties of the two control strategies are

Probing Strategy

+ Gives the ability to track changes in P_e^{crit} due to varying wood ash qualities.

− Since we differentiate the data, the probing strategy will be sensitive to disturbances in the measurement of $P_e(k)$. The differentiated signal may then have to be low-pass filtered before used in the probing strategy in a real-time application. This will delay the detection time.

− The controller is disabled precisely at, or slightly after the point P_e^{crit}.

GMA Strategy

+ Gives the ability to track changes in P_e^{crit} due to varying wood ash qualities.

+ Uses the full potential of the RLS.

+ Gives the possibility to disable the controller just before the point P_e^{crit}.

− The threshold γ and the parameter α used to tune the low pass effect may be hard to select.

5.5 On-line Detection

The change detector based on the GMA-test and the CUSUM-test are now applied to two data sets that represent a typical behavior of the WAS process. Here random pulses are inserted to the system input and the results are shown in Figures 5.7 and 5.8. When the normalized effective power $P_e(k)$ reaches the level P_e^{crit}, the gain of the WAS process switches sign from positive to negative, which implies that the residuals $\varepsilon(k)$ become negative. In both figures it is seen that both implemented change detectors are successful in detecting the mixture saturation, i.e., when the level P_e^{crit} is reached. The data filters $L(q)$ (see Section 4.8) uses $f = 0.9$. In Figure 5.8 we see that from $t = 800$ s to $t = 1800$ s the normalized effective power $P_e(k)$ is still decreasing even if the input signal $u(k)$ is zero. This phenomenon was also observed in the simulations shown in Figures 5.5 and 5.6.

Conclusions

In this section, a change detector has been presented using the one-filter approach for detecting the abrupt parameter change that occurs in a WAS process. Two stopping rules were evaluated, the GMA-test and the CUSUM-test. The implemented change detectors are both successful in detecting when the mixture becomes saturated, i.e., when the level P_e^{crit} is reached. However, the CUSUM-test has a more distinct detection. Further, prefiltering with the Δ operator to cancel the natural integrator of the process dynamics does not yield any better detection. It should also be noticed that the selected ARX model could be exchanged for a recursively identified Output Error (OE) model.

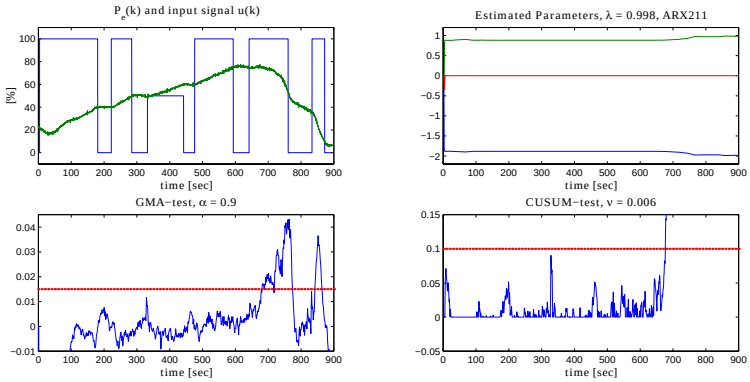

Figure 5.7: The change detector applied to the first data set. The plot to the upper left shows the applied input $u(k)$ and the system response $-$ $P_e(k)$. In the upper right plot the parameter convergence for the RLS is shown for $\lambda = 0.998$. The thresholds $\gamma_{GMA} = 0.015$ and $\gamma_{CUSUM} = 0.1$ are used, which are plotted in the two lower figures as dotted lines.

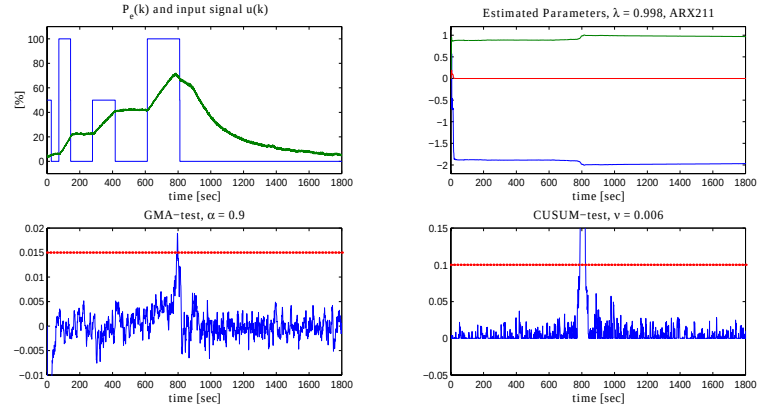

Figure 5.8: The change detector applied to the second data set. The upper left plot shows the applied input $u(k)$ and the system response $-$ $P_e(k)$. In the upper right plot the parameter convergence for the RLS is shown for $\lambda = 0.998$. The same thresholds are used as in Figure 5.7. Successful detection of the point P_e^{crit} is obtained.

5.6 Real-Time Implementation

The result of identification is dependent upon a careful choice of input to the system under investigation. During the auto-tuning, a Pseudo Random Binary Sequence (PRBS) is used as process input. This input signal shifts between two levels in a certain pattern such that its mean value and covariance function are quite similar to those of a white noise process [54]. This signal is therefore adequate for identification purposes since a white noise sequence is PE of any order [63].

PRBS Signal Generator

In order to generate a PRBS sequence with an auto-correlation function as given in equation (4.28), it is necessary to generate random numbers, *uniformly distributed* between, for example, zero and one. A numerous of methods for generating uniformly distributed random numbers have been devised, see e.g. [2]. The sequence of numbers generated is determined by the initial seed of the PRBS signal generator. Since the generator resets the initial seed at start-up, the sequence of numbers generated will be the same unless the initial seed is changed.

Definition 5.6.1 *Uniform distribution* [2].

A random variable X is *uniformly* distributed on the interval $[a, b]$ if its *probability density function* is given by

$$f_X(x) = \begin{cases} \frac{1}{b-a} & , \, a \leq x \leq b \\ 0 & , \, otherwise \end{cases} \tag{5.32}$$

The *probability distribution function* is given by

$$F_X(x) = \begin{cases} 0 & , \, x < a \\ \frac{x-a}{b-a} & , \, a \leq x \leq b \\ 1 & , \, x > b \end{cases} \tag{5.33}$$

The *mean* and *variance* of the distribution are given by

$$E\{X\} = \frac{a+b}{2} \tag{5.34}$$

and

$$Var\{X\} = \frac{(b-a)^2}{12} \tag{5.35}$$

□

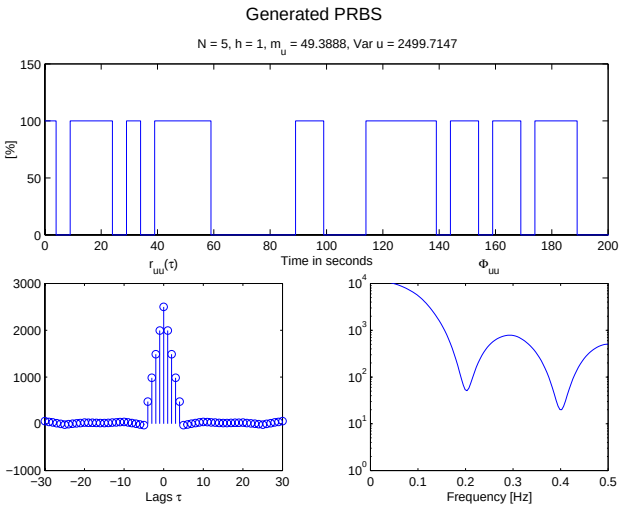

Figure 5.9: The upper plot shows the first 200 samples of the PRBS sequence. The two lower plots show the estimated auto-correlation function and the estimated auto-spectrum.

In order to generate random numbers uniformly distributed in the interval $[0, 1]$ we put $a = 0$ and $b = 1$. The PRBS signal generator is implemented in the `CALC-IDE` environment described in Section 7.4. The result of a `MATLAB` simulation using the PRBS signal generator for $N = 5$, $h = 1$ and 10000 generated samples is shown in Figure 5.9. See Appendix A, section A.2, for the definition of the auto-correlation function and the auto-spectrum. The result of the simulation confirms equation (4.28) and the number of dips in the estimated auto-spectrum is equal $(N - 1)/2$. Note that (4.28) is an asymptotic result, which means that it is valid for an infinite sequence.

Anti-Aliasing Filter

Filtering reduces noise errors in the signal. For most applications a low-pass filter is used. This allows through the lower frequency components but attenuates the higher frequencies. The cut-off frequency must be compatible with the frequencies present in the actual signal (as opposed to possible contamination by noise) and the sampling rate used for the A-D conversion. A low-pass filter that is used to prevent higher frequencies, in either the signal or noise, from introducing distortion into the digitized signal is known as an

anti-aliasing filter. These generally have a sharper cut-off than the normal low-pass filter used to condition a signal. Anti-aliasing filters are specified according to the sampling rate of the system and there must be one filter per input signal.

Very little is lost by sampling a continuous-time signal if the sampling instants are sufficiently close, but much of the information about a signal can be lost if the sampling points are too far apart. It is, of course, essential to know precisely when a continuous-time signal is uniquely given by its sampled version. Shannons sampling theorem (see the Appendix given in Section 5.9) gives the conditions for the case of periodic sampling. Note that Shannon gives conditions only for an infinite time signal. Also note that in practice we have to be more conservative, i.e., sample a little more frequently.

Practically all analog sensors have some kind of filter, but the filter is seldom chosen for a particular control problem. It is therefore often necessary to modify the filter so that the signals obtained do not have frequencies above the *Nyquist frequency* (see the Appendix given in Section 5.9). The simplest solution is to introduce an analog filter in front of the sampler. The analog inputs of the used control system `SattCon 200` (See Section 7.3) all have prefilters. However, for the selected sampling time $h = 1\ s$, the available filter has only a gain of about $-0.4\ dB$ at the Nyquist frequency $\omega_N = \omega_s/2 = \pi$, which is not sufficient. Therefore, a first order filter is designed that serves as an extra anti-aliasing filter. The filter has the transfer function

$$G_{aa}(s) = \frac{1}{s+1} \tag{5.36}$$

and has a gain of about $-10.4\ dB$ at the Nyquist frequency. Due to the slow process dynamics, the dynamics of the anti-aliasing filter are neglected.

Experimental Results

An adaptive controller that utilizes the CUSUM-test for detection of the level P_e^{crit} is implemented in the `CALC-IDE` environment (see Section 7.4) to enable real-time control of the WAS process. However, when using change detection based on a one-filter approach, experiments show that the complexity of the control algorithm may be decreased to a minimum. Then the control sequence produced by the GPC can be exchanged for a simple sequence that runs in open-loop.

The final choice of implementation is therefore summarized as follows: at each batch produced, a PRBS sequence is generated in order to obtain a good estimate of the process dynamics. This is to ensure an adequate performance

of the CUSUM-test. After the PRBS sequence is completed, the control signal attains the level $u_{\max}$ until a suitable mixture viscosity is obtained. This control strategy is, despite its simplicity, optimal in the sense that the level P_e^{crit} is reached in minimum time. As a result, this implementation also gives a decrease in the number of floating point calculations. This is positive, since most of the available time at the Programmable Logic Controller (PLC) has normally to be used for purposes other than the control algorithm itself, as for example, communications and alarms. See Chapter 7.

5.7 Summary and Concluding Remarks

In this chapter, different methods are developed in order to detect the critical mixture viscosity of the ash/dolomite/water. Three strategies are evaluated; a probing strategy, the GMA-test and the CUSUM-test, all three adequate for successful implementation. However, the final implementation is based on a simple control sequence performed in open-loop combined with a change detector that uses the one-sided CUSUM-test as a stopping rule.

It should be stressed that varying the threshold of the CUSUM-test affects the final moisture content of the mixture. Experimental results show that a threshold $\gamma_{CUSUM} = 0.2$ yields a mixture suitable for granulation, whereas the threshold $\gamma_{CUSUM} = 0.1$ presented in Section 5.5 yields a faster detection and thus a less moistened mixture. However, the threshold $\gamma_{CUSUM} = 0.2$ must be tested during a longer time-period in order to validate its robustness at seasonal variations of the wood ash quality.

5.8 Appendix 5A - Recursion of Diophantine Equations

It is simple to show that the two Diophantine equations (5.6) and (5.9) can be solved recursively. The recursion of the Diophantine equation has been demonstrated in [10]. A more detailed derivation is presented in [20]. Notice that the recursions given in this Appendix are valid for a time delay $d = 0$.

Calculation of E and F

$\boxed{i = 1 \text{ initialization}}$

$$\begin{cases} e_0^{(1)} = 1 \\ f_j^{(1)} = -e_0^{(1)}(a_{j+1} - a_j) \qquad 0 \leq j \leq na \end{cases} \tag{5.37}$$

$\boxed{i \geq 2 \text{ recursion}}$

$$\begin{cases} e_{i-1}^{(i)} = f_0^{(i-1)} \\ f_j^{(i)} = f_{j+1}^{(i-1)} - e_{i-1}^{(i)}(a_{j+1} - a_j) \qquad 0 \leq j \leq na \end{cases} \tag{5.38}$$

Calculation of G and H

$\boxed{i = 1 \text{ initialization}}$

$$\begin{cases} g_0 = e_0^{(1)} b_1 \\ h_j^{(1)} = b_{j+2} e_0^{(1)} \qquad 0 \leq j \leq nb - 2 \end{cases} \tag{5.39}$$

$\boxed{i \geq 2 \text{ recursion}}$

$$\begin{cases} g_{i-1} = h_0^{(i-1)} + b_1 e_{i-1}^{(i)} \\ h_j^{(i)} = h_{j+1}^{(i-1)} + e_{i-1}^{(i)} b_{j+1} \qquad 0 \leq j \leq nb - 2 \end{cases} \tag{5.40}$$

□

5.9 Appendix 5B - Sampling and Reconstruction

Very little is lost by sampling a continuous-time signal if the sampling instants are sufficiently close, but much of the information about a signal can be lost if the sampling points are too far apart. It is, of course, essential to know precisely when a continuous-time signal is uniquely given by its sampled version. The following theorem gives the conditions for the case of periodic sampling.

Theorem 5.9.1 *Shannons sampling theorem* [46].

A continuous-time signal with a Fourier transform that is zero outside the interval $(-\omega_0, \omega_0)$ is given uniquely by its values in equidistant points if the sampling frequency ω_s is higher than $2\omega_0$. The continuous-time signal can be computed from the sampled signal by the interpolation formula

$$f(t) = \sum_{k=-\infty}^{\infty} f(kh) \frac{\sin(\omega_s(t-kh)/2)}{\omega_s(t-kh)/2} = \sum_{k=-\infty}^{\infty} f(kh) sinc \frac{\omega_s(t-kh)}{2} \quad (5.41)$$

where ω_s is the sampling frequency in radians per second (rad/s).

Proof. See for example [64].

□

Remark 5.9.1 The frequency $\omega_N = \omega_s/2$ plays an important role. This frequency is called the *Nyquist frequency.*

Remark 5.9.2 Notice that equation (5.41) defines the reconstruction of signals whose Fourier transforms vanish for frequencies larger than the Nyquist frequency.

The Fourier transform $F_s(\omega)$ of the sampled variable is given by

$$F_s(\omega) = \frac{1}{h} \sum_{k=-\infty}^{\infty} F(\omega + k\omega_s) \quad (5.42)$$

where h denotes the sampling interval and $F(\omega)$ is the Fourier transform of the continuous-time signal $f(t)$

$$F(\omega) = \int_{-\infty}^{\infty} e^{-i\omega t} f(t) dt \quad (5.43)$$

Thus, the function $F_s(\omega)$ is periodic with a period equal to the sampling frequency ω_s. If the continuous-time signal has no frequency components higher than the Nyquist frequency, the Fourier transform is simply a periodic repetition of the continuous-time signal $f(t)$.

It follows from (5.42) that the value of the Fourier transform of the sampled signal at ω is the sum of the values of the Fourier transform of the continuous-time signal $f(t)$ at the frequencies $\omega+n\omega_s$. After sampling, it is thus no longer possible to separate the contributions from these frequencies. The frequency ω can thus be considered to be the *alias* of $\omega+n\omega_s$. It is customary to consider only positive frequencies. The frequency ω is then the alias of $\omega_s-\omega$, $\omega_s+\omega$, $2\omega_s-\omega$, $2\omega_s+\omega$, ..., where $0 \leq \omega \leq \omega_N$. After sampling, a frequency thus cannot be distinguished from its aliases. The fundamental alias for a frequency $\omega_1 > \omega_N$ is given by [64]

$$\omega_{alias} = |(\omega_1 + \omega_N) \bmod(\omega_s) - \omega_N| \tag{5.44}$$

A practical difficulty is that real signals do not have Fourier transforms that vanish outside a given frequency band. The high-frequency components may appear to be low-frequency components due to aliasing. The problem is particularly serious if there are periodic high-frequency components. To avoid the alias problem, it is therefore necessary to filter the analog signals with an *anti-aliasing filter* before sampling as discussed in Section 5.6.

Chapter 6

Operations in the Earlier Prototype

6.1 Granulation Process

After the mixture has passed the size reduction the actual granulation occurs. The *drum granulator* (shown in Figure 6.1 and in Appendix B) consists of two rotating parallel cylinders. The mixture enters the drum granulator at the left end and passes through the cylinders from the left to the right in Figure 6.1. The *time* required for the material to pass the cylinders is the variable that controls the *granule size distribution.* This time can be controlled using two parameters [30]: the first is the angular velocity ω of the rotating cylinders; the second is the inclination θ. The angular velocity has to be quite precise − it cannot be too great or too small. This will cause the material to either be smashed or not granulated. When the material follows the inner wall of the cylinders up to a distance equal its radius, the desired angular velocity is obtained [30]. It is important to note that neither the inclination should be too small. Then no material would pass the drum granulator. Two variables that cannot be affected, but also have impact on the size distribution, are the length and diameter of the rotating cylinders. At present, the inputs to the actuators of the drum granulator have static values, which correspond to a desired granule mean diameter $\overline{d}$.

6.2 Granule Hardening

After the granulation is completed, the granulated material enters the drying stage in the ash transformation process. The idea is to use the flue gas

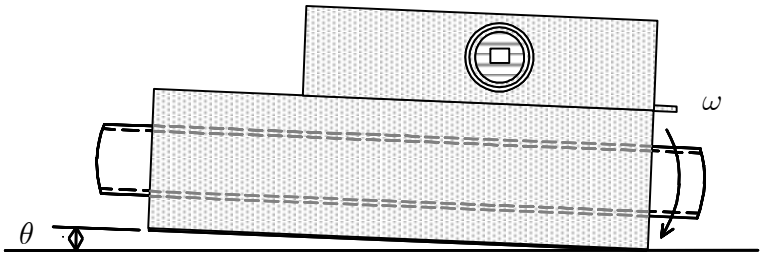

Figure 6.1: The drum granulator used to granulate the ETEC-dolomite, ash and water.

produced during combustion to dry the granules. This approach is quite attractive, since there is no need to produce any extra energy at the drying procedure. The flue gas, which has a temperature of 150-170 $^{\circ}C$, is today not used for anything and is therefore discharged immediately.

At present the flue gas is not used in the hardening procedure. The reason for this is that it is still not clear whether the flue gas produced at Graninge-Kalmar Energi is appropriate for granule hardening or not. This is under investigation. Instead, the hardening furnace is heated by hot air. The furnace, which is depicted in Figure 6.2 and shown in Appendix B, contains four conveyor belts that transport the granulated material. It is possible to vary the conveyor belt velocity (fixed today) and thus control the time δ that each granule is present in the hardening furnace.

6.3 Sorting and Packing

The final stage of the ash transformation process is the sorting and packing. This stage is at present not implemented and is thus handled manually. The setpoint for the granule size distribution is that 80% should have a diameter range of $0.5 - 4$ mm. The largest accepted diameter is 6 mm. In the future, if necessary, an industrial vibrating screen station (oversized and undersized screens) will be applied. On the other hand, if it is possible to control the granule size distribution with such a precision that the vibrating screens are not needed, the total solution would be less expensive. However, if this is not the case, for the screen we will have:

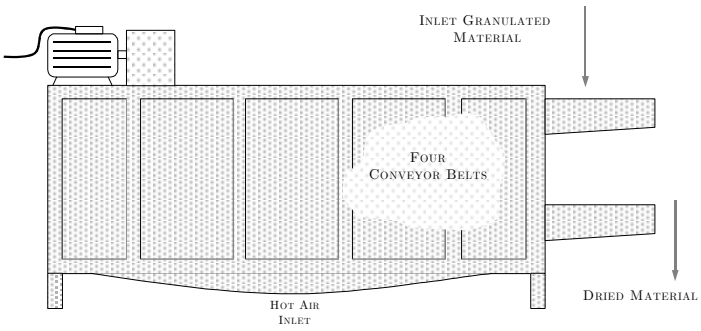

Figure 6.2: The furnace used in the drying process.

$$w_s^o > 6\ mm \qquad (6.1)$$
$$w_s^p \leq 6\ mm$$

where w_s^o is the mesh diameter for the *oversized* screen, and w_s^p is the mesh diameter for the *product* screen. How to deal with the granules that have a diameter range less than 0.5 mm is still not decided. The exact mesh diameter is to be obtained through experiments. After the granules have passed the vibrating screen they are packed and stored in big sacks or containers for later transportation. The use of containers are recommended [18].

6.4 Summary and Concluding Remarks

The stages of granulation and hardening are at present only controlled to a certain extent. With control, we here mean that the inputs to the actuators of the drum granulator and hardening furnace have static values, which correspond to a desired system response (granule mean diameter and granule moisture content). This is not an adequate implementation if a uniform product quality is desired. For example, in the hardening process, the dynamics will change with the speed of the material through the dryer and the moisture content of the incoming material. On the other hand, this implementation serves as a good initial solution. In the future work, controllers for the granulation and hardening processes should be developed, and the sorting and packing, which today are handled manually, should be automatic. The physical equipment should also be built to comply with the industrial requirements for continuous operation.

Chapter 7

Co-ordination of Control

7.1 Introduction

The control system and the physical process must of course work well together. For example, a controller is normally designed for operation around one operating state. It is, however, necessary to make sure that the system will work well also during start-up and shutdown and under *emergency conditions*, such as process failures. During normal conditions it is natural to design for maximum efficiency. At a failure, it may be much more important to recover and quickly return to safe operating conditions. In any automated manufacturing system that is in operation 24 hours a day the *robustness* of a control system is crucial. The discussion above implies that a *robust* and *safe* control system must be designed for the ash transformation process in order to meet all possible situations that may occur during operation.

Because of the industrial environment, an industrial control system is suitable as a base to solve the computer real-time problem. The control system should not only be able to interact with the process but also with the *operator*. It is important to emphasize that the *man-machine interface* plays an essential role in these kind of applications. If the operator does not understand the information he/she is receiving, it is impossible to make the correct decision about the next step in the process. Therefore, it is important to facilitate the exchange of information between the user and the equipment to be controlled. A well designed interface not only makes work conditions more pleasant but also helps considerably to reduce errors and thus limit the extent of possible damage.

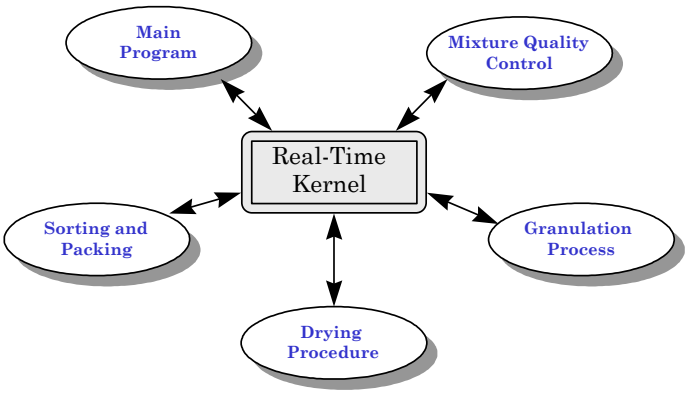

Figure 7.1: The real-time environment.

The ash transformation process consists mainly of five different tasks that will run concurrently, as depicted in Figure 7.1. Some of the processes can be divided into smaller parts, for example, the ash scheduling is included in the main program. These tasks run in parallel and need information from the "world outside" through measurements to be able to execute the next step in the program code. This implies that a numerous amount of sensors must be included to convey this information. In order to physically connect the computer to the process many technologies have to be applied. Since it is impossible to become an expert in all the related fields, it is important to be aware of the different interfacing problem in order to get a functional closed-loop system. If poor measurements are obtained of the quantity that is to be controlled, it is waisted time to use any theory from automatic control. In this case, when dealing with a true physical process, we can not ignore what is happening beyond the A-D-converters. A good reference to a book that clearly remark the importance of this topic is [40].

As mentioned earlier, each process needs different kinds of sensors. Therefore, numerous digital and analog inputs-outputs must be connected to the control system.

7.2 Control System Philosophy

This section presents the general philosophy applied during the development and implementation of the control program for the ash transformation process.

Two Mode Operations

To enable flexible operation it is possible to run the ash transformation process in two different modes:

Mode1 : *Bypass operation*
Mode2 : *Ash transformation*

It is the operator that manually sets the current mode for the transformation process.

Bypass Operation Mode

In this mode, the ash will never pass through the ash transformation process and no granules are thus produced. The ash will instead be transported to an ash container, see Appendix B. By having this mode, it is possible to reschedule the ash transportation and shut down the transformation process if a failure occurs. Hence, running the process in mode 1 is the same solution as applied earlier: the ash is deposited as waist. In this mode no alarms are allowed from any object that is a member of the ash transformation process. This is so because the staff should be able to do repairs/services on the equipment without any unmotivated alarms occurring, for example, if any safety switch is turned off during the service. Alarms are thus still allowed to be triggered from the parts of the process still active, for example, if the spiral-feeder for the ash transportation fails.

Ash Transformation Mode

In this mode the ash is granted to be transformed into fertilizing granules in the manufacturing line. The process will run in this mode until the operator orders shut down, or if any failure occurs. The ash falling from the electrostatic precipitators is, if necessary, analysed by a CIFA monitor independent of the process mode. If *mode 2* is active, and the analyzed ash is qualified, it is transported to an ash buffer (see Appendix B) for later granulation. If not, it is transported to the ash container. If *mode 1* is active, the ash is always transported to the ash container.

Fault Detection

During operation of any manufacturing system, many predictable and unpredictable sources for system failure may occur. When dealing with a production line, as the ash transformation process, it may be fruitful to divide the total manufacturing system into several successively smaller pieces as

depicted in Figure 7.1. If a failure occurs in one stage of operation, the control system must make a proper decision whether to shut down the whole production line or to keep some part of the system running.

Fault detection is to determine as quickly as possible if something in the production line has gone wrong based on knowledge of the system and observations. Based on the detection we have to make a *fault isolation*, i.e., from observations of the system we wish to determine if a fault has occurred, where it occurred, and what it is. In our case the problem is to decide which component has failed. Components can be arbitrary items such as sensors, actuators, electric drive systems, feeders etc. Since the process can run in two different *modes,* some failures can occur in any of these two modes. If a failure occurs, the control system identifies the failure and then classifies how serious it is depending on the current mode. The failures are classified as *serious* or *less serious*. The control systems then gives an alarm and take proper actions depending on in which mode (mode1/mode2) the process is running. Hence, irrespectively of the process mode, it is always necessary for the operator to correct the source of error and acknowledge before the process can be put in operation after the failure. If any source of error is not corrected accurately, and the operator anyway acknowledges, it is not possible to restart the ash transformation process until the source of error is properly corrected.

In this application two alarm-types are used. The first type is alarms caused by the hardware, called Hardware Alarms (HA) and the second type is alarms caused by the software, called Software Alarms (SA). An example of a HA may be that a safety switch is switched off to the electrical motor used in the ash spiral-feeder conveying system. On the other hand, a SA could be that the hardware does not indicate any failure, but no ash is filled into the mixer. This is monitored by the control system. Also if the execution of any of the implemented control-algorithms fails, this is regarded as a SA and the control system should take proper actions.

7.3 Distributed Control

The microprocessors have had a profound impact on the way computers have been applied to control entire production plants. It became economically feasible to develop systems consisting of several interactive microcomputers sharing the overall workload. Such systems generally consist of process stations, controlling the process; operator stations, where process operators monitor the activities; and various auxiliary stations, for example, for system configuration and programming, data storage and so on. All of them are in-

teracting by means of some kind of communication network. The allure was to boost performance by facilitating parallel multi-tasking, to improve overall availability by not putting "all the eggs in one basket" to further expandability and to reduce the amount of control cabling. The term "distributed control" was coined. The first systems were oriented towards regularity control, but over the years distributed control systems have adopted more and more of the capabilities of programmable (logic) controllers, making today's distributed control systems able to control all aspects of production and enabling operators to monitor and control activities from a single computer console.

Distributed control is adopted to solve the co-ordination problem of control, see Figure 7.2. The total system contains a local Central Processing Unit (CPU) that is connected to the ash transformation process through several I/O units. This CPU (`SattCon 200`) is independent and programmed via a Personal Computer (PC), which is easily connected to the front end of the `SattCon 200` unit. The software `DOX10` is used to design the program to be downloaded. `DOX10` supports five different types of programming methods: Sequential Function Chart (SFC), Function Blocks, Ladder, Enhanced Instruction List and Structured Text, which is floating point in `SattCon 200`. The local control system `SattCon 200` is communicating with the `SattGraph Server` by using the protocol COMmunication LInk (COMLI)[1]. Ethernet is utilized to transfer data to `SattGraph 5000`, which is used for supervision at the district heating plant. Four load cells are connected to the weight transmitter E-2 WEI. The WEI unit is a slave under `SattCon 200` and is used as a transmitter between the load cells and the PLC. The data communication is carried out over an isolated RS 485 serial interface with COMLI used as protocol, see Figure 7.2.

SattGraph 5000

`SattGraph 5000` is a modular PC-based Supervision, Control and Data Acqusition (SCADA) system. The open, object orientated system architecture is founded on true client/server principles. The SattGraph Human Machine Interface (HMI) concept used for operator interactions employs modern graphical interaction techniques, supports object orientation and features information zooming and pop-up windowing. `SattGraph 5000` is a scalable system concept. The architecture for a small single node combi system is exactly the same as for an enterprise size installation. `SattGraph 5000` is developed for the 32 bit Windows NT^{TM} platform providing connectivity to a world of Windows^{TM} applications. Configuration of process signals, detected events

[1] This communication is at present not implemented.

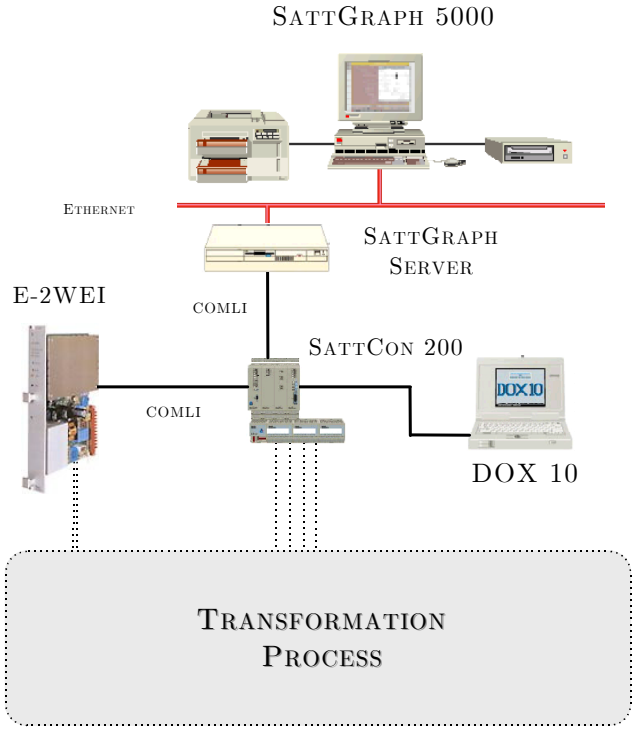

Figure 7.2: Co-ordination of control.

and alarms, and long-term process history are stored in true Open Data Base Connectivity (ODBC) databases. This enables any type of user specific report to be generated by the use of standard Windows components, such as Microsoft Excel^{TM}, Access^{TM}, SQL Server^{TM}, Visual Basic and Visual C++. This feature helps the operator to analyze the process output and further to make decisions about long-range improvements.

Communication with PLCs like `SattCon 200` is handled by the communication server. See Figure 7.2. This server supports the used protocol COMLI, and also an open Dynamic Data Exchange (DDE) interface. An *event* or *alarm* may be triggered by a binary signal or by an internal limiter in the server. Printouts and event logs can be generated for all state changes with a configurable status description. Printouts can be sent to any configuration of printers. The latest events can be inspected in an event list. Alarms are displayed in the alarm list and on the alarm line in the `SattGraph` opera-

tor station. Alarms may be delayed a certain amount of time to avoid false detection.

Some limited *control* could be implemented in `SattGraph`, but since the distance between the different units may be large, it is recommended that the control algorithms are implemented at the local unit near the physical process.

7.4 Used Programming Methods

In this section the used programming methods in `DOX10`; Grafcet and CALC-IDE are described. Function Blocks are also used but not discussed here.

Grafcet

Grafcet was proposed in France in 1977 as a formal specification and realization method for logical controllers. The name Grafcet was derived from graph, since the model is graphical in nature, and AFCET (Association Francaise pour la Cybernétique Economique et Technique), the scientific association that supported the work.

During several years, Grafcet was tested in French industries. It quickly proved to be a convenient tool for representing small and medium scale sequential systems. Grafcet was therefore introduced in the French educational programs and proposed as a standard to the French association AFNOR where it was accepted in 1982. In 1988 Grafcet, with minor changes, was also adopted by the International Electrotechnical Commission (IEC) as an international standard named IEC848 [25]. In this standard Grafcet goes under the name Sequential Function Chart (SFC). Seven years later, in 1995, the standard IEC1131-3, with Grafcet as essential part, arrived [26]. The standard concerns programming languages used in Programmable Logic Controller (PLC)s. It defines four different programming language paradigms together with SFC. No matter which of the four different languages that is used, a PLC program can be structured with SFC. Because of the two international standards, Grafcet, or SFC, is today widely accepted in industry where it is used as a representation format for sequential control logic at the local PLC level. In Section 7.8 (Appendix) a brief overview of Grafcet is given. A more thorough presentation is to be found in [14].

CALC-IDE

CALC-IDE, an extension of DOX10, is utilized to implement the more advanced control algorithms. CALC-IDE is a stand alone program in Windows^{TM} that is used for arithmetic calculations in SattCon 200. Floating-point calculations for controllers, mean-value calculations, handling of arrays, statistical analyses etc. are all solvable with CALC-IDE. The language is based on selected parts of the system program specification for programmable logic controllers, described in the international standard IEC1131-3 [26]. Compared to Structured Text, this programming language has some prominent differences.

Variables

The following class of variables are not implemented:

VAR_ACCESS . . . END_VAR
VAR_CONSTANT . . . END_VAR

A program that follows the rules in IEC1131-3 declares the absolute variables in a VAR . . . END_VAR − construction. A program in SattCon 200 uses VAR . . . END_VAR, VAR_INPUT . . . END_VAR, VAR_IN_OUT . . . END_VAR and/or a VAR_OUTPUT . . . END_VAR − constructions. The variables are further not affected directly. They are copied to a reserved memory area in a data-segment at the instance before the execution begins. The variables are then copied back to the memory or register at the end of the execution.

Datatypes

Generic datatypes, time, date and ascii-strings are not implemented. The following datatypes are missing:

BOOL	INT	REAL	STRING	TIME
SINT	LINT	USINT	UINT	UDINT
ULINT	DATE	TIME_OF_DAY	TOD	DATE_AND_TIME
DT	BYTE	WORD	DWORD	LWORD

and datatypes triggered by flanks.

7.5 Implementation

Totally, to control and monitor the ash transformation process, fifteen three-phase asynchronous machines, eight discrete control valves and fifteen sensors are incorporated. The asynchronous machines that are sources of mechanical

power, are used as movers for: spiral-feeder conveying systems, fans, high-pressure pump operation, stirrer drive, size reduction, drum granulation and conveyor belts. Some of these induction motors are speed regulated. It is possible to run each individual motor manually *or* via the PLC. Furthermore

- A power transducer is utilized to measure the normalized effective power $P_e(t)$ as discussed in Chapter 4.
- Inductive proximity sensors are applied to control the mixer outlet in order to adjust the feeding rate to the size reduction stage.
- Load cells with high resistance for lateral and longitudinal forces are used to measure the shear stress in the bars at which the mixer is placed upon. The stress is measured by straingauges in a fullbridge giving an analog output. The load cells are connected to the WEI unit shown in Figure 7.2, section 7.3.
- Electromechanical sensors are used for level monitoring in the buffers.

Ultrasonic Sensors

Ultrasonic sensing is applied for level monitoring and control of the size reduction stage. Ultrasonic sensing, which is a non-contact measuring method, is well suited since the mixture of ash/dolomite/water is very sticky. This type of level sensor is based upon high-frequency sound waves that are generated by the application of an alternating current to a piezoelectric crystal. Sonic waves may undergo surface reflection. They also have a velocity of propagation which is medium dependent. If such a wave is launched into a medium towards a level interface, it will undergo reflection. The wave takes a finite time to travel a distance equal to twice the distance between the sensor and the interface. Hence, by measuring the time from launch to reception of the reflected wave, the calculation of the distance is made using the velocity of propagation of the sound wave. If a wave travels in, for example, an empty cylindrical space with a velocity v (m/s), and takes the time t (s) to travel the distance $2(h_2-h_1)$ (m), where h_2 (m) is the length from the sensor to the bottom of the cylindrical space and h_1 (m) is the length from the sensor to the surface of the interface. Then the relevant equation for these conditions is [37]

$$2(h_2 - h_1) = tv \tag{7.1}$$

Ultrasonic sensing is affected by several factors including the target's surface, size angle and the distance from the sensor. Environmental conditions such as temperature, humidity, gases, and pressure may also affect the measurement. Therefore, a sensor that automatically compensates for most of these

environments is selected. The measured level from the ultrasonic sensor is compared to different pre-determined levels yielding three discrete values of the feeder level: `feeder_full, feeder_half_empty` and `feeder_empty.`

Component Failures

If any of the components mentioned above fails, it is crucial to detect this and take proper actions. For the motors, *overcurrent relays* or *thermal overload relays* (the first operates when the current through the relay, during its operating period, is equal to or greater than its setting), *safety switches* (a manual on/off switch that ensures, in off-mode, that the motor is not started during, for example, service/repair) and *contactor failures* must be monitored in order to ensure a functional hardware. For some motors, it is crucial that the source of error is corrected before a certain time-interval has expired, i.e., some acknowledgments for hardware alarms are time constrained. This is to guarantee safe operation of the ash transformation process. Also, to further ensure safe and robust operation, several tasks have time constraints. If a task is not completed during a predetermined time-interval, an alarm becomes active. This is used to monitor:

- Mixture quality control failures.
- Failures during the ash/dolomite dosage.
- Failure of the ultrasonic sensor.
- Failure of the size reduction stage.

Fault detection is further applied to check:

- Superstructure in mixer.
- Absence of water.
- Failure of the dust preventing equipment.

To ensure safe (and dry) operation of the *high-pressure cleaning procedure*, the gross weight of the mixer is monitored during this period.

7.6 Program Structure

`DOX 10` enables the user to structure the program (project) in ProgramModules (PM) and SubModules (SM). It is possible to include 255 PM:s in a project, where each PM can contain up to 1000 SM:s. With this feature, the user can structure the program so that each PM is controlling a specific

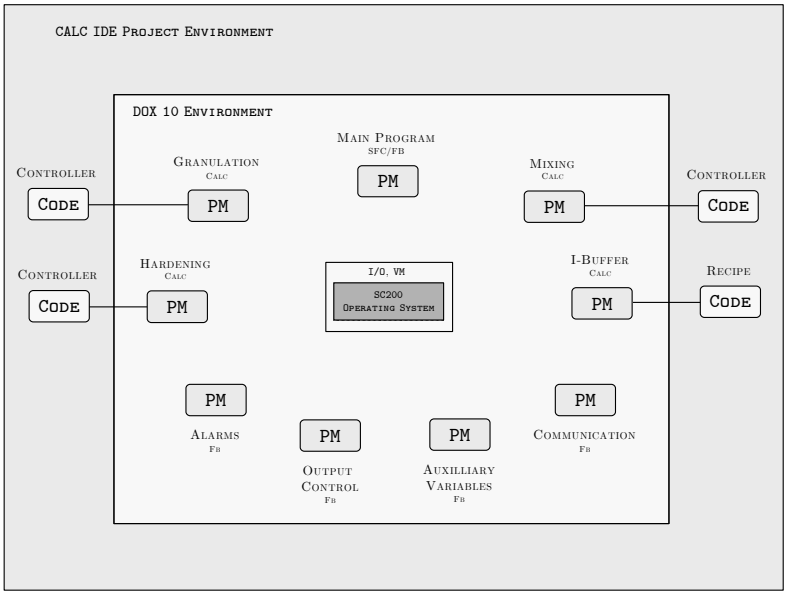

Figure 7.3: The DOX 10 program structure used when controlling the transformation process.

part of the process, where each SM in the PM is controlling, for example, a specific object. Another option is to structure the program in such way that each PM is handling special events, as for example alarms. Each PM and SM can be given a name and be documented. In order to make communication between the different PM:s possible, forty VariableModules (VM) are available to the user. All user variables are located in this real-time protected area. It is possible to connect any VM to an arbitrary chosen PM, which enables flexible programming.

The selected program structure for the ash transformation process is depicted in Figure 7.3. Here nine program modules are implemented to control specific parts of the ash transformation process, c.f., Figures 7.1 and 1.2. The main program also includes the ash scheduling. The approach of having special program modules for alarm events, output control etc. is adopted. The PM for communication is handling all interactions between SattCon 200 and SattGraph 5000[2]. The communication line uses an asynchronous serial RS485 interface, which is well suited for long distance transmissions.

[2] At present not implemented.

The used protocol is `COMLI`. SFC procedure steps (see Section 7.8) are implemented in order to enable effective usage of the weight transmitter. The PM labeled `I-buffer` is for future use, if a CIFA monitor is installed. This PM is then utilized to determine the recipe for the dry material − dolomite and ash − at each batch produced in the ash transformation process.

All Program Modules are implemented in the `DOX 10` environment. Program codes, which are implemented in the `CALC IDE` project environment, are connected to the corresponding PM in the `DOX 10` environment via a real-time configuration. In this configuration, it is possible to choose if the program code should be executed periodically or if it should be triggered and executed once by a bit changing state from false to true. If the program code is set to be executed periodically, it is possible to enable/disable the periodical execution, which gives the opportunity to run, for example, a control algorithm in some special SFC step in the main program. All implemented program codes uses the program skeleton suggested in [63]:

Algorithm Skeleton

```
Analog_Digital_Conversion
Compute_control_signal
Digital_Analog_conversion
IF estimate THEN
  begin{estimate}
    Covariance_update
    Parameter_update
    IF tune THEN
      begin{tune}
        th_design:=th_estimated
        Design_calculations
     end{tune}
  end{estimate}
Organize_data
Compute_as_much_as_possible_of_control_signal
```

Line 1 implements the conversion of the measured output signal, the reference signal, and possible feedforward signal. All the converted signals are supposed to be filtered through an appropriate anti-aliasing filters. Line 3 sets the control signal to the process. Lines 15 and 2 contain the calculation of the terms of the control signal that are independent of whether the process parameters are estimated or not. Notice the division of the calculations of the control signal to avoid overly long computation times. Only calculations that contain the last measurements are done in Line 2.

Lines 4-13 contain calculations that are specific for an adaptive algorithm. There are two logic variables, `estimate` and `tune`, which control whether the parameters are to be estimated and whether the controller is to be redesigned, respectively. The estimation is done in Lines 5-7, and the design calculations are done in Line 11. Line 14 organizes the data such that the algorithm is always ready to start the estimation when desired. For a non-adaptive controller, some parts of the suggested program skeleton are neglected.

7.7 Summary and Concluding Remarks

In this chapter, the general philosophy applied during implementation of the control system has been presented. Also a detailed description of the used sensors, the selected program structure and programming methods are outlined. The usage of fault detection has also been presented. The program is implemented and tested. However, the HMI is not yet available. The academical potential of the work presented in this chapter may not be the greatest, but on the other hand, for the operator of any process controlled by computers, a well designed, robust and good structured program/operator interface is of most value. This takes a considerable time to achieve practically, but the academical writing about it is minor. However, it increases the engineering significance of the work.

7.8 Appendix 7A - Grafcet

The purpose of this appendix is to give a short description of the graphical language Grafcet that was presented as an implementation method in Section 7.4. An example containing the basic Grafcet building blocks is shown in Figure 7.4.

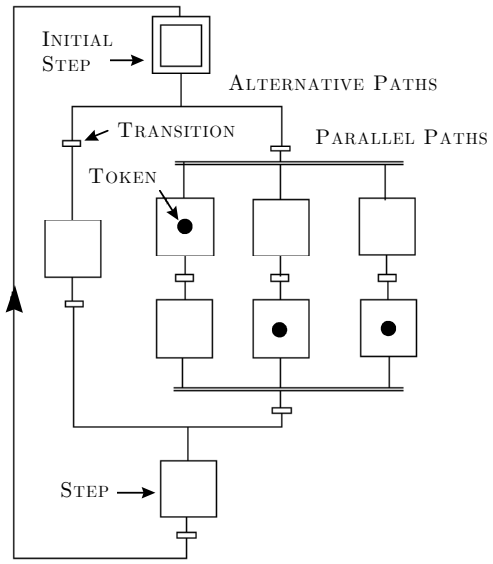

Figure 7.4: Grafcet graphical syntax.

Syntax

Grafcet has a graphical syntax. It is built up by steps, drawn as squares, and transitions, represented as bars. The initial step, i.e., the step that should be active when the system is started, is represented as a double square. Grafcet has support for both alternative and parallel branches, see Figure 7.4.

Steps

A step can be active or inactive. An active step is marked with one (and only one) token placed in the step. The steps that are active define the situation or

the state of the system. To each step one or several actions can be associated. The actions are performed when the step is active.

Actions

There are two major categories of actions: *level actions* and *impulse actions*. A level action is modeled by a binary variable and has a finite duration. The level action remains set all the time while the step, to which the action is associated, is active. A level action may be conditional or unconditional. An impulse action is responsible for changing the value of a variable. The variable can, but must not, be a binary variable. An impulse action is carried out as soon as the step changes from being inactive to active. A variable representing time may be introduced to create time-delayed actions and time-limited actions. For a more thorough discussion of related topics, see for example [28].

Transitions

Transitions are used to connect steps. Each transition has a receptivity. A transition is enabled if all steps preceding the transition are active. When the receptivity of an enabled transition becomes true the transition is firable. A firable transition will fire immediately. When a transition fires the steps preceding the transition are deactivated and the steps succeeding the transition are activated, i.e., the tokens in the preceding steps are deleted and new tokens are added to the succeeding steps. The transitions are programmed with, for example, Function Blocks, Ladder or Enhanced Instruction List.

Procedure Steps

A procedure step is equivalent of a procedure call in an ordinary programming language. When the procedure step becomes active it calls an underlying procedure (Grafcet sequence) that should be executed. When the procedure is finished, it confirms this by making the transition after the procedure step firable. This scheme is very useful if the program to be implemented contain several steps where the same task should be executed.

Chapter 8

Concluding Remarks

This work has discussed the control of an ash transformation process, which automatically transforms wood ash produced at district heating plants into fertilizing granules. The manufactured granules are recycled back to the forest grounds, as a fertilizer, or as a tool to reduce the acidification in the forest soil at the spreading area. Other areas of application are, for example, structural fill and substitute for cement in ready-mix concrete.

Today CIFA analyzers based on microwave methods are too expensive for the application of wood ash transformation. Therefore, at present, no on-line measuring device is installed. Instead, all wood ash is transformed into granules, i.e., no ash is sorted out to be reburnt. However, an attempt to optimize the burner efficiency has been launched and is ongoing. Furthermore, it is concluded that the presence of $Ca(OH)_2$ and $CaCO_3$ does not affect the color of the wood ash, since these components are not visible to the eye. On the other hand, this may result in gross errors in the LOI tests for fly ashes. Experimental results show that the color of the wood ash varies with different fuels used at combustion. This implies that a measuring method based on machine vision would be poor.

In Chapter 4, the viscosity of the ash/dolomite/water mixture is estimated by measuring the normalized effective power $P_e(t)$, which represents the rate of useful work being performed by the three-phase asynchronous machine used as stirrer drive. It is shown that this measurement is well suited for control of the amount of added water to the WAS process. A second order ARX model structure is selected and RLS is applied to estimate the time-varying dynamics. Since the mixture is accumulating water, the physical interpretation of the viscosity dynamics is that an integrator is to be found in the process dynamics. Further, a time-constant is present, which depends

on how the water is "diffused" into the mixture; in the beginning of the WAS procedure the dry mixture absorbs water fast, whereas at the end the mixture becomes more and more saturated and is not able to absorb water as fast as in the beginning. It is also concluded that the process gain switches sign when the mixture totally saturates.

Methods to predict the critical water-to-ash ratio are presented in Chapter 5. The final implementation is based on a simple control sequence performed in open-loop combined with a change detector that uses the one-sided CUSUM-test as stopping rule. The controller is implemented in the `CALC-IDE` environment to enable real-time control of the WAS process. The total ash transformation process is controlled by an industrial control system in order to enable automatic manufacture. A personal concluding remark is that the major problem of building a machine for automated manufacture is to design an apparatus that does not obtain superstructures on the mechanical parts when processing the sticky mixture of ash/dolomite/water.

Extensions and Future Work

There is a number of open problems that need to be further investigated regarding automated manufacture of fertilizing granules. A list for future research and development is:

- Since the produced granules do not benefit from high carbon content, the necessity of an on-line measuring device for the assessment of the carbon in fly ash must be established. Furthermore, the attempt to optimize the burner efficiency must be evaluated.
- The threshold $\gamma_{CUSUM} = 0.2$ must be tested during a longer time-period in order to validate its robustness at seasonal variations of the wood ash quality.
- The granulation and hardening processes must be modified, or maybe rebuilt in order to comply with the industrial requirements for continuous operation. Furthermore, the approach to dry the granules by using the flue gas produced during combustion must be investigated.
- Controllers for the granulation and hardening processes should be developed, and the sorting and packing, which today are handled manually should be automatic.
- A HMI must be implemented to enable proper exchange of information between the user and the equipment to be controlled.

Appendix A

Prerequisites

A.1 Vectors and Matrices

Definition A.1.1 *Definition of a Vector*

Let $x_1, x_2, \ldots, x_n$ be any n real numbers and x an ordered set of these numbers, that is

$$\mathbf{x} = [x_1 \; x_2 \; \ldots \; x_n]^T \tag{A.1}$$

then $\mathbf{x}$ is called an *n-vector* (or simply a *vector*). Here T denotes the *transpose* of the column vector $\mathbf{x}$, i.e.,

$$\mathbf{x} = \begin{bmatrix} x_1 \\ \vdots \\ x_n \end{bmatrix} = [x_1 \; \ldots \; x_n]^T \tag{A.2}$$

□

Definition A.1.2 *Definition of a Matrix*

A *matrix* is a rectangular array of real elements. The $(i,j)-$th element a_{ij} of the matrix $\mathbf{A}$ stands in the $i-$th row and $j-$th column of the array. The *order* (size) of a matrix is said to be $m \times n$ if the matrix includes m rows and n columns. For example,

$$\mathbf{A} = \{a_{ij}\} = \begin{bmatrix} a_{11} & a_{12} & \cdots & a_{1n} \\ a_{21} & \ddots & & \vdots \\ \vdots & & \ddots & \vdots \\ a_{m1} & \cdots & \cdots & a_{mn} \end{bmatrix} \tag{A.3}$$

is a $m \times n-$matrix. □

Definition A.1.3 *Inverses of Nonsingular Square Matrices*

If $\mathbf{A}$ and $\mathbf{B}$ are square matrices of the same dimension, and such that their product

$$\mathbf{AB} = \mathbf{I} \tag{A.4}$$

where $\mathbf{I}$ is the *identity matrix,* which has ones along the main diagonal and zeros everywhere else, then $\mathbf{B}$ is the *matrix inverse* of $\mathbf{A}$ and $\mathbf{A}$ is the matrix inverse of $\mathbf{B}$. The matrix inverse is unique, if it exists, and is denoted by $\mathbf{A}^{-1}$.

□

Definition A.1.4 *Quadratic forms*

Given

$$\mathbf{x} = [x_1 \; x_2 \; \ldots \; x_n]^T \tag{A.5}$$

and the square matrix $\mathbf{A}$

$$\mathbf{A} = \begin{bmatrix} a_{11} & a_{12} & \cdots & a_{1n} \\ a_{21} & \ddots & & \vdots \\ \vdots & & \ddots & \vdots \\ a_{n1} & \cdots & \cdots & a_{nn} \end{bmatrix} \tag{A.6}$$

then

$$\mathbf{x}^T\mathbf{Ax} = \sum_{i=1}^{n}\sum_{j=1}^{n} a_{ij}x_i x_j \tag{A.7}$$

is called a *quadratic form.*

□

Definition A.1.5 *Positive definite matrix*

A square symmetric matrix $\mathbf{A}^T = \mathbf{A}$ is said to be *positive definite*, denoted by $\mathbf{A} \succ 0$ if

$$\mathbf{x}^T\mathbf{Ax} > 0 \quad \forall \mathbf{x} \neq 0 \tag{A.8}$$

□

Definition A.1.6 *Positive semi-definite matrix*

A square symmetric matrix $\mathbf{A}^T = \mathbf{A}$ is said to be *semi-definite*, denoted by $\mathbf{A} \succeq 0$ if

$$\mathbf{x}^T\mathbf{Ax} \geq 0 \quad \forall \mathbf{x} \neq 0 \tag{A.9}$$

□

A.2 Stochastic Processes

Definition A.2.1 *Stochastic process*

A sequence of random (stochastic) variables

$$\{y(k), \quad k = 1, 2, 3, \ldots\} \tag{A.10}$$

shorter denoted $\{y(k)\}$ is called a *stochastic process.*

□

Expectation

The statistical average value $m_y(k)$ of a random variable $y(k)$ is given by the mathematical *expectation operator* denoted E. Hence

$$m_y(k) = E\{y(k)\} \tag{A.11}$$

Assume that a number of realizations $y^{(1)}(k)$, $y^{(2)}(k), \ldots, y^{(n)}(k)$ of the random variable $y(k)$ are available. The expectation can then be considered as the average value when an infinite numbers of realizations are utilized. Thus

$$m_y(k) = E\{y(k)\} = \lim_{n\to\infty} \frac{1}{n} \sum_{i=1}^{n} y^{(i)}(k) \tag{A.12}$$

For a stochastic process $\{y(k)\}$ this means that the average value generally is a time-varying function $m_y(k)$. However, if the expectation operator acting on a stochastic process implies a constant function, we obtain a *stationary stochastic process.* The average value, m_y, for instance, then becomes

$$m_y = E\{y(k)\} = E\{y(k+i)\} \qquad i = \pm 1, \pm 2, \ldots \tag{A.13}$$

For stationary processes the average taken over a number of realizations can naturally be replaced by a time average of one single realization $\{y(k)\}_{k=1}^{N}$. Hence, (A.12) is then replaced by

$$m_y = E\{y(k)\} = \lim_{N\to\infty} \frac{1}{N} \sum_{k=1}^{N} y(k) \tag{A.14}$$

Correlation

The *auto-correlation* for a stochastic process $\{y(k)\}$, defined as

$$r_{yy}(k,\tau) = E\left\{\left(y(k+\tau) - m_y(k+\tau)\right)\left(y(k) - m_y(k)\right)\right\} \tag{A.15}$$

describes how the process is correlated in time. For a slowly varying process, there is a strong correlation between values at different time instances, while the correlation is insignificant for a rapidly varying process except for very short time differences τ.

Assuming a stationary process, the correlation does not depend on the time k, but only on the time difference τ. Thus, we simplify the notation for the correlation to $r_{yy}(\tau)$, and experimentally it can be determined by the time average as

$$\begin{aligned} r_{yy}(\tau) &= E\left\{\left(y(k+\tau) - m_y\right)\left(y(k) - m_y\right)\right\} \\ &= \lim_{N\to\infty} \frac{1}{N} \sum_{k=1}^{N} \left(y(k+\tau) - m_y\right)\left(y(k) - m_y\right) \end{aligned} \tag{A.16}$$

If the average $m_y = 0$ we also note that the *variance* becomes

$$Var\ y(k) = E\left\{y^2(k)\right\} = r_{yy}(0) \tag{A.17}$$

It is also important to know how two different stochastic processes are related to each other. Assume that $\{y(k)\}$ and $\{u(k)\}$ are stationary stochastic processes. The dependence between these processes is then described by the *cross-correlation*

$$\begin{aligned} r_{yu}(\tau) &= E\left\{y(k+\tau)u(k)\right\} \\ &= \lim_{N\to\infty} \frac{1}{N} \sum_{k=1}^{N} \left(y(k+\tau) - m_y\right)\left(u(k) - m_u\right) \end{aligned} \tag{A.18}$$

Example A.2.1 (White-noise)

White noise is a type of stochastic process that often is used as a unit disturbance. It is simply defined as an uncorrelated stationary process with zero mean. Assume that the stochastic process $\{e(k)\}$ is white noise with variance r_e. Then the average is

$$m_e = E\left\{e(k)\right\} = 0 \tag{A.19}$$

and the auto-correlation

$$r_{ee}(\tau) = \begin{cases} r_e & , \tau = 0 \\ 0 & , \tau \neq 0 \end{cases} \tag{A.20}$$

□

Spectrum

The frequency content of a signal is described by its *spectrum.* Depending on the property of a signal, different types of spectra are defined. For a stochastic process $\{y(k)\}$ the *auto-spectrum* can be considered as the expectation of the power spectrum for realizations of $y(k)$, i.e.,

$$\Phi_{yy}(\omega) = \lim_{N\to\infty} \frac{1}{Nh} E\left|Y_N(\omega)\right|^2 \tag{A.21}$$

where Y_N is given by the *Discrete Fourier Transform* (N measurements)

$$Y_N(\omega) = h\sum_{m=1}^{N} y(mh)e^{-i\omega mh} \tag{A.22}$$

The normalizing factor Nh is the real time between the first and last non-zero value of the signal. Hence, $\Phi_{yy}(\omega)$ describes the average frequency content of $\{y(k)\}$. Hence, equation (A.21) can also be written as

$$\Phi_{yy}(\omega) = \frac{1}{2\pi}\sum_{\tau=-\infty}^{\infty} r_{yy}(\tau)e^{-i\omega\tau} \tag{A.23}$$

which shows that the spectrum for a stochastic process can be considered as the fourier transform of the correlation function $r_{yy}(\tau)$. In fact, (A.21) is the original definition of spectrum for a stochastic process.

In the same way, the *cross-spectrum* for two stochastic processes is defined as

$$\Phi_{yu}(\omega) = \frac{1}{2\pi}\sum_{\tau=-\infty}^{\infty} r_{yu}(\tau)e^{-i\omega\tau} \tag{A.24}$$

This means that the cross-spectrum for two *independent* signals is zero since $r_{yu} = 0$.

Example A.2.2 (White-noise cont'd)

For white noise $e(k)$ with variance r_e, (A.20) and (A.24) imply that

$$\Phi_{ee}(\omega) = \frac{1}{2\pi} r_e \tag{A.25}$$

i.e., the spectrum is constant. This is in fact the reason for the designation *white noise,* since the white color has an equal mix of all colors (frequencies).

□

Appendix B

Magnificus Apparatus

Rome was not built in a day.

Fejmert Mixer
Hardening Furnace
Dolomite buffer
Ash buffer

If mixture control fails

Drum granulators

Dust preventer

Ash container

Index

Bibliography

[1] H. Ban, J. L. Schaefer and J. M. Stencel. *Energia,* Vol 6, Nr. 7, 1995.

[2] J. Banks and J. S. Carson. *Discrete-Event System Simulation*, Prentice-Hall International Inc., London, 1984.

[3] M. Basseville and I.V. Nikiforov. *Detection of abrupt changes: theory and application*. Information and system science series. Prentice Hall, Englewood Cliffs, NJ., 1993.

[4] I. B. Benson. *The characteristics and scope of continuous on-line near infrared measurement.* Spectroscopy Europe 7(6):18-24, 1995.

[5] G. J. Bierman. *Factorization Methods for Discrete Sequential Estimations*. Academic Press, New York, 1977.

[6] R. R. Bitmead, M. Gevers and V. Wertz. *Adaptive Control: The Thinking Man's GPC.* Englewood Cliffs, N.J. Prentice Hall, 1990.

[7] R. C. Brown and J. R. Dykstra. *Systematic-Errors in the use of loss-on-ignition to measure unburned carbon in fly-ash.* FUEL, 7(4):570-574, April 1995.

[8] H. Brunzell. *Signal Processing Techniques for Detection of Buried Landmines using Ground Penetrating Radar*. Ph.D. thesis, Department of Signals and Systems, School of Electrical and Computer Engineering, Chalmers University of Technology, Sweden, 1998.

[9] E.F. Camacho and C. Bordons. *Model Predictive Control.* Springer - Verlag London Limited, 1999.

[10] D.W. Clarke, C. Mohtadi and P.S. Tuffs. Generalized Predictive Control. Part I. The Basic Algorithm. *Automatica,* 23(2):137-148, 1987.

[11] D.W. Clarke and T.T.C. Tsang. Generalized predictive control with input constraints. *IEEE Proceedings Part D*, Vol. 135, Nov., 1988.

[12] D.W. Clarke and C. Mothadi. Properties of Generalized Predictive Control. *Automatica,* 25(6):859-875, 1989.

[13] D. W Clarke, and P. J. Gawthrop. Self-tuning control, *IEE Proceedings, Part D*, 126:663-640, 1979.

[14] R. David and H. Alla. *Petri Nets and Grafcet: Tools for modelling discrete events systems*. Prentice-Hall International UK Ltd, 1992.

[15] D. Dodgen and L. Larrimore, Southern Company Services. "*Issues Impacting Coal Ash Utilization*" for Presentation at the SME Annual Meeting - Denver, Colorado - February 24-27, 1997.

[16] J. R. Dykstra and R. C. Brown. *Comparison of optically and microwave excited photoacoustic detection of unburned carbon in entrained fly-ash.* FUEL, 74(3):368-373, March 1995.

[17] EG$_\Sigma$G Berthold. *On-line Analyzer for the Measurement of Carbon of Fly-Ash in Power Stations.* (30/8-2000), `http://berthold.com.au/industrial_pages/fly%20ash.html.`

[18] S-O. Ericson, A. Lundborg and R. Oskarsson. *Wood ash in the forest - collected experiences and knowledge from the project Skogskraft.* Södra, Vattenfall, January 1994. (In Swedish).

[19] J. Eriksson. *Characterization of wood-ash with respect to contents and solubility of plant nutrients and heavy metals.* Vattenfall Research, Bioenergy, 1993.

[20] J. Gangloff. *Asservissements visuels rapides d'un robot manipulateur à six degrés de liberté.* Thèse de l'Université Louis Pasteur, Ecole Nationale supérieure de Physique de Strasbourg, 15, février 1999. (In French).

[21] K. F. Gauss. *Theory of Motion of the Heavenly Bodies.* New York, Dover 1963.

[22] F. Gustafsson. *Adaptive filtering and change detection*. John Wiley & Sons, Ltd, 2000.

[23] M. Harayama and M. Uesugi. *On-line measurement of average pellet size with spatial frequency analysis.* Proceedings of the 1992 International Conference on Industrial Electronics, Control, Instrumentation, and Automation, 1992. Power Electronics and Motion Control. 3:1613-1618, 1992.

[24] T. Hägglund. The problem of forgetting old data in recursive estimation. *Prepr. IFAC Workshop Adaptive System Control, Signal Processing*, San Francisco, Paper SAC-6, 1983.

[25] IEC848: *Preparation of function charts for control systems.* International Electrotechnical Commission.

[26] IEC1131-3. *Technical Report.* International Electrotechnical Commission.

[27] R. Johansson. *System Modeling & Identification,* Prentice Hall Inc., 1993.

[28] C. Johnsson. *Recipe-Based Batch Control Using High-Level Grafchart.* Licentiate thesis, TFRT – 3217. Department of Automatic Control, Lund Institute of Technology, June 1997.

[29] C. L. Larrimore and J. Sorge. *Evaluation of On-line Carbon-In-Ash Measurement Technologies.* FETC Publications, Conference Proceedings, Third Annual Conference on Unburned Carbon on Utility Fly Ash, 1997.

[30] M. Lindahl and T. Claesson. *Recycling of ashes. Granules made of wood ash, ETEC-dolomite and water.* Kalmar University College, Kalmar Energi & Miljö, 1996. (In Swedish).

[31] L. Ljung. *System Identification: Theory for the User.* Prentice Hall Inc., 1987.

[32] L. Ljung. Model Validation and Model Error Modeling. *Åström Symposium on Control*, Lund, Sweden, August 1999.

[33] S. Ljung and L. Ljung. Error propagating properties of recursive least-squares adaptive algorithms. *Automatica* 21(2):157-167, 1985.

[34] L. Ljung and T. Söderström. *Theory and Practice of Recursive Identification.* The MIT Press Cambridge, Massachusetts, London, England 1983.

[35] Load measurement – EL-FI G3 Power meter, Emotron AB, `http://www.emotron.com/.` (30/8-2000).

[36] A. Lundborg. *Ash Recycling,* BIOENERGI, Nr 6. 1997 (In Swedish).

[37] J. Mc Ghee, I. Henderson, W. Kulesza, J. Korczynski. *Measurement Science for Engineering.* Lodart, 1998.

[38] A. Nilsson. *Techniques for wood ash processing.* NUTEK R 1993:42. Stockholm (In Swedish).

[39] F. Nordenberg. *Granulation with stirrer technique.* Dimploma work, Inst. för Energiteknik, Mälardalens Högskola, 1996. (In Swedish)

[40] G. Olsson and G. Piani. *Computer Systems for Automation and Control.* Prentice Hall Inc., 1992.

[41] B. G. Osborne, F. Fearn and P. H. Hindle. *Practical NIR Spectroscopy with applications in food and beverage analysis, Second Edition.* Longman Group UK Limited, 1993.

[42] J. Peetz-Schou. *Economics of On-Line Ash, Coal and Unburned Carbon Monitors in Coal-Fired Power Plants.* FETC Publications, Conference Proceedings, Conference on Unburned Carbon on Utility Fly Ash, 1998.

[43] RENOMA: `http://www.renoma.se/` (Before 30/8-2000).

[44] S.W Roberts. Control charts based on geometric moving averages, *Technometrics*, 8:411-430, 1959.

[45] S. L. Shah and W. R. Cluett. Recursive least-squares based estimation schemes for self-tuning control, *The Canadian Journal of Chemical Engineering* 69:89-96, 1991.

[46] C. E. Shannon. Communication in presence of noise. *Proc. IRE*, 37:10-21, 1949.

[47] SIMULINK: *Writing S-Functions*, Version 3. The MathWorks Inc., 1998.

[48] B-M. Steenari. *Chemical Properties of FBC Ashes,* Ph.D. Thesis, Department of Environmental Inorganic Chemistry. Postgraduate Programme in Environmental Sciences, Chalmers University of Technology, Sweden, 1998.

[49] T. Sundqvist. *A High Temperature Granulation Process for Ecological Ash Recirculation.* Licentiate thesis, Luleå University of Technology, 1999.

[50] T. Svantesson. *Real-Time Implementation of Adaptive Algorithms in dSPACE/SIMULINK.* Report LiTH-ISY-EX-1958, Department of Electrical Engineering, Linköping University, Linköping, Sweden, June 1997.

[51] T. Svantesson, A. Lauber and G. Olsson. Automated Manufacture of Granules from Burnt Wood Ash, *Fifth National Science − Technical Conference. Macro-Levelling and Reclamation of Areas with use of By Products Combustion*, 14-17 October 1998, Swinoujscie, Poland.

[52] Swedish Standard: SS 02 81 13, *Determination of dry matter and ignition residue in water, sludge and sediment.*

[53] B. Snowdon. *Sekam On-Line Carbon-in-Ash Monitor, Application Examples and Operating Experience.* FETC Publications, Conference Proceedings, Conference on Unburned Carbon on Utility Fly Ash, 1998.

[54] T. Söderström and P. Stoica. *System Identification.* Prentice Hall Inc., 1989.

[55] J. D. Taylor. *Introduction to Ultra-Wide Band Radar Systems.* CRC Press, 1995.

[56] C. L. Thornton and G. J. Bierman. UDU^T covariance factorization for Kalman filtering. *Control and Dynamic Systems 16.* New York Academic Press, 1980.

[57] D. N. Trerice, A. M. DiGioia, Jr. and J. B. Reid. *Experience with Microwave-Based Systems for Measurement of LOI.* FETC Publications, Conference Proceedings, Conference on Unburned Carbon on Utility Fly Ash, 1998.

[58] P. Ulriksen. *Application of impulse radar to civil engineering.* Doctoral Thesis, Department of Engineering Geology, Lund University of Technology, Sweden, 1982.

[59] C.S. Van Dobben de Bruyn. *Cumulative sum tests: theory and practice.* Hafner, New York, 1968.

[60] K. Widelhed. *Mekanisk bearbetning av bioaskor.* The Swedish National Energy Administration, ER 12:1998, Stockholm, Sweden. 1998. (In Swedish).

[61] T.W. Yoon and D.W. Clarke. *Advances in Model-Based Predictive Control.* Chap. Towards Robust Adaptive Predictive Control, pp. 402-414, Oxford University Press, 1994.

[62] M. Åkesson. *Probing Control of Glucose Feeding in Escherichia coli Cultivations,* Ph.D. thesis, TFRT – 1057. Department of Automatic Control, Lund Institute of Technology, Sweden, December 1999.

[63] K. J. Åström and B. Wittenmark. *Adaptive Control, Second Edition.* Addison Wesley, 1995.

[64] K. J. Åström and B. Wittenmark. *Computer-Controlled Systems: Theory and Design, Third Edition.* Prentice Hall Inc., 1997.